The role of cyclin B3's phosphate-binding pocket in female meiosis I of *Xenopus laevis*

Doctoral thesis for obtaining the

academic degree

Doctor of Natural Sciences

(Dr. rer. nat.)

submitted by

Demmig, Rebecca

at the

Universität Konstanz

Faculty of Science

Department of Biology

Date of Oral Examination: 25th April 2024

1st Referee: Prof. Dr. Thomas U. Mayer

2nd Referee: Prof. Dr. Martin Scheffner

Table of Contents

Abstract

Cyclins are the main driver of the cell cycle and are indispensable for correct cell division. Cyclins prevent aneuploidy, which is a hallmark of cancer in the case of mitosis and a risk factor for embryonic mortality or the development of trisomy disorders in the case of meiosis. The different cyclin classes are involved in different cell cycle phases with B-type cyclins mainly responsible for mitosis and meiosis. Cyclin B3 (cycB3) is an understudied member of B-type cyclins with sequence similarity to other B-type cyclins as well as to A-type cyclins. This leads to a unique mix type cyclin with the function of preventing premature metaphase I arrest in meiosis. This metaphase I arrest is circumvented by phosphorylation of the anaphase-promoting complex/cyclosome (APC/C) inhibitor XErp1 by cycB3 in complex with the cyclin-dependent kinase 1 (Cdk1) which leads to further polo-like kinase 1 (Plx1) phosphorylation and results in XErp1 degradation. For the first time, a cycB3-specific phosphate-binding pocket mediating the main function of cycB3 in meiosis is described in this thesis. By comparison of a phosphate-pocket deficient cycB3 version, cycB3^{TEM}, with wild-type cycB3, cycB3^{WT}, the role of the phosphate-binding pocket in XErp1 degradation was investigated. The phosphate-binding pocket in cycB3 directly interacted with threonine 97 residue in XErp1, which was pre-phosphorylated by cycB3/Cdk1. The binding of cycB3/Cdk1 to XErp1 mediated by the phosphate-binding pocket then led to multisite phosphorylation of XErp1 by cycB3/Cdk1 and consequently to binding of Plx1. The number of phosphorylation sites, sufficient for resembling wild-type XErp1 degradation pattern, could be narrowed down to four phosphorylation sites in the M-cluster and several phosphorylation sites in the N-cluster. Therefore, the order of events occurring on XErp1 in metaphase I—consisting of preceding cycB3/Cdk1 phosphorylation of T97, then multisite phosphorylation mediated by phosphate-binding pocket dependent cycB3 binding, followed by Plx1 phosphorylation—was characterised. Furthermore, the comparison of different B-type cyclins revealed a difference in substrate binding which might depend on the phosphate-binding pocket and further structural difference of cycB3 and cycB1. Finally, further possible phosphate-binding pocket dependent substrates of cycB3/Cdk1 were identified. Thus, this thesis contributes to a better understanding of cycB3 function in meiosis and broadens our knowledge about cyclin-mediated Cdk phosphorylation by identifying a phosphate-binding pocket in cycB3.

Zusammenfassung

Cycline sind die treibende Kraft für das Voranschreiten des Zellzyklus und sind unersetzbar für einen korrekten Ablauf der Zellteilung. Cycline verhindern Aneuploidie, welche im Falle von Mitose, ein Kenzeichen von Krebs ist, und im Falle von Meiose, ein Risikofaktor für Embryosterblichkeit oder die Entstehung von Trisonomien. Die verschiedenen Cyclin Typen sind in unterschiedlichen Zellzyklusphasen involviert, mit den B-Typ Cyclinen als Hauptverantwortliche für Mitose und Meiose. Cyclin B3 (CycB3) ist ein noch wenig untersuchtes B-Typ Cyclin mit Sequenzähnlichkeiten sowohl mit anderen B-Typ Cyclinen als auch mit A-Typ Cyclinen. Dies führt zu einer Art „Misch"-Cyclin, dessen Funktion es ist einen verfrühten Arrest in Metaphase I zu verhindern. Der Metaphase I Arrest wird dadurch umgangen, das der APC/C (anaphase-promoting complex/cyclosome) Inhibitor XErp1 von CycB3 im Komplex mit der „cyclin-dependent kinase 1" (Cdk1) phosphoryliert wird. Diese Phosphorylierung führt zur weiteren Phosphorylierung durch „polo-like kinase" (Plx1) und endet im Abbau von XErp1. In dieser Arbeit wird zum ersten Mal eine spezifische Phosphatbindungstasche in CycB3, die zur Hauptfunktion von CycB3 in der Meiose beiträgt, beschrieben. Indem Wildtyp CycB3 (CycB3^{WT}) mit einer Phosphatbindungstaschen-Mutante (CycB3^{TEM}) verglichen wurde, wurde die Rolle der Phoshatbindungstasche für den Abbau von XErp1 untersucht. Die Phosphatbindungstasche in CycB3 interagierte direkt mit Threonin 97 Rest in XErp1, welches von CycB3/Cdk1 vor-phosphoryliert wurde. Bindung durch die Phosphatbindungstasche führte dann zu weiteren Phosphorylierung von XErp1 durch CycB3/Cdk1, was zu Plx1 Bindung führte. Die Anzahl an Phosphorylierungstellen in XErp1, die notwendig für einen Wildtyp-ähnlichen XErp1 Abbau waren, konnten auf alle M-cluster Stellen und mehrere N-cluster Stellen eingegrenzt werden. Dadurch wurde die Reihenfolge der Events an XErp1 in Metaphase I—die aus vorangehender CycB3/Cdk1 T97 Phosphorylierung, dann weiteren Phosphatbindungstaschen-abhängigen Phosphorylierungen durch CycB3/Cdk1, gefolgt von Phosphorylierungen durch Plx1 besteht—aufgeschlüsselt. Zudem wurde im Vergleich von verschiedenen B-Typ Cyclinen ein Unterschied in der Substratbindung festgestellt, der von der Phosphatbindungstasche und eventuell weiteren strukturellen Unterschieden abhängen könnte. Abschließend wurden noch weitere mögliche Substrate von CycB3/Cdk1, die von der Phosphatbindungstasche abhingen, identifiziert. Somit trägt diese Arbeit zu einem besseren Verständnis der Funktion von CycB3 in Meiose bei und erweitert unser Wissen über Cyclin mediierte Cdk Phosphorylierung durch die Identifizierung einer Phosphatbindungstasche in CycB3.

1. Introduction

Cell division—the mitotic cell cycle—is a fundamental process of life where all genetic information, stored in chromosomes, is transported from one mother cell to two daughter cells, which then contain the same genetic information as the mother cell. On the other hand, for sexual reproduction, two gametes—egg and sperm—fuse to develop a new organism to generate genomic variability a main driver of evolution. To prevent doubling of the genome in each generation, gametes only possess one copy of each chromosome and are therefore haploid. After the fusion of two gametes a diploid cell arises, and mitosis takes over for further development. To produce a haploid gamete, two consecutive rounds of chromosome segregation have to occur without an intervening duplication phase (S-phase). This specialized cell division is called meiosis and can be subdivided into meiosis I and meiosis II, respectively. Correct meiotic division is essential for creating a new organism as errors in meiosis can lead to aneuploidy linked to many different diseases or even death in early developmental stages (Petracchi et al., 2009; Warburton & Fraser, 1964). Understanding the biochemical processes which underlie meiosis is crucial for improving reproductive medicine.

Here, I aim to elucidate the role of cyclin B3 in meiosis in more detail. The introduction is structured into two main parts: The first part describes female meiosis to illustrate all relevant pathways and proteins necessary to understand the presented results, while the second part comprises a more detail description of cyclins and their mode of action, with an emphasis on the current knowledge about cyclin B3. As this thesis was performed with African clawed frogs, *Xenopus laevis*, the focus of the introduction will be on the meiotic mechanism in this model organism.

1.1. Oogenic meiosis

Female gametes precursor cells called oocytes were produced already in early embryonic stages in mammals like mice and humans (Jorgensen & Rajpert-De Meyts, 2014; Slizynski, 1957). These primary oocytes are derived from pluripotent cells, oogonia. In most mammals, these precursor cells divide to create a limited number of oocytes while in species like amphibians or fishes, oogonia are self-renewing stem cells that can generate new oocytes each year. After the pre-meiotic S-phase of oogonia, these cells enter meiosis and arrest at the end of meiosis I. Upon entry into meiosis, these cells are termed primary oocytes and pass through meiotic prophase consisting of four phases, where chromosome pairing, cross-over formation, and recombination of homologous chromosomes take place. In the last prophase stage, the diplotene stage, oocytes arrest to grow and stockpile all necessary components for the following two divisions (Jessus et al., 2020). This first arrest is conserved in metazoans and can last for months in mice and up to decades in humans until these oocytes are triggered for meiotic maturation. Meiotic maturation is induced by maturation-inducing hormones (MIH) and only fully grown oocytes are sensitive toward MIH stimulus. In *Xenopus laevis,* this MIH is the steroid hormone progesterone released by surrounding follicle cells upon receiving an ovulatory gonadotropin signal. Then, oocytes undergo nuclear envelop break-down, which is termed germinal vesicle breakdown (GVBD) in oocytes, followed by assembly of the metaphase I spindle and the first separation of chromosomes (homologous chromosomes) (Fig. 1). One set of homologous chromosomes is removed by extrusion of the first polar body. The now secondary oocyte enters directly the second meiotic division and arrests at metaphase of meiosis II to await fertilization (Fig. 1). The metaphase arrest in meiosis II, also termed cytostatic factor (CSF) arrest, is only conserved throughout most vertebrates (Von Stetina & Orr-Weaver, 2011). These metaphase II arrested oocytes are also termed eggs. The term egg refers here to fertilizable oocytes and not specifically to oocytes which already finished meiosis II (Duncan et al., 2020). In species like starfish or jelly fish, secondary oocytes directly go through metaphase II, separate sister chromatids and extrude the second polar body. In metaphase II arrested oocytes the second meiotic division is induced upon fertilization. Both meiotic divisions are highly asymmetric with the most cytoplasm retained for the oocyte, compared to the very symmetric cell division in mitosis. Correct meiotic arrests and resumptions are regulated by a variety of proteins. Understanding the interplay and regulation of these proteins helps to reveal causes for miscarriages and aneuploidy.

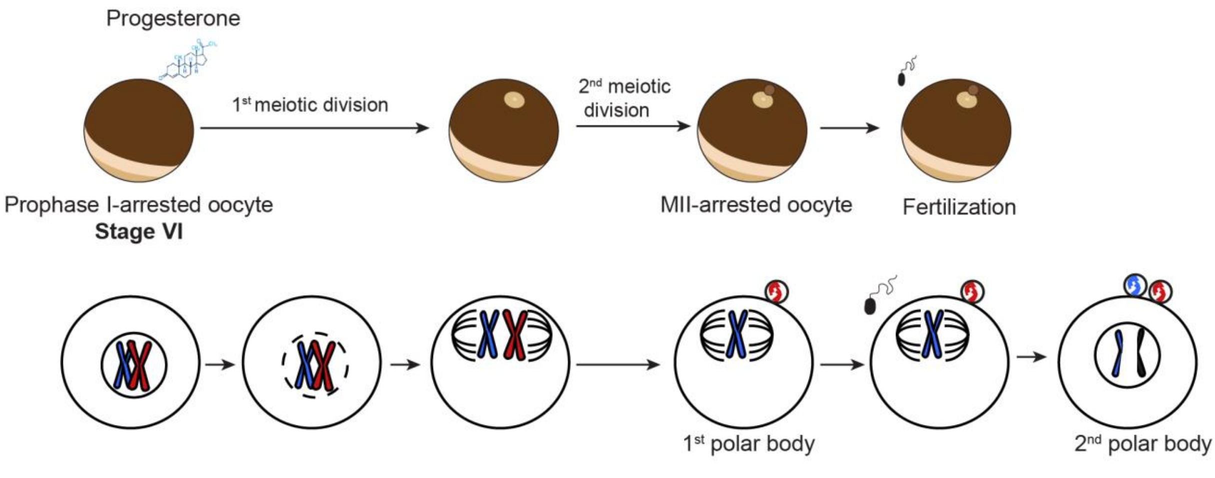

Figure 1: Female meiosis in *Xenopus laevis*. The upper scheme shows a cartoon of meiosis from stage VI oocytes arrested in prophase I to oocytes ready for fertilization, while in the lower panel, the behaviour of chromosomes is depicted. Primary oocytes arrest in the diplotene stage of meiosis I. Upon a stimulus they continue with the meiotic program and a white spot appears at the animal pole of the oocytes. The white spot results from the metaphase I spindle migrating to the animal pole after germinal vesicle breakdown (GVBD). The GVBD spot helps to score oocytes which resume meiosis. The first polar body is extruded after anaphase I has occurred and can be observed by microscopy after staining. In metaphase II, the second arrest occurs with oocytes containing a metaphase II spindle and the extruded first polar body. After fertilization, anaphase II is initiated and the second polar body is extruded.

To investigate and study meiosis different model organisms are available and, as this work was conducted with *Xenopus laevis* oocytes, the focus of the introduction lays on meiosis in this model organism. *Xenopus laevis* or African clawed frog is a great model organism to study meiosis, as large quantities of oocytes can be obtained from one single frog without the need for euthanasia. Furthermore, the oocytes are larger compared to mouse oocytes with a diameter of 1.2 to 1.3 mm compared to around 100 µm, respectively. The size allows visual staging, sorting, and manipulation by microinjection. As research with *Xenopus laevis* oocytes has been performed for decades a very detailed knowledge about the genome and proteome is available simplifying the development of tools, like antibody creation or cloning. A specialty of *Xenopus laevis* is its allotetraploidy and thus it contains two subgenomes (Session et al., 2016).

1.1.1. Prophase I arrest and release

Oocytes arrest in prophase I and await stimulation by MIH produced by surrounding follicle cells upon external or internal stimulus. Although the prophase I arrest is universal, the mechanism underlying the arrest is not. The universal component is the inhibition of MPF activity. MPF or M-phase promoting factor consists of the kinase Cdk1 and cyclin B which need to be activated to induce meiotic maturation. In *Xenopus laevis,* MPF activation is prevented by protein kinase A (PKA) activity in prophase I. High cAMP levels keep PKA active and MPF inhibited (Huchon et al., 1981; Maller & Krebs, 1977). Inhibition of PKA by a heat-stable protein inhibitor led to meiotic resumption without hormone stimulus, while the addition of the catalytic domain of PKA prevented meiotic resumption (Maller & Krebs, 1977). This PKA-sensitive period only lasts until GVBD as the addition of PKA after GVBD does not prevent meiotic resumption (Wang et al., 2006). One direct PKA target is Cdc25, the MPF-activating phosphatase. PKA phosphorylates Cdc25 on S287 which recruits the protein 14-3-3 sequestering Cdc25 away from its substrate (Duckworth et al., 2002). PKA also prevents new synthesis of protein which is essential for meiotic resumption in *Xenopus laevis* while in other organisms like mice or starfish protein synthesis is only necessary for metaphase II arrest but not MPF activation (Jessus et al., 2020). Just recently a link between the known PP2A-B55 inhibitor Arpp19 and PKA was found to be involved in prophase I arrest and meiotic resumption. In 2014, it was published that Arpp19 needs to be phosphorylated on S109 and this is both necessary and sufficient for maintaining prophase I arrest (Dupré et al., 2014). In a follow-up study this phosphorylation was found to be opposed by PP2A-B55, dephosphorylation of Arpp19 then creates a time window after PKA inactivation in which the program for meiotic resumption is further set up (Lemonnier et al., 2021). Further downstream targets and the complete mechanism how PKA prevent meiotic maturation still need to be elucidated.

To induce meiotic maturation, progesterone leads to the inhibition of the adenylate cyclase, followed by a drop in cAMP level and PKA inactivation (Finidori-Lepicard et al., 1981; Mulner et al., 1979; Sadler

& Maller, 1981). In *Xenopus laevis* protein synthesis is then activated and three essential proteins are synthesized, RINGO/Speedy, cyclin B, and Mos. Together these three proteins lead to a first activation of MPF sufficient to turn on a circuit of positive-feedback, the auto-amplification loop, which finally leads to full MPF activity and meiotic resumption. The core of the auto-amplification loop is the transformation of inactive, so-called pre-MPF, into active MPF. For activation, the Cdk1 protein in pre-MPF must be phosphorylated on the T-loop site T161 and dephosphorylated at the inhibitory sites T14/Y15. Activating phosphorylation on T161 is achieved by a constitutively active Cdk-activating-kinase (CAK) (Solomon et al 1992). The removal of the inhibitory phosphorylation (T14/Y15) is highly regulated. Myt1 is the inhibitory kinase while Cdc25 is the activating phosphatase. To trigger the first MPF activation two possible mechanisms were identified. On the one hand, RINGO (rapid inducer of G(2)/M transition in oocytes) can activate Cdk1 by binding to monomeric Cdk1 (Ferby et al., 1999) and is less sensitive to inhibitory phosphorylation on T14/Y15 (Karaiskou et al., 2001). So, RINGO can phosphorylate and inhibit Myt1 and therefore start the transformation of pre-MPF to active MPF (Ruiz et al., 2008). On the other hand, a maybe more important pathway starts with the synthesis of cyclin B1 and B4. In prophase I arrest there is mainly cyclin B2 and B5 bound to around 10 % of available Cdk1 protein (Hochegger et al., 2001). Therefore, newly synthesized cyclin B1 and B4 can directly interact with monomeric Cdk1 and build active cycB/Cdk1 complexes to start the auto-amplification loop. This hypothesis is underlined by data from Gaffré et al. showing that new synthesis of cyclin B results in rapid inactivation of Myt1 (Gaffré et al., 2011). Once a few active Cdk1 complexes are built, the auto-amplification loop induces full MPF activation by phosphorylation and therefore activation of Cdc25, and phosphorylation and therefore inhibition of Myt1 (Booher et al., 1997; Hoffmann et al., 1993; Izumi & Maller, 1993). Cdc25 is only active if fully phosphorylated by Cdk1 and dephosphorylated by PP1 at the above-mentioned S287 site, phosphorylated by PKA (Margolis et al., 2006). On the contrary, Myt1 needs to be hypophosphorylated to be active and is phosphorylated and inactivated upon MPF activation (Mueller et al., 1995). Myt1 and Cdc25 are regulated directly by cycB1/Cdk1 for positive feedback in the auto amplification loop, but cycB/Cdk also indirectly affects these two components by inhibiting the phosphatase PP2A-B55δ, the main Cdk1 opposing phosphatase (Castilho et al., 2009; Mochida et al., 2009; Vigneron et al., 2009) (Fig. 2). CycB/Cdk1 is activating the kinase Gwl (Greatwall) which then phosphorylates and activates the PP2A-B55 inhibitor Arpp19 (Dupré et al., 2013). The inhibition of PP2A-B55δ also results in remaining phosphorylation on Cdc25 and Myt1 which adds a second layer of regulation to the auto-amplification loop, resulting in the creation of a bistable switch, allowing MPF activation to be irreversible after a certain threshold is reached (Mochida et al., 2016; Pomerening et al., 2003; Sha et al., 2003). As Gwl is crucial in inhibiting PP2A-B55 and in the absence of Gwl a very high cycB/Cdk1 level is needed for meiotic resumption scored by GVBD, nowadays Gwl also belongs to the term of MPF (Hara et al., 2012). Therefore, MPF not only described the active

CycB/Cdk1 complex but also the components leading to full cycB/Cdk1 activity, namely cycB/Cdk1 and Gwl (Fig. 2).

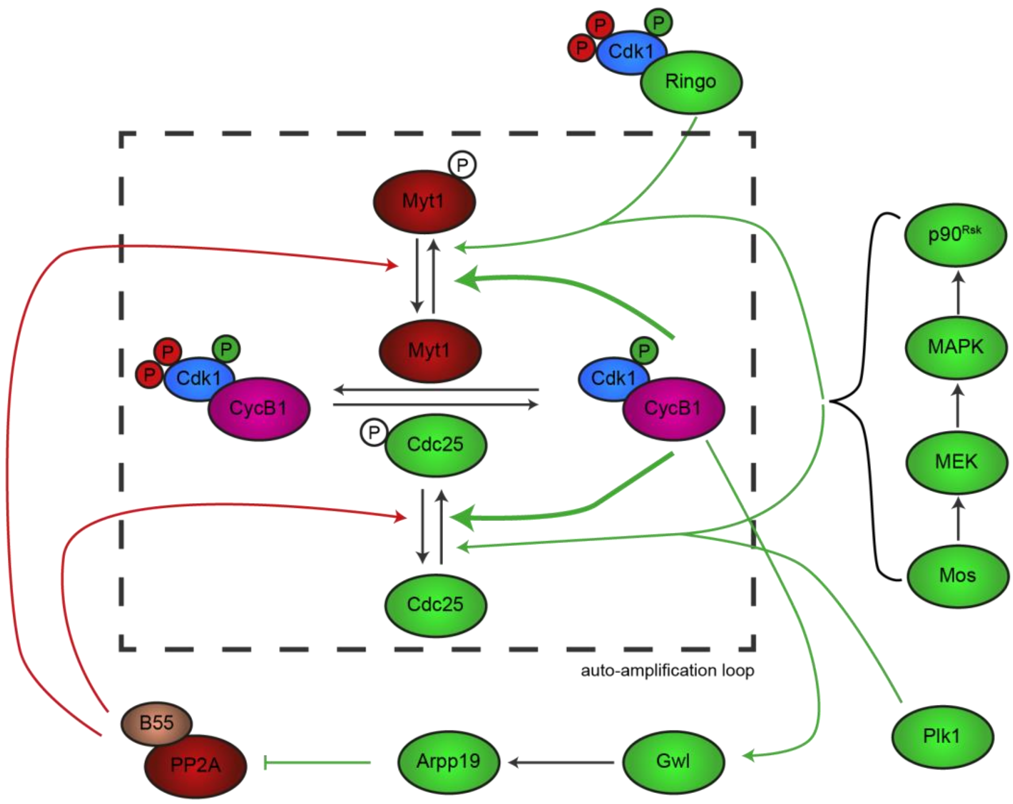

Figure 2: Auto-amplification loop for full MPF activation. For entry into metaphase I, MPF consisting of the cycB1/Cdk1 complex needs to be activated by removing inhibitory phosphorylation by the phosphatase Cdc25. The kinase for the inhibitory phosphorylation on MPF is Myt1. CycB1/Cdk1 itself can activate Cdc25 and inhibit Myt1. These proteins form the core of the auto-amplification loop (box in the middle). Several other kinases and proteins can support the auto-amplification loop (green proteins surrounding the box, with green arrows to the respective pathways they support). PP2A-B55 is the phosphatase opposing many cycB1/Cdk1 phosphorylation events and directly inhibits the activating phosphatase and activates the inhibitory kinase (red arrows). Proteins in red inhibit MPF activity while protein in green support MPF activity.

The third important protein synthesized after progesterone stimulation is Mos (N. Sagata et al., 1988). Mos is the upstream kinase of the MEK-MAPK-p90^{Rsk} cascade (Posada et al., 1993). Indeed, it was shown that injection of Mos was sufficient to induce meiotic maturation (Haccard et al., 1995) but its synthesis is not necessary for meiotic maturation induced by progesterone stimulation (Dupré et al., 2002). In fact, cycB/Cdk activity is necessary for full Mos activation as it stabilizes Mos by phosphorylation (Castro et al., 2001). Activation of Mos and its downstream effector p90^{Rsk} rather occurs simultaneously with MPF activation and supports stable MPF activity by phosphorylation of Myt1 (Mueller et al., 1995; Palmer et al., 1998; Peter et al., 2002). Furthermore, MAPK also directly phosphorylates Cdc25, increasing its phosphatase activity (Wang et al., 2007). Therefore, preventing Mos synthesis in *Xenopus laevis* did not result in prevention of meiotic maturation but delayed GVBD

(Dupré et al., 2002). Although Mos is dispensable for MPF activation followed by GVBD, the Mos kinase pathway is indispensable for establishment of a direct entry into meiosis II after anaphase I, which is followed by the metaphase II arrest (see below). Beside metaphase II arrest, Mos-MAPK pathway also is involved in correct metaphase I spindle assembly and asymmetric meiotic division (Avilov et al., 2023; Lefebvre et al., 2002; Terret et al., 2003).

Another kinase important for the auto-amplification loop and MPF stabilization is the polo-like kinase 1 (Plk1 or Plx1 in *Xenopus laevis*). Plk1 phosphorylates and therefore activates Cdc25 in vitro and in vivo (Abrieu et al., 1998; Qian et al., 1999) adding a further element for stable MPF activity upon meiotic resumption (Fig. 2). Importantly, Plk1 activity depends on Cdk1 activity, as the activating Plk1 kinase (Plkk1) is activated by Cdk1, as well as on the activity of aurora kinase A and its binding partner Bora (Archambault & Carmena, 2012; Blengini et al., 2021; Karaïskou et al., 1999).

After MPF activation meiosis I takes place by establishment of GVBD, a metaphase spindle, separation of homologous chromosomes, and PB extrusion.

1.1.2. Meiosis I to Meiosis II transition

After the separation of homologous chromosomes and the first polar body extrusion, oocytes directly continue entering meiosis II without an intervening S-phase. No DNA duplication is allowed between MI and MII, which is ensured by direct activation of cycB/Cdk1 after meiosis I exit (Furuno et al., 1994). Upon meiotic exit the E3 ligase APC/C in complex with its co-activator Cdc20 gets activated and ubiquitinates cycB, leading to the degradation of cycB via the proteasome. To achieve direct cycB/Cdk activation, the new synthesis of cycB1 and cycB4 and simultaneous Mos-MAPK activity are necessary. Mos-MAPK activates $p90^{Rsk}$ deactivating Myt1 and indirectly activating Cdc25 through Plk1 (Gross et al., 2000; Okano-Uchida et al., 2003; Palmer et al., 1998). Through Myt1 inhibition and Cdc25 activation, cycB/Cdk1 activity is ensured, and oocytes can enter MII. Another factor essential for entering MII is the accumulation of the F-box protein XErp1 (in *Xenopus laevis*) or Emi2 (in other vertebrates). Without synthesis of XErp1, oocytes would directly enter interphase (mechanistic details see next section) (Ohe et al., 2007). XErp1, the Mos-MAPK pathway together with fast activation of cycB/Cdk1 activity ensure entry into metaphase II. Here oocytes are arrested and await fertilization. The metaphase arrest in meiosis is maintained by CSF activity which is deactivated upon sperm entry and the accompanying Ca^{2+} increase.

1.1.3. CSF-arrest/Metaphase II arrest

The cytostatic factor (CSF) arrest or metaphase II arrest occurs in the metaphase of meiosis II in most vertebrates. Masui and Markert first described CSF when they injected cytoplasm from metaphase II arrested oocytes into one of two blastomeres of two-cell embryos and this blastomere stopped dividing and arrested in metaphase (Masui & Markert, 1971). These unknown factors in the cytoplasm were named cytostatic factors and have to fulfil three criteria: appear during oocyte maturation and peak in MII, cause metaphase II arrest by injection into blastomere, and must be inactivated by an increase in Ca^{2+} level which occurs upon fertilisation. Mos was first identified as part of the CSF because Mos injection into a blastomere of two-cell embryos also led to a metaphase arrest (Noriyuki Sagata et al., 1988). On a biochemical level, metaphase arrest is maintained with a constant high level of cycB/Cdk1 activity only possible by inhibiting the E3-ligase anaphase-promoting complex/cyclosome with its co-activator Cdc20 (APC/C^{Cdc20}). The E3-ligase leads to the destruction of cyclin B and securin and therefore initiates anaphase (Gerhart et al., 1984). The link between Mos and APC/C was discovered by Schmidt et al. when they identified XErp1 as an inhibitor of the APC/C necessary for MII arrest in *Xenopus laevis* (Schmidt et al., 2005). The mechanism was then further investigated also in other vertebrates, where the XErp1 orthologue was named Emi2 (Shoji et al., 2006). XErp1 can be divided into an N- and C-terminal part. The C-terminal part of XErp1 is able to inhibit the APC/C^{Cdc20} by direct interaction via its D-box, ZBR region, and RL tail (Ohe et al., 2010; Shoji et al., 2014; Tang et al., 2010). Furthermore, the C-terminal part of XErp1 also interferes with the interaction of APC/C and its ubiquitin-conjugating enzymes (Sako et al., 2014). The N-terminal part consists of many regulatory elements like two Cdk1 phosphorylation clusters (M- and N-cluster), in each there are four minimal consensus Cdk1 sites (SP or TP), two phosphodegron motifs (DSG and DSA) recognized by the E3-ligase $SCF^{\beta\text{-TRCP}}$, as well as calcium/calmodulin-dependent kinase II (CaMKII), $p90^{Rsk}$ and Plx1 phosphorylation sites (Fig. 3). As the several phosphorylation sites in XErp1 suggest, XErp1 is highly regulated through phosphorylation during CSF-arrest to ensure proper inhibition of APC/C^{Cdc20}.

The main goal during CSF-arrest is to keep a constantly high activity level of cycB/Cdk1, typical for a metaphase state, without inducing anaphase onset. To achieve the constant level of cycB/Cdk1 activity, XErp1 serves as a sensor for its activity. XErp1 is constantly phosphorylated at S335 and T336 by $p90^{Rsk}$, creating a docking site for PP2A-B56 and thus preventing any phosphorylation in the C-terminal and N-terminal of XErp1 ensuring APC/C^{Cdc20} interaction (Inoue et al., 2007; Isoda et al., 2011; Nishiyama et al., 2007; J. Q. Wu et al., 2007). Rising cycB/Cdk1 activity leads to increased phosphorylation of the N-terminal SP and TP sites, namely the M-cluster sites (S43, S73, T97, S157) and the N-cluster sites (S213, T239, T252, T267) which can no longer be opposed by PP2A-B56 (Isoda et al., 2011). The phosphorylation of these sites results on the one hand in further C-terminal phosphorylation of XErp1 by cycB/Cdk1 and casein kinase 1 (CK1) and on the other hand in Plx1 recruitment. C-terminal phosphorylation of XErp1 by cycB/Cdk1 on T545, T551, and S641 and by CK1 on S644 is interfering with XErp1 binding to APC/C^{Cdc20}, which leads to its activation (Isoda et al., 2011; Q. Wu et al., 2007). The N-terminal phosphorylation also recruits Plx1, which can then create its own docking site by phosphorylation of T195 and T170 (T195 is stronger phosphorylated). Full Plx1 recruitment results in phosphorylation of the two degron motifs DSG/DSA, followed by $SCF^{\beta\text{-TRCP}}$

mediated degradation (Isoda et al., 2011) (Fig. 3). Both pathways, induced by cycB/Cdk1-dependent N-terminal phosphorylation, lead to activation of the APC/C^{Cdc20} either by interfering with the interaction between XErp1 and the APC/C or by targeting XErp1 for degradation. APC/C^{Cdc20} activation will result in partial cyclin B ubiquitination and degradation. The drop in cyclin B level allows the dephosphorylation of XErp1 by PP2A-B56 to prevail over the phosphorylation by cycB/Cdk1 and thus results in stabilization of XErp1 in a state that actively inhibits APC/C^{Cdc20} (Isoda et al., 2011). This balance of phosphorylation and dephosphorylation creates a variable regulatory circuit for APC/C^{Cdc20} activity as high cycB/Cdk1 activity shifts the balance to highly phosphorylated XErp1, which can no longer inhibit the APC/C^{Cdc20} leading to the ubiquitination and degradation of cycB. The degradation of cycB results in a drop of Cdk1 activity, which leads to dephosphorylation of XErp1 by PP2A-B56 and thus in restored APC/C^{Cdc20} inhibition. This mechanism of partial and especially slow XErp1 degradation followed by partial cycB degradation mediates the metaphase II arrest and ensures that cycB is not completely degraded which prevents anaphase onset.

1.1.4. Fertilisation

Upon fertilisation, oocytes must efficiently transit from metaphase to anaphase and to this end, fast XErp1 degradation and APC/C^{Cdc20} activation have to occur. Fertilisation leads to a transient increase in the cytoplasmic Ca^{2+} concentration activating the CaMKII (Busa & Nuccitelli, 1985; Lorca et al., 1993). CaMKII directly phosphorylates XErp1 at residue T195, leading to recruitment of Plx1 followed by phosphorylation of the degron motifs DSG/DSA (Inoue et al., 2007; Rauh et al., 2005; J. Q. Wu et al., 2007) (Fig. 3). To add a further level of robustness to the Ca^{2+} dependent release from metaphase II the phosphatase Calcineurin (CaN) is activated (Mochida & Hunt, 2007). Calcineurin dephosphorylates XErp1 at S335 and T336, which results in loss of PP2A-B56 binding to XErp1 and stronger destabilization of XErp1 (Heim et al., 2018) (Fig. 3). Beside acting directly on XErp1, Calcineurin dephosphorylates Cdc20 on inhibitory sites facilitating binding of Cdc20 to the APC/C forming the activated APC/C^{Cdc20} (Heim et al., 2018; Mochida & Hunt, 2007). Both pathways support robust anaphase onset either by supporting the CaMK-induced degradation of XErp1 or mediating strong APC/C^{Cdc20} activity to induce the degradation of cycB and further APC/C^{Cdc20} substrates.

Upon fertilisation, meiosis II finishes and the now fertilized egg continues with mitotic cell cycles to further develop into an embryo.

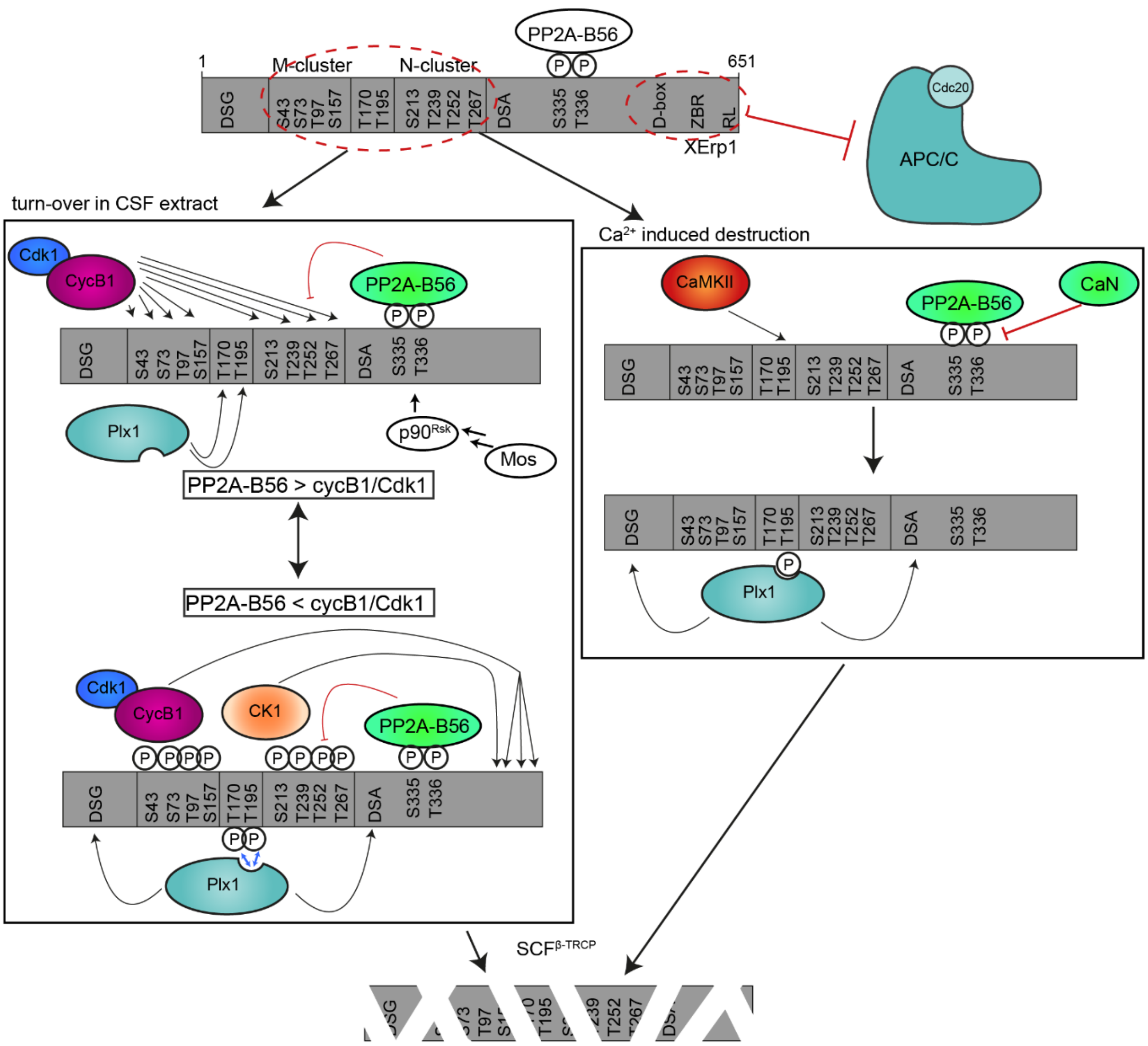

Figure 3: XErp1 scheme and degradation pathways. XErp1 contains several motifs and phosphorylation sites (upper scheme). The N-terminal domain contains regulatory sites (M- and N-cluster) as well as the two degron motifs DSG and DSA. The C-terminal part contains several domains important for APC/C^{Cdc20} interaction and inhibition, the D-box, the ZBR region, and the RL-tail. Two modes of XErp1 degradation can occur, the slow turn-over in CSF-arrested oocytes to keep constant levels of cycB1/Cdk1 activity (left panel) and the fast degradation upon fertilisation (right panel). Degradation of XErp1 is induced because the E3 ligase SCF$^{\beta\text{-TRCP}}$ recognizes the degron motifs phosphorylated by Plx1.

1.2. Cyclins in general

The first cyclin was described by Tim Hunt's group as a protein oscillating with each cell division in sea urchins (Evans et al., 1983). All genes designated to the family of cyclins comprise one common feature, the cyclin box. The cyclin box is a tertiary structure of five α-helices spanning a region of around 100 amino acids mediating the typical binding of cyclins to Cdk, which is a family of proline-directed serine/threonine kinases (Gibson et al., 1994; Noble et al., 1997; Wood & Endicott, 2018). Although the tertiary structure is very conserved, the primary amino acid sequence varies between different cyclins. Around 30 genes translated into cyclins are known to date in humans, which can be subdivided into three groups (Quandt et al., 2020). One group includes the canonical cyclins, which are the typical oscillating cyclins with major functions in the cell cycle, preferentially interacting with the Cdk1 family (Cdk1, Cdk2 and Cdk3) and Cdk4 family (Cdk4 and Cdk6). The second group comprises transcriptional cyclins and is involved in RNA polymerase regulation. The third group includes all atypical cyclins which are not well characterized yet so that the corresponding Cdk-partner is often unidentified (Quandt et al., 2020).

The canonical cyclins, lately also called “cell cycle cyclins”, can roughly be allocated to specific cell cycle phases where they fulfil their function (Martínez-Alonso & Malumbres, 2020). The attribution of cyclins to cell cycle phases is not as strict as depicted in Fig. 4. According to their presence and function in the different cell-cycle phases, canonical cyclins can be subdivided into four classes named G1-cyclins, G1/S-cyclins, S-cyclins, and M-cyclins (Morgan, 2007).

In the following the mitotic cell cycle will be described with the respective cyclin-Cdk complexes relevant for the specific phases (Fig. 4). This brief summary will focus on the mechanism in mammalian cells to give a broad overview of the categories of canonical cyclins in the cell cycle. The cyclins can differ in other species, like *Xenopus laevis* and yeast.

The mitotic cell cycle starts with G1-cyclins like cyclin C and cyclin D. CycC builds a complex either with Cdk3, Cdk8 or Cdk19 (Martínez-Alonso & Malumbres, 2020; Tassan et al., 1995). CycC/Cdk3 leads to G0 exit while cycC/Cdk8 interact with the Mediator complex and therefore regulates cell cycle entry (Knuesel et al., 2009; Ren & Rollins, 2004). CycD in complex with Cdk4 or Cdk6 build a link between growth signal and cell cycle entry by phosphorylation of the retinoblastoma protein (Rb) followed by release of the transcription factor E2F and transcription of E2F responsive genes (Malumbres & Barbacid, 2001; Weinberg, 1995; Yang et al., 2006). E-type cyclins are an example of proteins expressed due to cycD/Cdk activity. The next step in the cell cycle is DNA replication where all genes are duplicated for later cell division. For correct replication, the G1/S-cyclin, cycE, together with Cdk2 induces the assembly of the replication complex while the S-phase cyclin, cycA, in complex with Cdk2 regulates the start of DNA synthesis and simultaneously prevents the assembly of further replication complexes (Coverley et al., 2002). In frog embryos, cycE/Cdk2 starts DNA replication and cycA/Cdk activity is mainly responsible for mitosis (Jackson et al., 1995). A-type cyclins also induce chromosome condensation and entry into mitosis by indirectly activating Plk1 which activates the phosphatase Cdc25 and therefore cycB/Cdk1, the main driver of mitosis (M-phase) as well as meiosis (Gheghiani et al., 2017; Vigneron et al., 2018). The B-type cyclins or M-cyclins are finally taking over and regulate the M-phase in which correct chromosome alignment and segregation are orchestrated. At the transition from S to M-phase, DNA synthesis must be terminated as entry into mitosis with unfinished duplicated DNA can lead to DNA breaks, fatal for the developing daughter cells.

Degradation of S- and M-cyclins is achieved via ubiquitination via the E3-ligase APC/C depending on a destruction box (Glotzer et al., 1991). CycD is accumulating during the cell cycle again in G2 so that after the completion of mitosis a further cell cycle round can start (Yang et al., 2006).

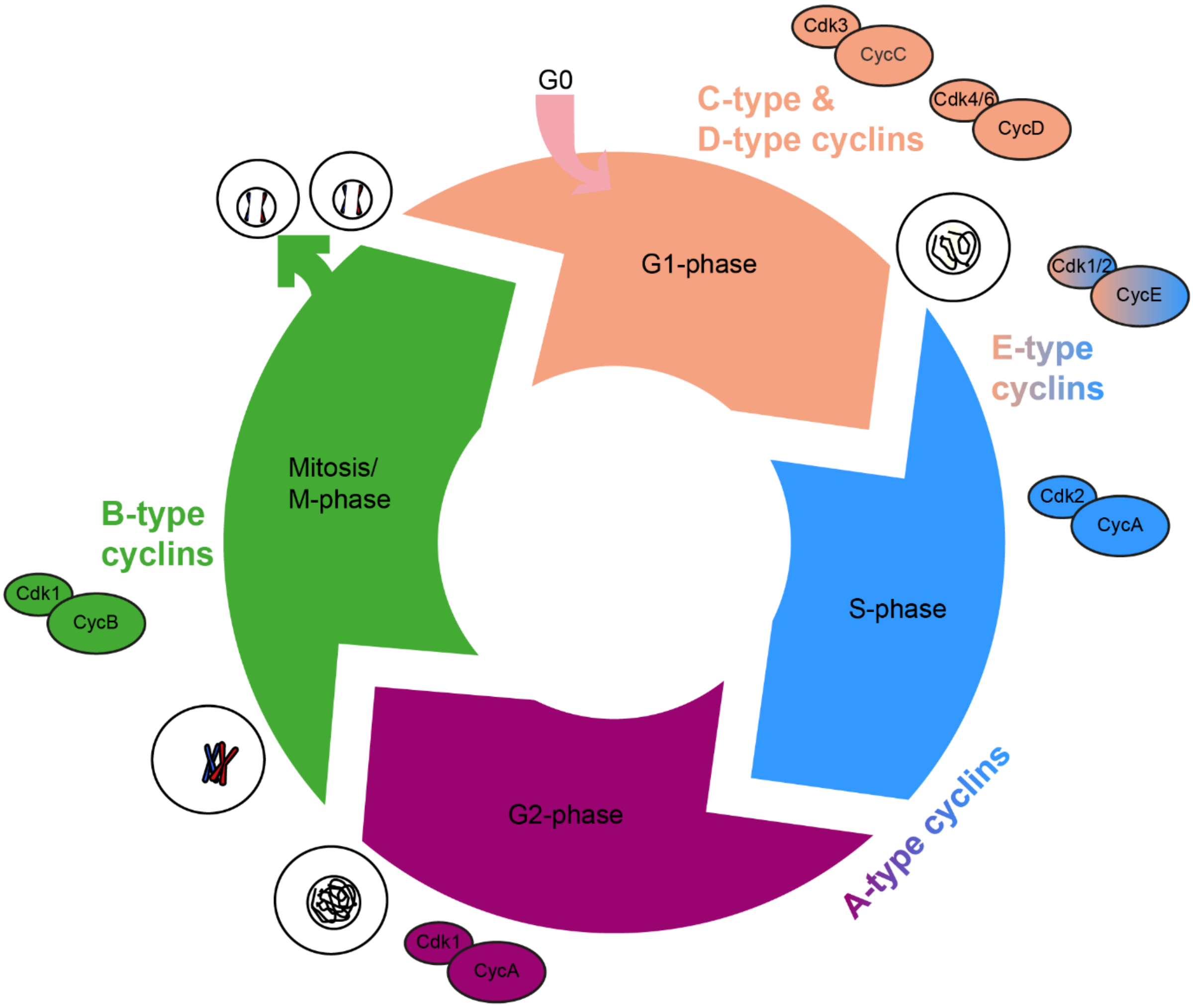

Figure 4: Cell cycle phase with corresponding cyclins. Scheme of the mitotic cell cycle phase with the corresponding cyclins involved in each phase. The assignment of cyclins to cell cycle phases is a simplification and only serves as a crude overview.

1.2.1. Cyclins regulating Cdks

This variety of cell cycle cyclins was raising the question of how these cyclins help their associated Cdk partner to phosphorylate their specific substrates as they are often also associated with the same Cdk. Especially in budding yeast and other unicellular organisms only one Cdk, more specific Cdk1, is present throughout the cell cycle (Morgan, 2007). Also in mice with knock-out of Cdk2, Cdk3, Cdk4 and Cdk4, embryos develop until embryonic day 12.5 and therefore Cdk1 is sufficient to drive the mammalian cell cycle (Santamaría et al., 2007). If Cdk1 alone is sufficient to set up a functional cell cycle, the diversity in substrate recognition has to be established by the cyclins. In mice, it was found that especially the early cyclins cannot compensate for the loss of A- or B-type cyclins, while the G1 and G1/S-cyclins are dispensable (Satyanarayana & Kaldis, 2009). Research in fission yeast reveals that one cyclin is enough to lead cells through the mitotic and meiotic cell cycle (Coudreuse & Nurse, 2010; Fisher & Nurse, 1996; Gutiérrez-Escribano & Nurse, 2015). These findings end up in a quantitative model as a basic fundament driving the cell cycle (Stern & Nurse, 1996; Uhlmann et al., 2011). This model describes cell cycle progression through an increase of Cdk activity from phase to phase, with a moderate increase leading to entry into S-phase and a further increase in Cdk activity initiating mitosis. Investigation of the capability of cyclins to activate Cdk1 towards the well-known substrate H1 revealed that the activity of Cdk1 increases from complex with G1/S cyclins to complex with M-phase cyclins in yeast, supporting the quantitative model (Kõivomägi, Valk, Venta, Iofik, Lepiku, Morgan, et al., 2011). The quantitative model can be extended by considering phosphatase activity, which lead to odered substrate phosphorylation during the cell cycle, explained in the following (Uhlmann et al., 2011). Each substrate can be defined as both a Cdk and phosphatase target. Considering constant phosphatase activity, a substrate which is a "bad" Cdk target will be only highly phosphorylated when Cdk activity is at its maximum, namely in M-phase, as the phosphatase will keep the substrate dephosphorylated at the cell cycle phases with low Cdk activity. A substrate which is a "good" Cdk target will be already highly phosphorylated in G1/S-phase, because the counteracting phosphatase is outcompeted by strong Cdk substrate phosphorylation. This can ensure different phosphorylation statuses of different proteins in different cell cycle phases, leading to the variety of events occurring in the distinct cell cycle phases.

Cyclins regulate Cdk activity toward substrates in two ways and therefore define "good" or "bad" substrates. On the one hand, cyclins influence the overall activity of Cdk toward a generic substrate, as shown in yeast and mention above (Kõivomägi, Valk, Venta, Iofik, Lepiku, Morgan, et al., 2011). On the other hand, there are specific docking-motifs of different cyclins. Each cyclin type has a different short-linear motif (SLiM) that it preferentially binds to: G1-cyclin/Cdk complexes to leucine and proline-rich motifs, S-cyclin/Cdk to RxL motifs and M-cyclin/Cdk to LxF motifs (Bandyopadhyay et al., 2020; Bhaduri & Pryciak, 2011; Kõivomägi, Valk, Venta, Iofik, Lepiku, Morgan, et al., 2011; Loog & Morgan, 2005; Örd et al., 2019). In 2021, a second docking motif, NLxxxL, for S-cyclins was identified to even more efficiently lead to the docking of S-cyclins to their respective substrate (Faustova et al., 2021). The binding of these docking motifs is mediated by a hydrophobic patch region in A and B-type cyclins (Örd et al., 2019), especially in A-type cyclins the amino acids in and near the MRAIL region bind to the RxL motif (Brown et al., 2007; Cheng et al., 2006). Cdk possesses activity toward the minimal consensus motif S/TP, with proline in position +1, but consists of higher activity toward the sequence S/TPxR/K, with a positively charged arginine or lysine in +3 position (Brown et al., 2015; Brown et al., 1999). The docking motifs can increase the activity of the respective cyclin/Cdk complex toward a substrate with minimal consensus sites or even nonconventional sites by optimal positioning of the Cdk1 active site (Brown et al., 2015; Faustova et al., 2021; Valk et al., 2023). In a recent study, they speculate on a "consensus sequence switch" between cyclin A and cyclin B, with cyclin A together with Cdk phosphorylating rather non-consensus sites while cyclin B together with Cdk rather phosphorylate consensus sites (Al-Rawi et al., 2023). Cyclins are therefore the main driver of substrate specificity in the cyclin/Cdk complex.

1.2.2. Cyclin B3

An understudied cyclin is cyclin B3 (cycB3), which was first identified in chicken and characterized as a B-type cyclin with features corresponding to an A-type cyclin (Gallant & Nigg, 1994). Like cycA, cycB3 accumulates in the nucleus but the expression pattern resembles the pattern of cycB (Gallant & Nigg, 1994). From sequence comparison, cycB3 is slightly more similar to cycB1 or cycB2 but in several conserved residues distinguish from both B- and A-type cyclins. Interestingly cycB3 is the only B-type cyclin whose translation does not increase upon hormone stimulus in meiosis of *Xenopus* oocytes (Piqué et al., 2008). The sequence of cycB3 is quite conserved throughout metazoans but increased during evolution in the mammalian lineage by 3-fold, which leads to an extended N-terminal region probably mediating interactions with different proteins (Lozano et al., 2012). CycB3 fulfils its cellular function in complex with either Cdk1, Cdk2 or both, depending on the studies (Jacobs et al., 1998; Nguyen et al., 2002). In *Drosophila*, cycB3 was characterized to be crucial, especially for female fertility, but not for mitotic cell division (Jacobs et al., 1998). These findings were confirmed in higher eukaryotes like mice (Nguyen et al., 2002). Just recently a direct link between cycB3 and the APC/C was revealed in *Drosophila*. Here, cycB3 mediates correct anaphase onset in mitosis and meiosis by directly promoting APC/C phosphorylation (Garrido et al., 2020). In *C. elegans*, lack of cycB3 leads to metaphase II arrest and failure in sister chromatid separation (van der Voet et al., 2009). CycB3 also promotes several mitotic events in early embryos of *C. elegans* for example pronuclear migration, chromosome condensation, centrosome maturation, spindle pole separation, and chromosome congression (Deyter et al., 2010). These mitotic effects are partially based on the indirect activation of dynein by cycB3.

CycB3 is indispensable for female meiosis because the lack of cycB3 leads to metaphase I arrest in *Drosophila* as well as mouse oocytes (Karasu et al., 2019; Li et al., 2019; Zhang et al., 2015). The phenotype of MI-arrested oocytes could be rescued in mouse oocytes by the expression of cycB3 from different species, which suggests a conserved mechanism for the function of cycB3 in female meiosis (Karasu et al., 2019). Also, untimely expression of cycB3 in metaphase II led to defects in meiosis as CSF-arrest is released prematurely in the absence of a fertilisation signal (Meng et al., 2020). So both, correct presence, as well as timely regulated degradation of cycB3, are crucial for an undisturbed meiosis. In line with these findings, reports revealed cases of recurrent pregnancy loss or miscarriages in humans caused by either cycB3 mutations or truncations (Fatemi et al., 2021; Rezaei et al., 2021) underlining the necessity to understand cycB3's function. Together with the Wassmann group, we were able to unravel the function of cycB3 in meiotic maturation (Bouftas et al., 2022). To prevent premature MI arrest, cycB3/Cdk primes XErp1 for degradation by direct phosphorylation at T97. Probable, this then leads to recruitment of Plx1, as degradation of XErp1 mediates by cycB3 depends on Plx1 activity. A potential docking site for Plx1 is T170 either phosphorylated directly by Plx1 or cycB3/Cdk1. Plx1 binding finally leads to phosphorylation of the two degron motifs, DSG and DSA, and rapid XErp1 degradation (Bouftas et al., 2022). As XErp1 synthesis starts after entry into MI (Tung et al., 2007), CycB3 deletion in oocytes leads to premature accumulation of XErp1 already at the end of metaphase I, which results in an untimely metaphase I arrest. Therefore, cycB3/Cdk activity in meiosis I is absolutely necessary for correct meiotic maturation. CycB1/Cdk1 is also active in meiosis I but cannot rescue cycB3 depletion (Karasu et al., 2019). In Bouftas et al., we showed that this might be due to the fact that T97, the major phosphorylation site for cycB3/Cdk mediated degradation, is a better cycB3/Cdk1 site than cycB1/Cdk1 site. Why XErp1 is a worse substrate for cycB1/Cdk1 compared to cycB3/Cdk1 is still unanswered. Investigation of the intrinsic special features of cycB3 compared to cycB1 might answer this question. Besides, the exact mechanism of Plk1 recruitment to XErp1 as well as the subsequent Plk1-dependent phosphorylation need to be addressed.

1.2.3. Phosphate-binding pocket of B-type cyclins

In 2021, the Boland group first described a conserved phosphate-binding pocket in B-type cyclins (Yu et al., 2021). The pocket consists of three positively charged amino acids: arginine, histidine and lysine (Fig. 5). Theses residues build a positively charged groove at the surface of cycB1, which in able cycB1 to bind phosphorylated residues of specific proteins. In the case of cycB1, it can bind separase at pre-phosphorylated Serine 1126. This phosphate-binding pocket dependent binding contributes to the inhibition of separase, as binding results in a state of mutual inhibition of separase and cycB1/Cdk1 (Yu et al., 2021). In yeast, the Clb2 phosphate-binding pocket was identified in the regulation of the transcriptional co-activator Ndd1 (Asfaha et al., 2022). The phosphate-binding pocket might be a mechanism to regulate multisite phosphorylation events, yet further targets must be identified.

The phosphate-binding pocket is highly conserved in all B-type cyclins throughout different species, except for cycB3, and completely absent in A-type cyclins (Fig. 5). Interestingly, in the region of the phosphate-binding pocket, cycB3 is more similar to cycB1 than to cycA. Therefore, cycB3 might possess a putative phosphate-binding pocket with different substrate partners compared to the other B-type cyclins. The putative cycB3 phosphate-binding pocket consists of an arginine, leucine and arginine instead of an arginine, histidine and lysine, which build the phosphate-binding pocket in both cycB1 and cycB2 (conserved in *Xenopus* cycB4 and B5) (Fig. 5).

cycB1 *X. laevis*	266-PLPLHFLRRASKIG	...	QHSLAKYLMELVMVDYD-301	identified phosphate-binding pocket
cycB1 *H. sapiens*	300-PLPLHFLRRASKIG	...	QHTLAKYLMELTMLDYD-335	
cycB1 *M. musculus*	297-PLPLHFLRRASKVG	...	QHTLAKYLMELSMLDYD-332	
cycB2 *X. laevis*	261-PLPLHFLRRASKSC	...	QHTLAKYLMELTLIDYE-296	
cycB2 *H. sapiens*	264-PLPLHFLRRASKAG	...	QHTLAKYLMELTLIDYD-299	
cycB2 *M. musculus*	264-PLPLHFLRRASKAG	...	QHTLAKYLMELTLVDYD-299	
cycB3 *X. laevis*	289-PVPYRFLRRFAKCA	...	TLTLARYICELTLQEYD-324	putative phosphate-binding pocket
cycB3 *H. sapiens*	1259-PIAYHFLRRYARCI	...	TLTLSRYICEMTLQEYH-1294	
cycB3 *M. musculus*	1265-PTAYNFLRRYASCI	...	TLTLSRFICEMTLQEYE-1300	
cycB3 *G. gallus*	276-PIPYRFLRRFAKCA	...	TLTLARFVCEMTLQEYD-311	
cycB3 *D. rerio*	272-PVPYRFLRRYAKCV	...	TLTLARFICELSLLEME-307	
cycB3 *C. elegans*	243-PLSYRYLRRFGRVC	...	TLTMGRFILETSLMVYE-278	
cycB3 *D. melanogaster*	435-PLSYRFLRRYARCA	...	TLTLARYILELSLMDYA-470	
cycB3 *C. hemispherica*	382-PVPYRFLRRFARVT	...	ILTLSRYLLELSLHESK-417	
cycA2 *X. laevis*	291-PTILQYLNQYFQIH	...	VESLSMFLGELSLVDAD-326	no phosphate-binding pocket
cycA2 *H. sapiens*	309-PTVNQFLTQYFLHQ	...	VESLAMFLGELSLIDAD-345	
cycA2 *M. musculus*	299-PTVNQFLTQYFLHL	...	VESLAMFLGELSLIDAD-335	

Figure 5: Alignment of phosphate-binding pocket from B-type cyclins. CycB1 and cycB2 aligned from different species at the region of the phosphate-binding pocket. Cyclin B3 aligned from different species at the region of the corresponding residues from cyclin B1 and B2. Marked in grey are all residues matching in the different B-type cyclins, while different but positively charged amino acids were marked in light grey in cycB1 and cycB2. In the alignment of cyclin A2 from different species, residues at the position of the phosphate-binding pocket in B-type cyclins were marked in red.

1.2.4. Cyclin-dependent kinase subunit – Cks

The Cks protein family consist of small proteins of about 9-18 kDa, first identified in yeast, where suc1/Cks1 suppressed defective alleles of *cdc2* (Cdk1 in higher eukaryotes) in fission yeast and interacted with Cdc28 (Cdk1 in higher eukaryotes) in budding yeast (Pines, 1996). Therefore, the original name was Cdc28 kinase subunit 1. In higher eukaryotes, two Cks proteins were identified termed Cks1 and Cks2 in humans. In *Xenopus laevis*, the first Cks protein described by Patra and Dunphy was named p9 and corresponds to the Cks2 family according to sequence alignment (Patra & Dunphy, 1996). Experiments performed with Cks2-depleted meiotic and mitotic extracts revealed a crucial role of Cks2 in the cell cycle. Cks2 is involved in activating MPF by affecting Myt1, Wee1 and Cdc25 phosphorylation, and in regulating mitotic exit by affecting APC/C phosphorylation (Patra & Dunphy, 1998; Patra et al., 1999). Due to these functions, Cks is indispensable for both mitotic entry and meiotic/mitotic exit. The underlying mechanism of Cks-mediated phosphorylation is the recruitment of the cyclin/Cdk1 complex to pre-phosphorylated substrates via a cationic pocket (Bourne et al., 1996). The binding of Cks to Cdk-primed phosphorylation sites leads to enhanced association of cyclin/Cdk with its substrate resulting in multisite phosphorylation (Kõivomägi et al., 2013). For example, the APC/C is phosphorylated at the APC3 (Cdc27) subunit, which recruits cycB/Cdk1 via Cks2 concluding in phosphorylation of APC1 and consequently in activation of APC/C^{Cdc20} (Fujimitsu et al., 2016; Rudner & Murray, 2000). Data from experiments in yeast showed that the recruitment mechanism of cycB/Cdk/Cks complex requires a pre-phosphorylated threonine which then lead to phosphorylation of a downstream site with in a specific distance from the priming site (Kõivomägi et al., 2013; McGrath et al., 2013). Therefore, the Cks protein serves as a phosphate adaptor in complex with cycB1 and Cdk1 (McGrath et al., 2013). Especially the phosphorylation of non-conventional Cdk sites received more and more attention in recent years and their role in cell cycle regulation seems yet to be underestimated. In a study in mice embryonic stem cells, a large number of non-conventional Cdk sites were identified (Michowski et al., 2020). Furthermore, in a study combining fixed cell assay with proteomic, 49 % of enriched Cks1 phosphorylation sites were sites without proline in the +1 position (Al-Rawi et al., 2023). Cks1 adds a further layer of substrate specificity for multisite phosphorylation also for non-conventional Cdk1 sites, in addition to the docking motifs and the phosphate-binding pocket of the cyclins (Örd et al., 2019; Valk et al., 2023) (Fig. 6).

Interestingly, Cks2 plays a crucial role in meiosis while Cks1 is dispensable for meiosis, as Cks1 knock-out mice are fertile while Cks2 knock-out mice are sterile arresting in metaphase I of meiosis (Spruck et al., 2003; Spruck et al., 2001). Furthermore, in mice, it was found that Cks1 needs to be absent during germ line development as it failed when Cks1 is expressed under the promoter of Cks2 (Ellederova et al., 2019). For other organisms, it is not clear if Cks2 is the major Cks protein in meiosis although the data of p9 depletion in CSF extract hint toward a strong dependency on Cks2 for correct meiotic exit in *Xenopus* oocytes.

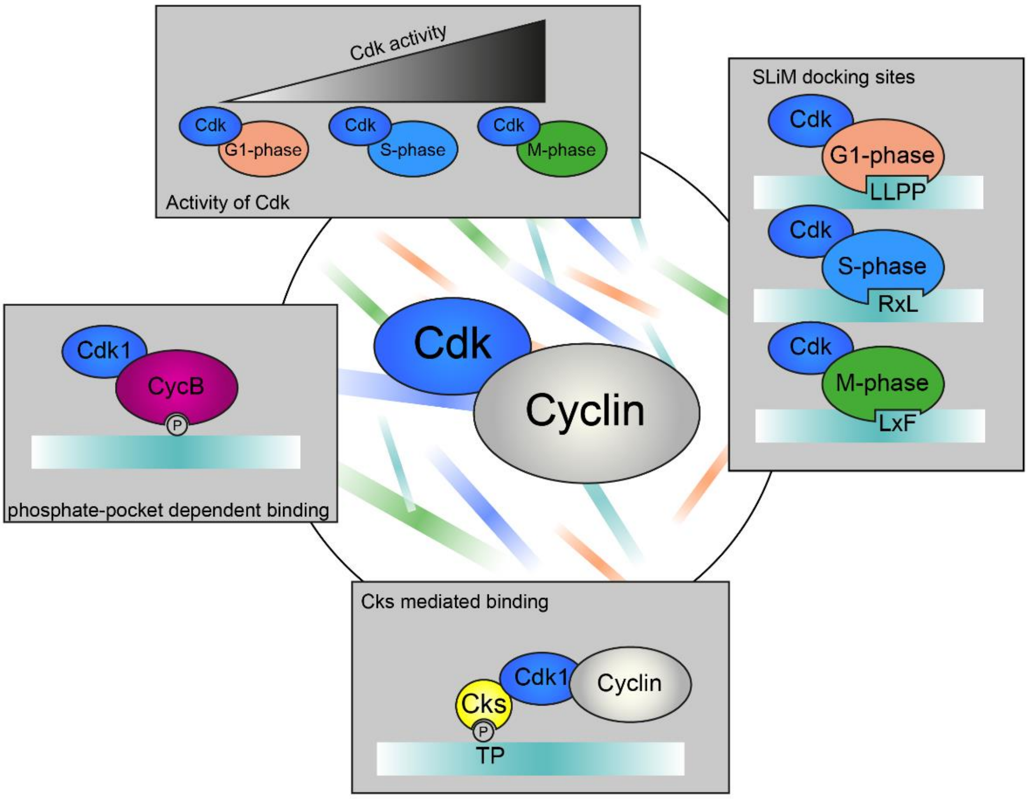

Figure 6: Mechanisms to modulate Cdk substrate phosphorylation. Summary of four different mechanisms of how cyclins or Cks mediate Cdk substrate phosphorylation. Especially when it comes to multisite phosphorylation, several of the strategies are used to fully phosphorylate specific substrates.

1.3. Aim of the study

This thesis aims to investigate the role of the putative phosphate-binding pocket of cycB3 for its role in meiotic maturation. Further, I want to investigate the potential binding partner for the putative phosphate-binding pocket and compare the putative phosphate-pocket of cycB3 with the phosphate-binding pocket of the other B-type cyclins. I also try to narrow down the position and number of the phosphorylation sites in XErp1 necessary for cycB3-mediated degradation and the influence of these sites on Plx1 binding.

2. Results

2.1. CycB3^{TEM} fails to reconstitute cycB3^{WT} function

CycB3 function is essential for oocyte development by preventing premature metaphase arrest in meiosis I as in the absence of cycB3 the APC/C inhibitor, XErp1, would already accumulate in meiosis I (Bouftas et al., 2022). Furthermore, Yu et al. described in a recent publication a conserved phosphate-binding pocket in B-type cyclins (Yu et al., 2021). In cycB3 the residues corresponding to the cycB1 phosphate-binding pocket are present but altered from RHK in cycB1 to RLR in cycB3 (Fig. 5). So, the questions arise if these residues also build a functional phosphate-binding pocket in cycB3 and if they fulfil a specific function during meiosis. To address this, the putative cycB3 wild-type (WT) phosphate-binding pocket (RLR) was mutated to the corresponding residues of the human and mouse A-type cyclins (TEM) (Fig. 5). These residues in A-type cyclins do not build a functional phosphate-binding pocket. This mutated cycB3, termed cycB3^{TEM}, was then tested for its capability to rescue metaphase I arrest in cycB3-depleted oocytes. CycB3 was depleted from stage VI oocytes using the Trim-Away approach by injection of an antibody against a short N-terminal peptide of cycB3 together with Flag-TRIM21 mRNA. For rescue experiments, N-terminal Flag-tag cycB3 constructs lacking a part of the recognition site of the antibody, the first 15 amino acids (cycB3$^{\Delta15}$), were co-injected as in vitro transcribed and translated proteins (IVTs), either Flag-cycB3$^{WT\Delta15}$ or the phosphate-binding pocket-mutant Flag-cycB3$^{TEM\Delta15}$. After incubation for 14-16 h at 19 °C, oocytes samples for western blot were taken. Endogenous cycB3 was depleted and the levels of ectopic Flag-cycB3 were comparable to endogenous cycB3 levels in the control depletion background (injection of Ctrl antibody) (Fig. 7A). To test if cycB3^{TEM} can fulfil the biological function of cycB3^{WT}, oocytes were treated with progesterone to induce meiotic maturation. Four hours after GVBD, the cell cycle state of the oocytes was analysed by fixation and staining for tubulin and DNA to investigate spindle and DNA morphology. As the timing of meiotic resumption varied between different oocytes, all oocytes containing only a spindle were counted as in metaphase of meiosis I (MI) arrested oocytes and all oocytes containing either an anaphase I spindle with clearly separated chromosomes, a metaphase II spindle and polar-body (PB) or only a PB were counted as post-MI (Fig. 7C). In control depleted oocytes, 81 % were post-MI 4 h after GVBD while in depletion background 95 % arrested in meiosis I. Re-expression of cycB3$^{WT\Delta15}$ rescued meiotic resumption with 73 % oocytes post-MI while re-expression of the mutant cycB3$^{TEM\Delta15}$ resulted in 99 % of metaphase I arrested oocytes, resembling the phenotype of cycB3-depleted oocytes (Fig. 7B/C). Next, I analysed meiotic maturation via western blot, as expected, there was no difference in MPF activation or GVBD timing as the signal of inhibitory phosphorylation of Cdk1 (on T14/Y15 detected by ppCdk) disappeared after around 5-6 h and the percentage of oocytes with GVBD

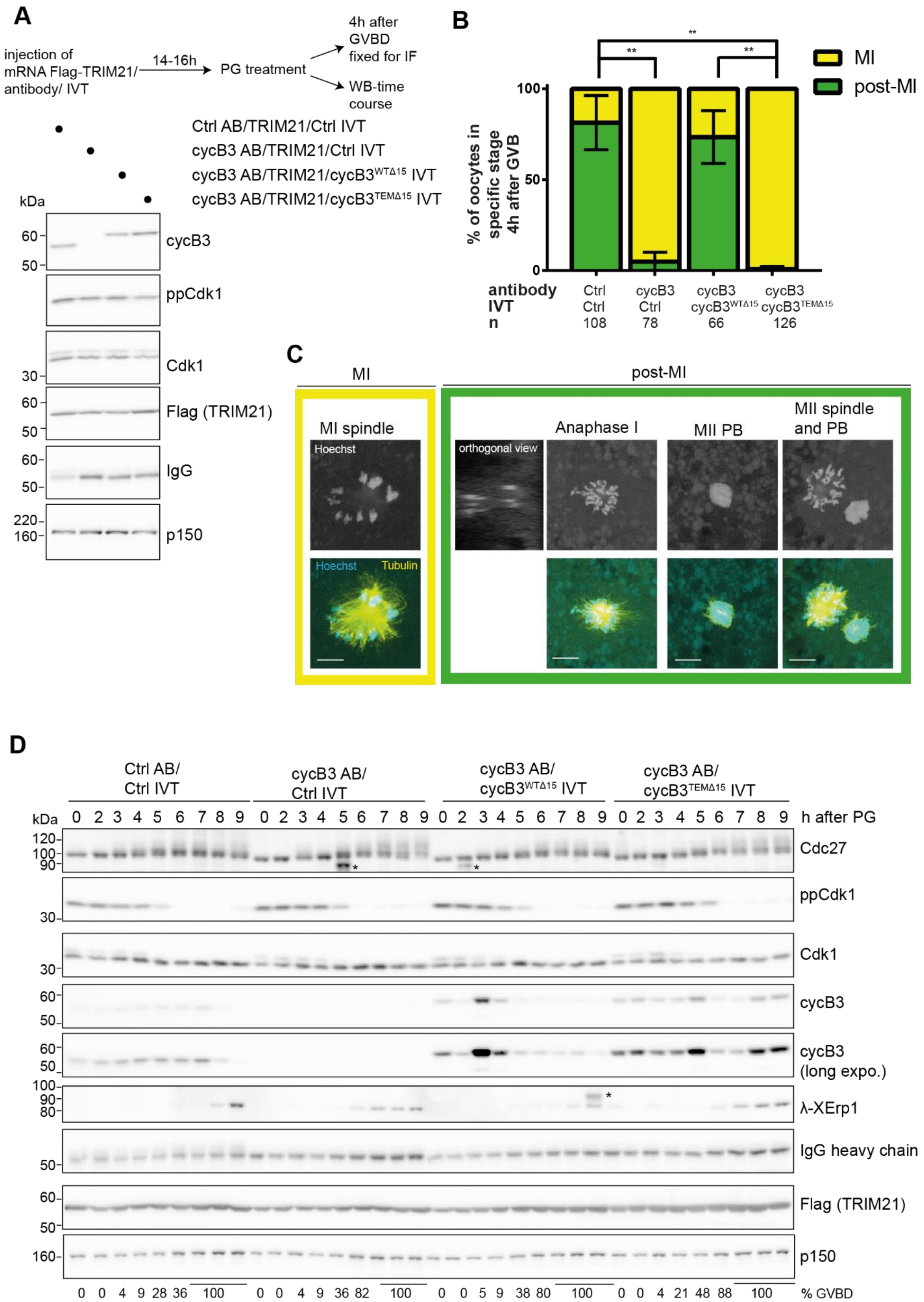

(Figure legend on next page)

Figure 7: CycB3^{TEM} fails to rescue metaphase I arrest in cycB3-depleted oocytes. (A) Upper part: Scheme of experimental procedure for cycB3 depletion by Trim-Away and rescue with either cycB3$^{WT\Delta 15}$ or cycB3$^{TEM\Delta 15}$. Stage VI oocytes were injected with Flag-Trim21 mRNA, antibody against N-terminal cycB3 peptide or control IgG (Ctrl AB) and either Ctrl, Flag-cycB3$^{WT\Delta 15}$ or Flag-cycB3$^{TEM\Delta 15}$ IVT. Oocytes were treated with progesterone (PG) and either fixed 4 h after GVBD for IF (B/C) or taken at specific time points for western blot (WB) (D). Lower part: western blot of samples from cycB3 depletion and rescue oocytes before PG treatment. For western blot, a cycB3 antibody created against N-terminal cycB3 (aa1-110) was used to detect rescue constructs lacking the first 15 amino acids. **(B)** Quantification of oocytes fixed 4 h after GVBD and stained with Hoechst and FITC-labelled anti-tubulin antibody. Number of experiments: n= 4, the total number of oocytes imaged is indicated under each condition. An unpaired two-sided t-test with Welch's correction was performed, ** = $p < 0.01$ **(C)** Representative images from (B). The scale bar is 10 µm. **(D)** Western blot time course of oocytes upon cycB3 depletion and rescue. Samples were taken at indicated time points and analysed via SDS-PAGE and western blot. Part of the samples were treated with λ-phosphatase to reduce phosphorylation-dependent mobility shifts (labelled with λ). Quantification of the relative number of oocytes which underwent GVBD (in %) is written below. One representative experiment from six biological replicates is shown. Asterisk marks unspecific bands. P150 serves as loading control.

was similar in all four conditions (Fig. 7D, GVBD quantification below blots). The APC/C subunit Cdc27 was phosphorylated after GVBD (between 6-7 h) and started to be dephosphorylated at the end of the time course in the control depletion and in the cycB3$^{WT\Delta 15}$ rescue condition, indicating release from metaphase I (Fig. 7D). In the cycB3 depletion background as well as in the cycB3$^{TEM\Delta 15}$ rescue no Cdc27 dephosphorylation took place, indicating metaphase I arrest in these conditions. CycB3 depletion leads to premature accumulation of XErp1 in meiosis I (Bouftas et al., 2022), which was observed in the depletion background and interestingly also in the cycB3 $^{TEM\Delta 15}$ rescue condition, indicating that cycB3 deficient in the phosphate-binding pocket cannot rescue cycB3^{WT} in meiosis I (Fig. 7D). CycB3$^{TEM\Delta 15}$ was incapable to prevent XErp1 accumulation which explains metaphase I arrest of these oocytes.

In a previous study, it was shown, that ectopic cycB3 leads to release from metaphase II and therefore needs to be degraded upon meiosis II entry (Bouftas et al., 2022; Meng et al., 2020). In *Xenopus laevis,* extract from metaphase II arrested oocytes can be easily obtained and manipulated by either the addition of proteins or depletion of proteins, being a beneficial tool to elucidate biochemical processes. Therefore, I wanted to investigate if ectopically added phosphate-binding pocket deficient cycB3 behaves differently from cycB3^{WT} in CSF extract, to utilize CSF extract for a detailed investigation of the effect of the phosphate-binding pocket in follow-up experiments. To address, whether cycB3^{TEM} was able to release metaphase II arrested CSF extract by inducing XErp1 degradation, cycB3^{TEM} IVT was added to CSF-extract. In agreement with previous findings, the addition of cycB3^{WT} to CSF extract led to rapid phosphorylation and degradation of XErp1, followed by cycB2 degradation and Cdc27 dephosphorylation, both markers for release from metaphase II (Fig. 8) (Bouftas et al., 2022; Meng et al., 2020). On the contrary, cycB3^{TEM} addition did not alter the state of the CSF extract, which maintained stable XErp1 and cycB2 levels and highly phosphorylated Cdc27 throughout the time course (Fig. 8). Addition of the inactive form of cycB3, cycB3^{MRL}, deficient in Cdk1 binding (Bouftas et al., 2022), had the same effect like cycB3^{TEM} (Fig. 8). Taken together, CycB3^{TEM} showed failure to mimic the phenotype of cycB3^{WT}, both in rescuing metaphase I arrest in cycB3 depleted oocytes and release of metaphase II arrested CSF extract.

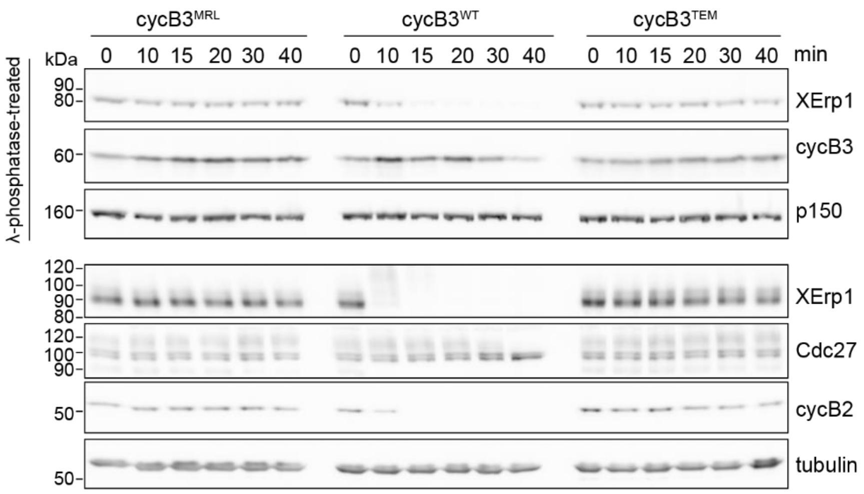

Figure 8: CycB3^{TEM} fails to induce metaphase II release. N-terminally Flag-tagged IVT of cycB3^{MRL}, cycB3^{WT} or cycB3^{TEM} was added to the CSF extract. Samples were taken at indicated time points and analysed via SDS-PAGE and western blot. Samples were either λ-phosphatase treated or left untreated to compare both XErp1 levels and phosphorylation status. Tubulin and p150 serve as loading control. One representative experiment from three biological replicates is shown.

2.2. CycB3^{TEM} is impaired in multisite phosphorylation of XErp1

One explanation why cycB3^{TEM} failed in rescuing cycB3 depletion and releasing metaphase II arrest could be that, compared to cycB3^{WT}, it is less efficient in activating Cdk1, which would result in decreased phosphorylation and degradation of XErp1. To examine the influence of the phosphate-binding pocket mutations on general activation of Cdk1, the activity of co-purified Strep-cycB3^{WT} or Strep-cycB3^{TEM} in complex with His-Cdk1^{AFE} against its reference substrate Histone H1 was measured in an in vitro kinase assay. In Cdk1^{AFE} both inhibitory phosphorylation sites were mutated to alanine (T14A) and phenylalanine (Y15F) (Solomon et al., 1992), respectively, and the activating phosphorylation site was mutated to the phosphomimetic amino acid glutamate (T161E) (Ducommun et al., 1991). The H1 kinase assay revealed the same activity for cycB3^{WT}/Cdk1^{AFE} and cycB3^{TEM}/Cdk1^{AFE} showing that cycB3^{TEM} is not compromised in activating Cdk1 (Fig. 9A/B). This kinase activity clearly depended on Cdk1 activity as cycB3^{WT}/Cdk1^{AFE} failed to phosphorylate H1 in the presence of the Cdk1 inhibitor Flavopiridol (FL) (Fig. 9A). As general Cdk1 activity is not influenced by the phosphate-binding pocket mutation, it was investigated whether specific substrate phosphorylation was altered. Therefore, the in vitro activity of the different cycB3/Cdk1 complexes (cycB3^{WT} or cycB3^{TEM}) toward N-terminal XErp1 constructs (1-350 aa) was tested, as cycB3/Cdk1 phosphorylation of XErp1 is essential for preventing premature metaphase arrest in meiosis I. The first 350 amino acids of XErp1 contain all relevant features for XErp1 degradation in CSF extract released by the addition of cycB3^{WT} as the timing of XErp$^{1\text{-}350}$ degradation was the same as for full-length XErp1 (master's thesis of Patrick Wehrle). The XErp1$^{1\text{-}350}$ constructs were purified with an N-terminal MBP-tag (for solubility reasons) and a C-terminal His-tag from bacteria. The activity of recombinant cycB3^{WT}/Cdk1^{AFE} towards individual XErp1 phosphorylation sites was examined with different XErp1 constructs that were wild-type for only one

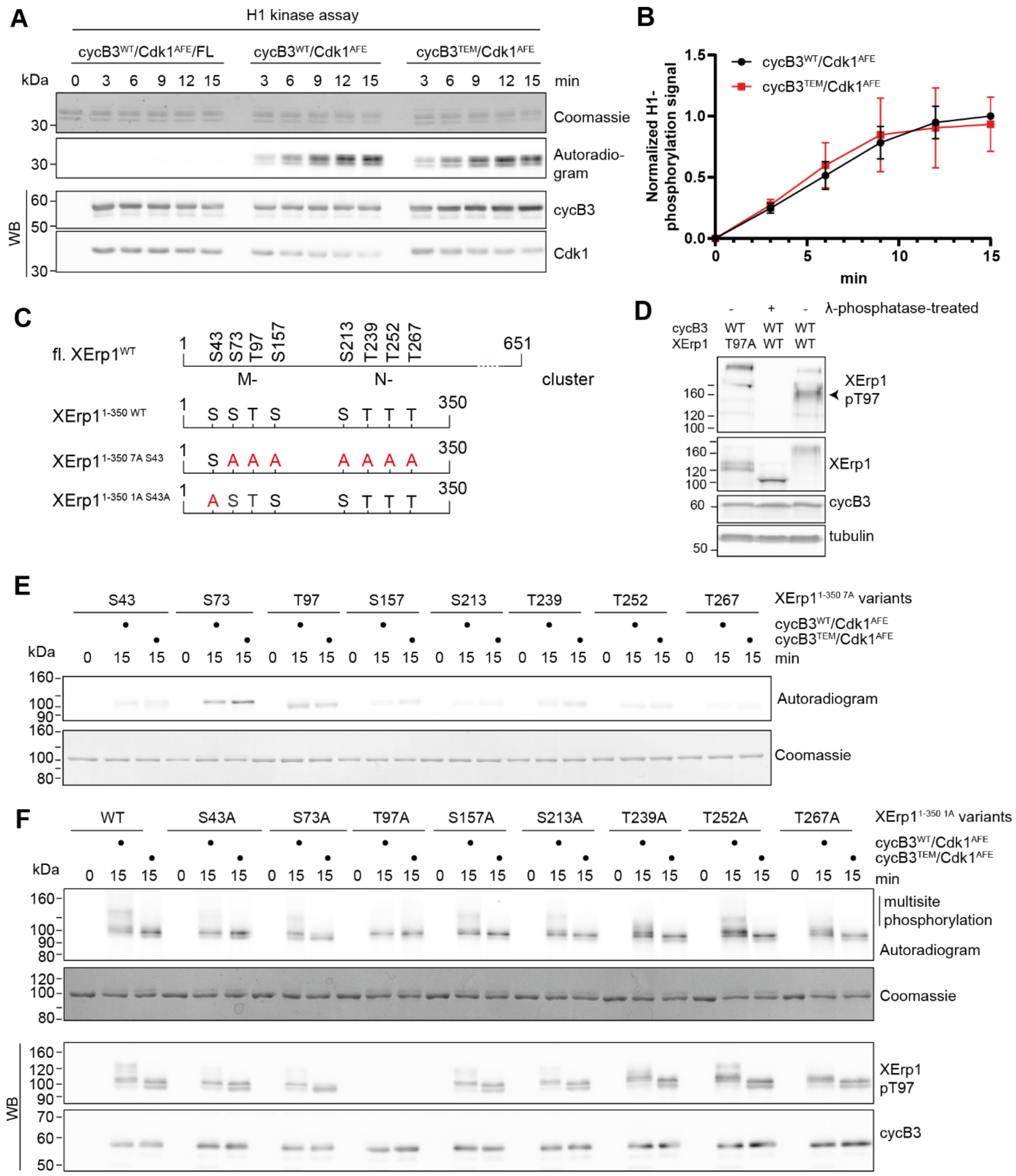

Figure 9: CycB3^{TEM} is impaired in multisite phosphorylation of XErp1. (A) In vitro H1 kinase assay with [γ-^{33}P]ATP. CycB3^{WT}/Cdk1^{AFE} treated with 10 µM Flavopiridol (FL), cycB3^{WT}/Cdk1^{AFE} and cycB3^{TEM}/Cdk1^{AFE} were tested. Samples were taken at indicated time points and analysed via SDS-PAGE. Coomassie shows equal distribution of H1, the autoradiogram is the read-out for substrate phosphorylation, while cycB3 and Cdk1 were detected via western blot. **(B)** Quantification of experiment in (A) and three further replicates. The H1 signal in the radiogram was quantified and normalized to the Cdk1 signal from the 3 min time point. Mean ± SD is shown. **(C)** Scheme of XErp1 constructs used in the following experiments. **(D)** CSF extract was arrested by the addition of MG262 and C-terminal XErp1. Flag-cycB3^{WT} IVT and respective XErp1$^{DSG/DSA}$ mutants IVT were added to CSF extract and incubated for 45 min. Samples were taken and either directly diluted in Lämmli buffer or λ-phosphatase treated. Arrowhead denoted specific XErp1 pT97 signal. One representative experiment from two biological replicates is shown. Tubulin serves as a loading control. **(E)** In vitro kinase assay with [γ-^{33}P]ATP with cycB3^{WT}/Cdk1^{AFE} or cycB3^{TEM}/Cdk1^{AFE} and XErp1^{7A} constructs as substrates. Samples were taken at indicated time points and analysed via SDS-PAGE. Coomassie shows an equal distribution of XErp1 and the autoradiogram serves as a read-out for the

phosphorylation signal. **(F)** In vitro kinase assay with [γ-^{33}P]ATP with cycB3^{WT}/Cdk1^{AFE} or cycB3^{TEM}/Cdk1^{AFE} and XErp1^{1A} constructs as substrate. Samples were taken at indicated time points and analysed via SDS-PAGE. Coomassie shows an equal distribution of XErp1 and the autoradiogram serves as a read-out for the phosphorylation signal. CycB3 was detected via western blot as well as pT97 signal. One representative experiment from two independent technical replicates is shown.

out of eight described Cdk1 sites in the M- or N-cluster (XErp1^{7A}) (Isoda et al., 2011)(Fig. 9C). These constructs allowed the analysis of the kinase activity against specific sites without effects corresponding to previous phosphorylation of other residues that could serve as recruitment sites. Again, cycB3^{TEM}/Cdk1^{AFE} showed no difference in phosphorylation efficiency towards the different XErp1$^{1\text{-}350\ 7A}$ sites compared to cycB3^{WT}/Cdk1^{AFE} (Fig. 9E). Interestingly, cycB3^{WT}/Cdk1^{AFE} and cycB3^{TEM}/Cdk1^{AFE} phosphorylated residues S73 and T97 in the M-cluster more efficiently than the other sites (Fig. 9E). T97 was shown to be one of the main phosphorylation sites for cycB3-mediated degradation of XErp1 (Bouftas et al., 2022). CycB3^{TEM}/Cdk1^{AFE} was able to phosphorylate this site with the same efficiency then cycB3^{WT}/Cdk1^{AFE}, revealing no alteration in Cdk1 activation toward single sites in XErp1. As the phosphate-binding pocket mutant might be impaired in binding to these single sites, multisite phosphorylation on XErp1 by cycB3/Cdk1 was addressed next. To evaluate, if mutation of the phosphate-binding pocket influenced multisite phosphorylation of XErp1, XErp1$^{1\text{-}350\ 1A}$ constructs were created. These XErp1 constructs contained seven wild-type Cdk1 phosphorylation sites in the M- and N-cluster and only one site was mutated to alanine. First of all, XErp1$^{1\text{-}350\ WT}$, containing all eight phosphorylation sites were phosphorylated by both cycB3^{WT}/Cdk1^{AFE} and cycB3^{TEM}/Cdk1^{AFE} (Fig. 9F). CycB3^{WT}/Cdk1^{AFE} strongly phosphorylated XErp1$^{1\text{-}350\ WT}$ at several sites, indicated by an upward smear in the autoradiogram. Phosphorylation of proteins leads to an increase in their negative charge influencing their separation in SDS-PAGE, with strong multisite phosphorylation leading to retardation and diffuse smeary signal of higher molecular weight in the case of XErp1. The phosphorylation signal (autoradiogram) in the case of XErp1$^{1\text{-}350\ WT}$ phosphorylated by cycB3^{TEM}/Cdk1^{AFE} was from less molecular weight and no upward smear was visible instead strong distinct bands with lower molecular weight were detected in the autoradiogram (Fig. 9F). Comparing the phosphorylation signal on XErp1$^{1\text{-}350\ WT}$ by cycB3^{WT}/Cdk1^{AFE} and cycB3^{TEM}/Cdk1^{AFE}, therefore showed strong multisite phosphorylation of XErp1 in case of cycB3^{WT}/Cdk1^{AFE} and strong but single sites phosphorylation in case of cycB3^{TEM}/Cdk1^{AFE} (Fig. 9F). This multisite phosphorylation, apparent through an upward smear, induced by cycB3^{WT}/Cdk1^{AFE} disappeared when T97 was mutated to alanine (XErp1$^{1\text{-}350\ T97A}$). Furthermore, this was the only condition with the same phosphorylation pattern for cycB3^{WT} and cycB3^{TEM} (Fig. 9F). This strongly suggests that T97 phosphorylation by cycB3/Cdk1 and its subsequent recruitment via cycB3's phosphate-binding pocket is a prerequisite for phosphorylation of several other sites. The residual phosphorylation signal with the XErp1$^{1\text{-}350\ T97A}$ was probably S73 phosphorylation as this site was independently phosphorylated in the kinase assay with XErp1$^{1\text{-}350\ 7A}$ constructs and was therefore phosphate-binding pocket independent (Fig. 9E). To verify if T97 phosphorylation was presence in all other XErp1$^{1\text{-}350\ 1A}$ constructs, we raised an antibody against pT97 (phosphorylated T97) by immunization of rabbits with pT97-peptide. The obtained sera were purified against pT97 and non-phosphorylated peptide and tested in CSF extract to verify substrate specificity (Fig. 9D). Detection of the kinase assay samples revealed pT97 signal in all phosphorylation conditions except for XErp1$^{1\text{-}350\ T97A}$ as well as in all detected bands and smear in each condition, resembling the autoradiogram pattern (Fig. 9F). This underlines the assumption of pT97 binding as the primary step in multisite phosphorylation of XErp1 by cycB3/Cdk1. In summary, the XErp1$^{1\text{-}350}$ kinase assays showed that CycB3^{TEM}/Cdk1^{AFE} was not impaired in single site substrate phosphorylation but failed in multisite phosphorylation of XErp1$^{1\text{-}350}$.

2.3. Phosphate-binding pocket dependent interaction of cycB3 and XErp1

The failure of cycB3^{TEM}/Cdk1^{AFE} to mediate XErp1 multisite phosphorylation might result from the lack of binding to phosphorylated T97, as the potential phosphate-binding pocket is mutated to a non-functioning cycA-like pocket. Impaired binding might then lead to less phosphorylation of downstream phosphorylation sites, resulting in deficient multisite phosphorylation. To test this hypothesis, Flag-cycB3 immunoprecipitation (IP) from CSF extract was performed and beads for co-IP of XErp1 were analysed. CSF extract would be released by the addition of cycB3^{WT} (Fig. 8, Bouftas et al. 2022). To prevent the release of CSF extract from metaphase II due to the degradation of XErp1 induced by the addition of ectopic cycB3 (Bouftas et al. 2022), the extract was supplemented with the proteasome inhibitor MG262 and non-degradable and non-phosphorylatable C-terminal Myc-XErp1 (aa 491-651) IVT. In addition, ectopic XErp1 constructs with mutated degron motifs (XErp1$^{DSG/DSA}$) were used to exclude any side effects from the destabilisation of XErp1 by cycB3^{WT}. Immunoprecipitation of IVT of cycB3^{WT} and cycB3^{TEM} from CSF extract via their Flag-tag led to co-immunoprecipitation of Cdk1 and Cks2 in similar levels in both cases (Fig. 10A). The Cks2 levels strongly varied between experiments, with less Cks2 bound to cycB3^{TEM} in further replicates (data not shown), which will be addressed below. XErp1$^{DSG/DSA\ WT}$, on the contrary, was only present in the cycB3^{WT} IP and completely absent in the cycB3^{TEM} IP condition (Fig. 10A). This interaction of XErp1 with cycB3^{WT} depended on T97 phosphorylation as a non-phosphorylatable T97 XErp1 mutant (XErp1$^{DSG/DSA\ T97A}$) was not co-precipitated with cycB3^{WT} (Fig. 10A). This finding was underlined by an experiment performed with pT97-peptides. SulfoLink^{TM} beads coupled covalently to a peptide corresponding to XErp1 amino acid 90 to 104 either phosphorylated or non-phosphorylated at T97 were incubated with CSF extract supplemented with cycB3^{WT}, cycB3^{TEM} or cycB3^{MRL}. Only beads coupled to pT97-peptide co-precipitated cycB3^{WT} from CSF extract (Fig. 10B, experiment performed by Michael Schäfer). Furthermore, the pocket-mutant and the MRL-mutant of cycB3 did not bind to pT97-peptide. CycB3^{MRL} failed in binding to the pT97 peptide although it contains an intact phosphate-binding pocket according

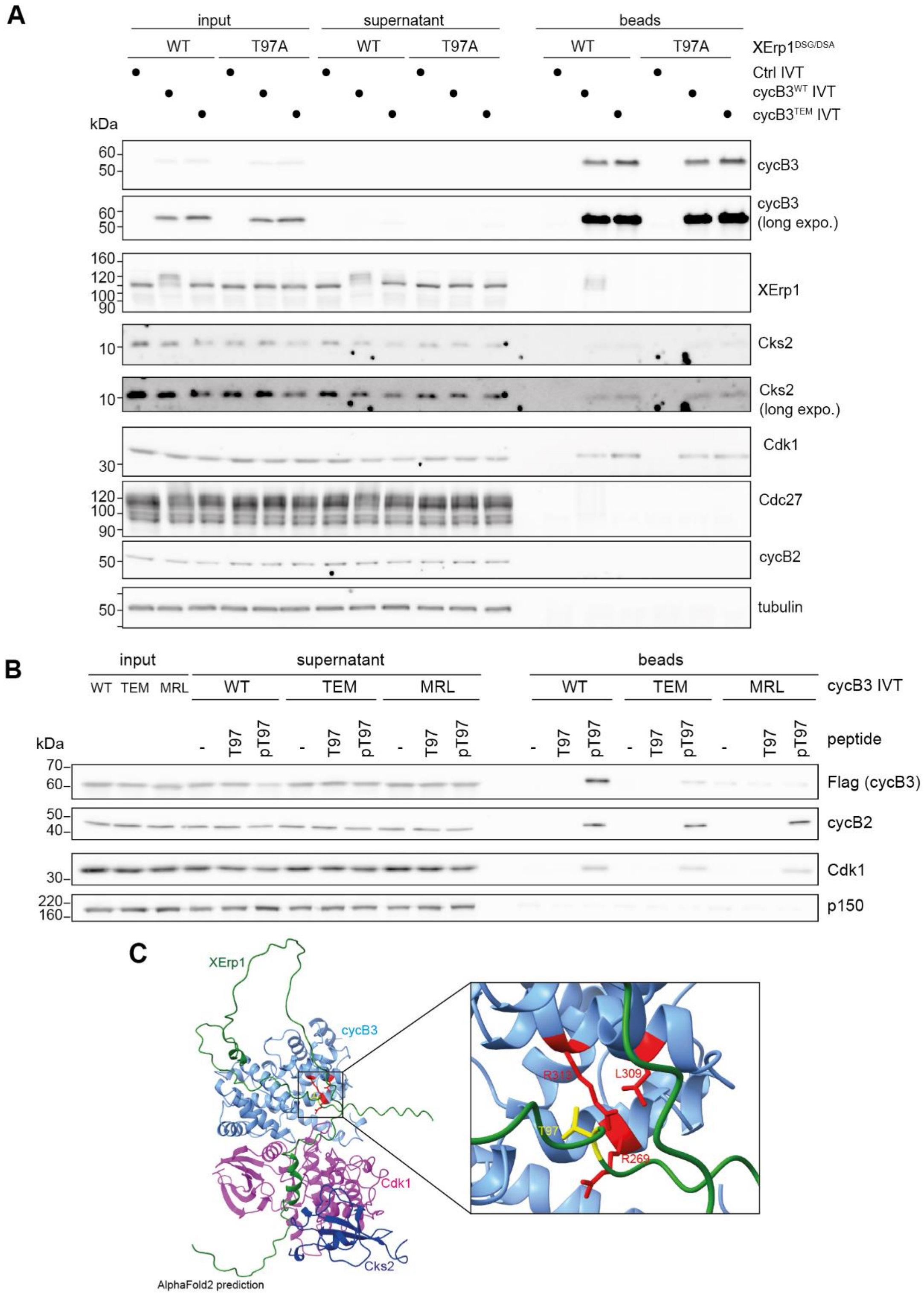

Figure 10: CycB3^{TEM} is deficient in pT97 binding. (A) IP of ectopic Flag-cycB3 IVT from CSF extract arrested in metaphase II by addition of C-terminal XErp1 IVT and proteasome inhibitor MG262. IP reaction was either supplemented with Myc-XErp1$^{DSG/DSA}$ or Myc-XErp1$^{DSG/DSA\ T97A}$. Flag-IP was performed for 30 min at RT. Beads were washed and λ-treated. Samples were taken at indicated time points and analysed via SDS-PAGE and western blot. Tubulin serves as a loading control. One representative experiment from four biological replicates (two performed by Michael Schäfer) is shown. **(B)** Peptides comprising the XErp1 amino acids 90 to 104 either phosphorylated on T97 or not were coupled to SulfoLink beads. Beads were incubated with CSF extract supplemented with IVTs of the indicated Flag-cycB3 variants. Samples were analysed via SDS-PAGE and western blot. One representative experiment from three biological replicates is shown. P150 serves as a loading control. Experiments were performed by Michael Schäfer. **(C)** AlphaFold2 prediction of cycB3/Cdk1/Cks2 with XErp1 aa 1-300. Cks2 in dark blue, Cdk1 in magenta, cycB3 in light blue, and XErp1 in green. N-terminal parts of XErp1 and CycB3 are not depicted for clearer visualization. The right panel shows a close-up of the phosphate-binding pocket of cycB3 (red residues) and XErp1 T97 (yellow) directed towards it.

to the amino acid sequence. Its failure in binding Cdk1 as well as the constant precipitation during purification led to the conclusion that cycB3^{MRL} is probably completely misfolded whereby a functional phosphate-binding pocket is most likely absent. The MRL-condition could be therefore considered a control condition for binding in the absence of cycB3. Interestingly, in all pT97-peptide pull-down conditions Cdk1 and cycB2 were isolated from CSF extract (Fig. 10B). As XErp1 is also a substrate for cycB2/Cdk1 this binding is not unexpected, as cycB2 possesses a phosphate-binding pocket which might also bind to XErp1 (Fig. 5, see below section 2.7.). The co-immunoprecipitation experiments with full-length XErp1 and phosphorylated T97-peptide both show that the postulated cycB3 pocket is indeed a phosphate-binding pocket, necessary for efficient binding of cycB3 to XErp1 at pre-phosphorylated T97.

The finding of phosphate-binding pocket dependent cycB3 binding to pT97 was also strengthened by the predicted structure of cycB3/Cdk1/Cks2 and XErp1 (aa 1-300) with AlphaFold2. More specifically, I wanted to test if T97 was predicted to be in the range of hydrogen-bond to the phosphate-binding pocket of cycB3. Indeed, the AlphaFold2 prediction located T97 into the phosphate-binding pocket of cycB3 (Fig. 10C). The backbone of XErp1 (in the region of Y95 and E96) builds hydrogen-bonds with the phosphate-binding pocket residues R296 and R313 in cycB3. As AlphaFold cannot predict phosphorylated residues, one can only speculate if phosphorylated T97 fits into the phosphate-binding pocket but the prediction with T97 mutated to a phosphomimetic glutamate was also performed. This prediction placed E97 into the phosphate-binding pocket in the same position as the prediction with T97.

The phosphate-binding pocket of cycB3 serves as an intrinsic adaptor of cycB3 and guides Cdk1 toward pre-phosphorylated XErp1, leading to multisite phosphorylation followed by XErp1 degradation. Another known phosphate adaptor of Cdk1 to bind pre-phosphorylated substrates resulting in multisite phosphorylation is Cks (Kõivomägi et al., 2013; Kõivomägi, Valk, Venta, Iofik, Lepiku, Balog, et al., 2011; Kõivomägi, Valk, Venta, Iofik, Lepiku, Morgan, et al., 2011; McGrath et al., 2013). There are two Cks proteins in higher eukaryotes, Cks1 and Cks2. In meiosis, Cks2 is essential as knock-down in mice leads to infertility of both sexes and metaphase I arrest in oocytes (Spruck et al., 2003). Cks1 needs to be absent from oocytes leading to failure in embryonic development if expressed under the promoter of Cks2 in mouse oocytes (Ellederova et al., 2019). I therefore focus on the potential role of Cks2 in cycB3-mediated degradation of XErp1. Immunoprecipitation of cycB3^{WT} versus cycB3^{TEM} from CSF extract showed diverse patterns of Cks2 binding with Cks2 most often stronger bound to cycB3^{WT} (data not shown). To exclude that the varying association to Cks2 is the cause for the difference between cycB3^{WT} and cycB3^{TEM} in mediating degradation of XErp1, Cks2 was depleted from CSF extract to test if this affect cycB3^{WT} dependent XErp1 degradation. Cks2 depleted extract was supplemented with Flag-cycB3^{WT} IVT and XErp1 degradation kinetics were analysed. The timing of XErp1 degradation between the control and Cks2 depleted extract was very similar (Fig. 11). In both conditions, the XErp1 signal disappeared after 20 min but the signal of XErp1 at the 10 min time point was stronger in Cks2 depleted extract compared to control depleted extract (Fig. 11). Besides this minor effect on the XErp1 degradation kinetic, Cks2 depletion led to slower cycB2 degradation (Fig. 11). The slower cycB2 degradation indicated decreased APC/C activity, which correlates with the detectable decrease of hyperphosphorylated Cdc27 signal (Fig. 11). Full activity of APC/C also depends on multisite phosphorylation mediated by cycB/Cdk1/Cks2 complex (Fujimitsu et al., 2016) implicating that loss of Cks2 in CSF extract leads to decrease in Cdc27 phosphorylation. In conclusion, Cks2 depletion from CSF extract via Cks2-IP impaired the phosphorylation level of Cdc27 and cycB2 degradation but did not influence XErp1 degradation mediated by cycB3. These findings strengthen the hypothesis that the phosphate-binding pocket in cycB3 is the main phosphate adaptor for XErp1 multisite phosphorylation.

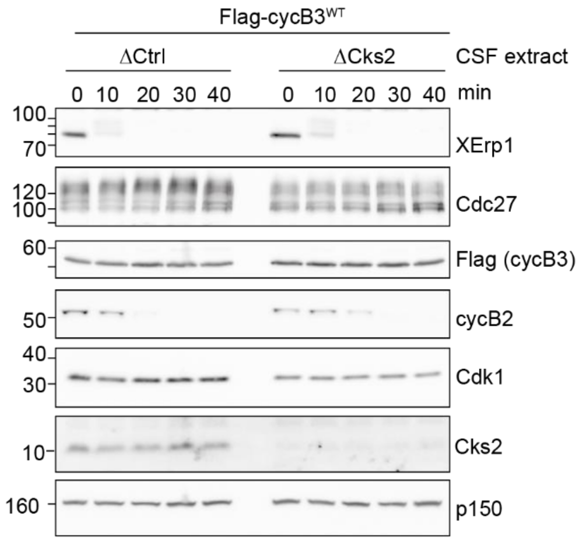

Figure 11: CycB3-mediated XErp1 degradation is unaffected by Cks2 depletion. CSF extract was depleted of Cks2 by performing three rounds of immunoprecipitation with Cks2-antibody bound beads. Either control or Cks2 depleted extract was supplemented with Flag-cycB3 IVT and samples were taken at indicated time points. The time course was analysed via SDS-PAGE and western blot. P150 serves as a loading control. One representative experiment from three biological replicates is shown.

2.4. Fusion of cycB3 to XErp1 rescues phosphate-binding pocket mutations

The mutations in the phosphate-binding pocket of cycB3^{TEM} lead to loss of binding to pre-phosphorylated XErp1, which reduced multisite phosphorylation although cycB3^{TEM}/Cdk1 is as active toward single sites in XErp1 as cycB3^{WT}/Cdk1 (Fig. 9E). Therefore, a fusion of cycB3^{TEM} to XErp1 should rescue the biological function of cycB3 by superseding the phosphate-binding pocket dependent binding step. To test this idea, either an N- or C-terminal fusion of full-length cycB3 WT or TEM to an N-terminal XErp1 fragment (aa 1-350) was created. Both variants were tested for their degradation pattern in CSF extract. For detection of the fusion construct the XErp1 and the cycB3 antibody were used to confirm correct in vitro transcription and translation (only the XErp1 antibody is shown). Both fusions of cycB3^{TEM} and XErp1 successfully rescued the degradation of XErp1 in CSF extract indicated by the degradation of the complete fusion construct (N-terminal fusion not shown; Fig. 12A). To verify that the degradation observed with the fusion construct was Plx1 mediated leading to recruitment of $SCF^{\beta\text{-}TRCP}$ followed by proteasomal degradation and not APC/C mediated by the D-box motif in cycB3, the Plx1 inhibitor BI2536 was supplemented in one condition. The addition of BI2536 completely blocked the degradation of XErp1-cycB3^{WT} fusion (Fig. 12A, first condition) confirming that degradation was Plx1 dependent and not induced through the APC/C. The degradation of XErp1$^{1\text{-}350}$-cycB3^{TEM} fusion was still not as efficient as the degradation of XErp1$^{1\text{-}350}$-cycB3^{WT} fusion. However, comparing the stability of endogenous XErp1 in presence of cycB3^{TEM}, the fusion of XErp1$^{1\text{-}350}$ to cycB3^{TEM} led to a significant increase in degradation (Fig. 8 compared to Fig. 12A). These data suggest that fusion of cycB3 to XErp1 skips the binding step necessary to mediate full XErp1 phosphorylation, which ultimately leads to XErp1 degradation. If this is the case, T97 phosphorylation, normally required to recruit cycB3 via the phosphate-binding pocket, should also be dispensable for the degradation of the XErp1-cycB3 fusion constructs.

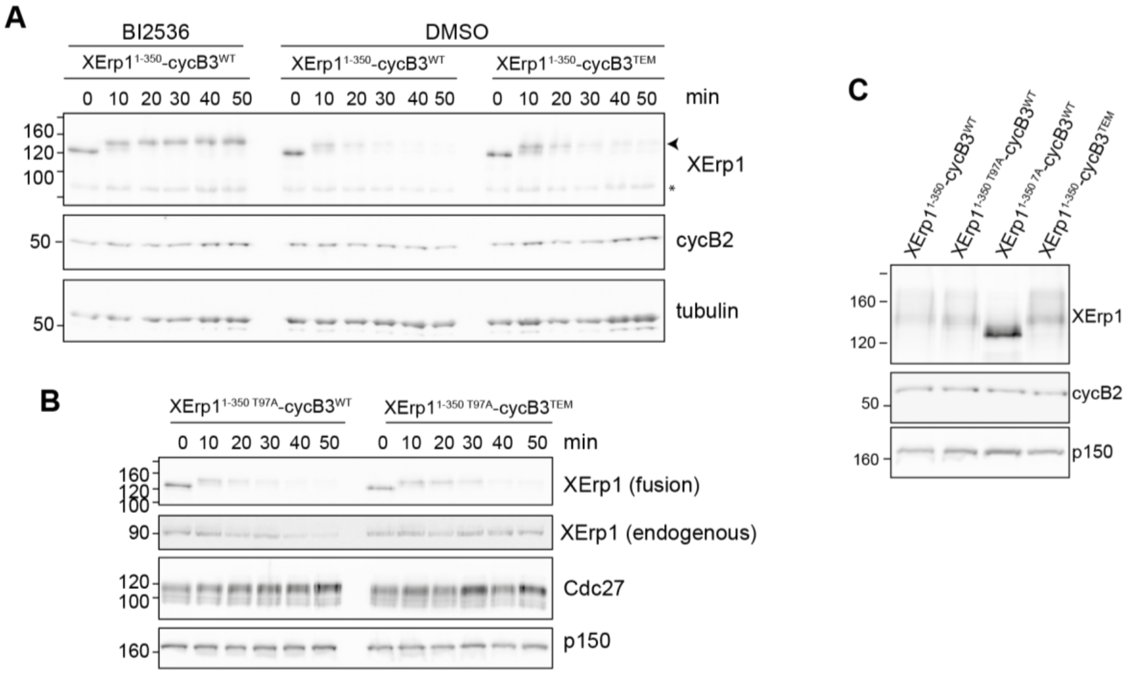

Figure 12: Fusion of cycB3^{TEM} to XErp1 rescues degradation. (A) IVTs of the indicated Myc-tagged fusion constructs were added to CSF extract and samples were taken at indicated time points. The extract was either treated with BI2536 (20 µM) or treated with solvent control DMSO. Samples were analysed via SDS-PAGE and western blot. The fusion construct (arrowhead) was detected with the anti-XErp1 antibody and endogenous XErp1 is marked with a star. P150 serves as a loading control. One representative experiment from three biological replicates is shown. **(B)** IVTs of the indicated Myc-tagged fusion constructs (XErp1^{T97A} (1-350aa) fused to either cycB3^{WT} or cycB3^{TEM}) were added to CSF extract and samples were taken at indicated time points. CSF extract was additionally supplemented with C-terminal XErp1 to prevent premature exit from MII. P150 serves as a loading control. One representative experiment from three biological replicates is shown. **(C)** CSF extract was arrested by the addition of MG262 and C-terminal XErp1. Indicated Myc-XErp1$^{1\text{-}350}$-cycB3 fusion IVTs were added to arrested CSF extract and incubated for 45 min. Samples were taken and analysed via SDS-PAGE and western blot. One representative experiment from two biological replicates is shown. The fusion constructs were detected with the XErp1 antibody. P150 serves as a loading control and cycB2 as a cell cycle marker.

To test this, cycB3 was fused to XErp1 containing a T97A mutation and added to the CSF extract. The XErp1$^{1\text{-}350\ T97A}$-cycB3 constructs were degraded with very similar kinetics in case both cycB3^{WT} and cycB3^{TEM} fusions (Fig. 12B). This result underlines the proposed mechanism that T97 is the binding site for the cycB3 phosphate-binding pocket and that this is necessary for further downstream multisite phosphorylation of XErp1. Tethering cycB3 to XErp1 circumvents phosphate-binding pocket dependent binding of cycB3 to XErp1 and therefore directly leads to multisite phosphorylation of XErp1 (Fig.12C). How many of the M- or N-cluster phosphorylation sites are in total necessary for inducing XErp1 degradation, even in the context of the XErp1-cycB3 fusion, is still unclear. Therefore, it will be addressed how many of the eight Cdk1-phosphosites in the M- and N-cluster are necessary for wild-type XErp1 degradation kinetic in the next section.

2.5. All M-cluster sites are necessary for efficient XErp1 degradation mediated by cycB3

CycB3^{TEM} phosphorylates residue T97 in XErp1 with the same efficiency as cycB3^{WT} (Fig. 9E) indicating that only T97 phosphorylation in the M- and N-cluster is not sufficient to induce XErp1 degradation. To gain further insights into the necessary phosphorylation sites, degradation assays using Flag-

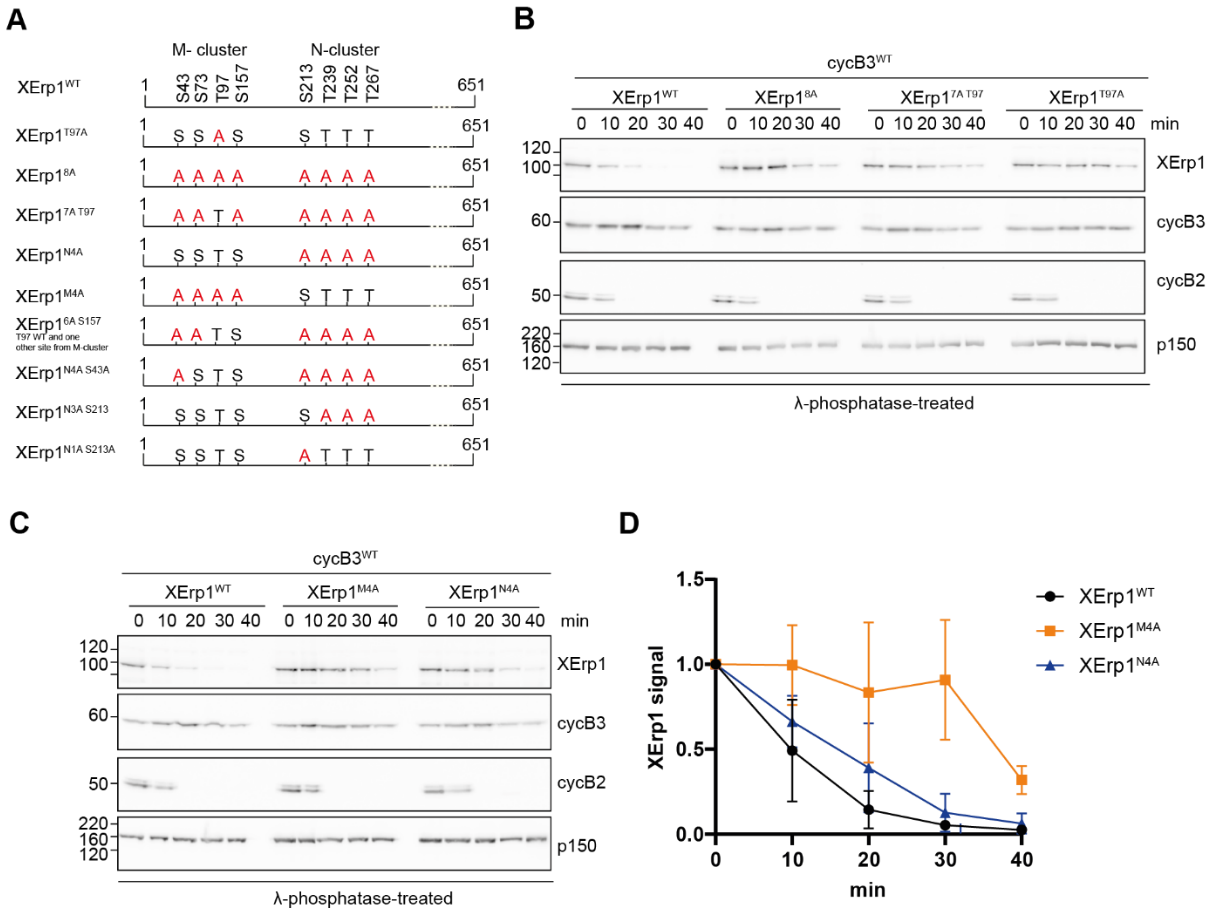

Figure 13: XErp1 T97 is necessary but not sufficient for XErp1 degradation. (A) Scheme of XErp1 variants tested in XErp1 degradation assay. Mutated residues were marked in red. **(B)** XErp1 degradation assay with indicated Myc-XErp1 IVT constructs ectopically added to CSF extract. After a short incubation time, Flag-cycB3^{WT} IVT was added and the time course was started. Samples were taken at indicated time points and directly treated with λ-phosphatase. Samples were analysed via SDS-PAGE and western blot. CycB2 serves as a cell cycle marker while p150 serves as a loading control. One representative experiment from three biological replicates is shown. **(C)** Same experiment as in (B) with different Myc-XErp1 constructs. **(D)** The graph shows the mean ± SD of quantification from three biological experiments depicted in (C). XErp1 signal was quantified and normalized to the p150 signal.

cycB3^{WT} and different Myc-XErp1^{ZBR} mutants were conducted (Fig. 13A). Ectopic Myc-tagged XErp1 was mutated in the ZBR region to prevent interference of ectopic XErp1 with the cell cycle by preventing XErp1 mediated inhibition of the APC/C (Heim et al., 2018). To observe the degradation of ectopically supplemented XErp1, IVTs of these Myc-XErp1 mutants and Flag-cycB3^{WT} were added to CSF extract and samples were taken at specific time points. As reported previously, a comparison of XErp1^{WT} with XErp1^{T97A}, revealed that T97 was necessary for effective degradation (Bouftas et al., 2022). However, it is not sufficient to induce degradation on its own as XErp1$^{7A\ T97}$ was still degraded slower than XErp1^{WT} and was as stable as the XErp1^{8A} construct, in which none of the N-terminal Cdk1 consensus sites in the M-and N-cluster are phosphorylatable (Fig. 13B). This indicates that T97 phosphorylation is a prerequisite for XErp1 degradation, but it is not the only phosphorylation site essential for inducing XErp1 degradation.

I next investigated whether the phosphorylation site mutations in the M- or the N-cluster showed higher stability to narrow down the phosphorylation sites sufficient for efficient XErp1 degradation. Both the XErp1^{M4A}- and the XErp1^{N4A}-construct were stabilized compared to XErp1^{WT} with a stronger

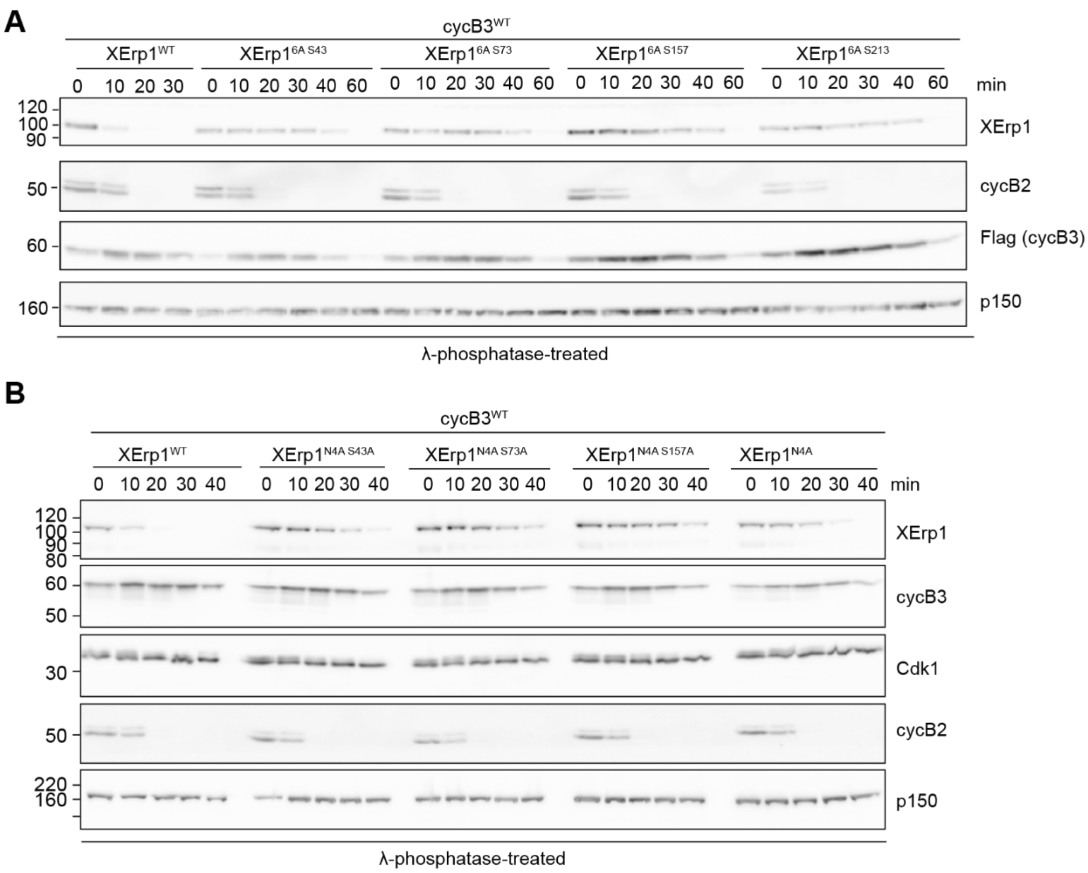

Figure 14: All M-cluster sites are necessary for efficient XErp1 degradation. (A) XErp1 degradation assay with indicated Myc-XErp1 IVT constructs ectopically added to CSF extract. After a short incubation time, Flag-cycB3^{WT} IVT was added and the time course started. Samples were taken at indicated time points and directly treated with λ-phosphatase. Samples were analysed via SDS-PAGE and western blot. CycB2 serves as a cell cycle marker while p150 serves as a loading control. One representative experiment from two biological replicates is shown. **(B)** Same experiment as in (A) with indicated Myc-XErp1 constructs. One representative experiment from two biological replicates is shown.

effect if the M-cluster sites were mutated to non-phosphorylatable alanine (Fig. 13C/D). This result fits the previous finding of T97 phosphorylation (one site in the M-cluster) to be absolutely necessary for efficient degradation. Single sites in the M-cluster were mutated back to WT to evaluate the influence of the single sites independent of the effect of T97. These XErp1^{6A} mutants contained T97 and one additional wild-type phosphorylation site (Fig. 13A/14A). These XErp1 constructs were strongly stabilized compared to XErp1^{WT} and in all conditions XErp1 was only completely degraded after 60 min (Fig. 14A). There was no significant difference between the different M-cluster sites in the XErp1^{6A} constructs. Adding a third wild-type site to the M-cluster, all possible XErp1$^{N4A\ M1A}$ combinations leaving T97 unmutated were tested. The XErp1$^{N4A\ S43A}$ mutant showed the weakest stabilization compared to the other XErp1$^{N4A\ M1A}$ mutants with the highest decrease in XErp1 signal at 40 min (Fig. 14B). Nevertheless, all XErp1$^{N4A\ M1A}$ showed higher stabilization compared to the XErp1^{N4A} construct (Fig. 14B). Consequently, all sites in the M-cluster contributes to XErp1 degradation efficiency.

To address the number of phosphorylation sites in the N-cluster necessary for normal XErp1 degradation, XErp1^{N3A} constructs were tested. If one single phosphorylation site in the N-cluster was

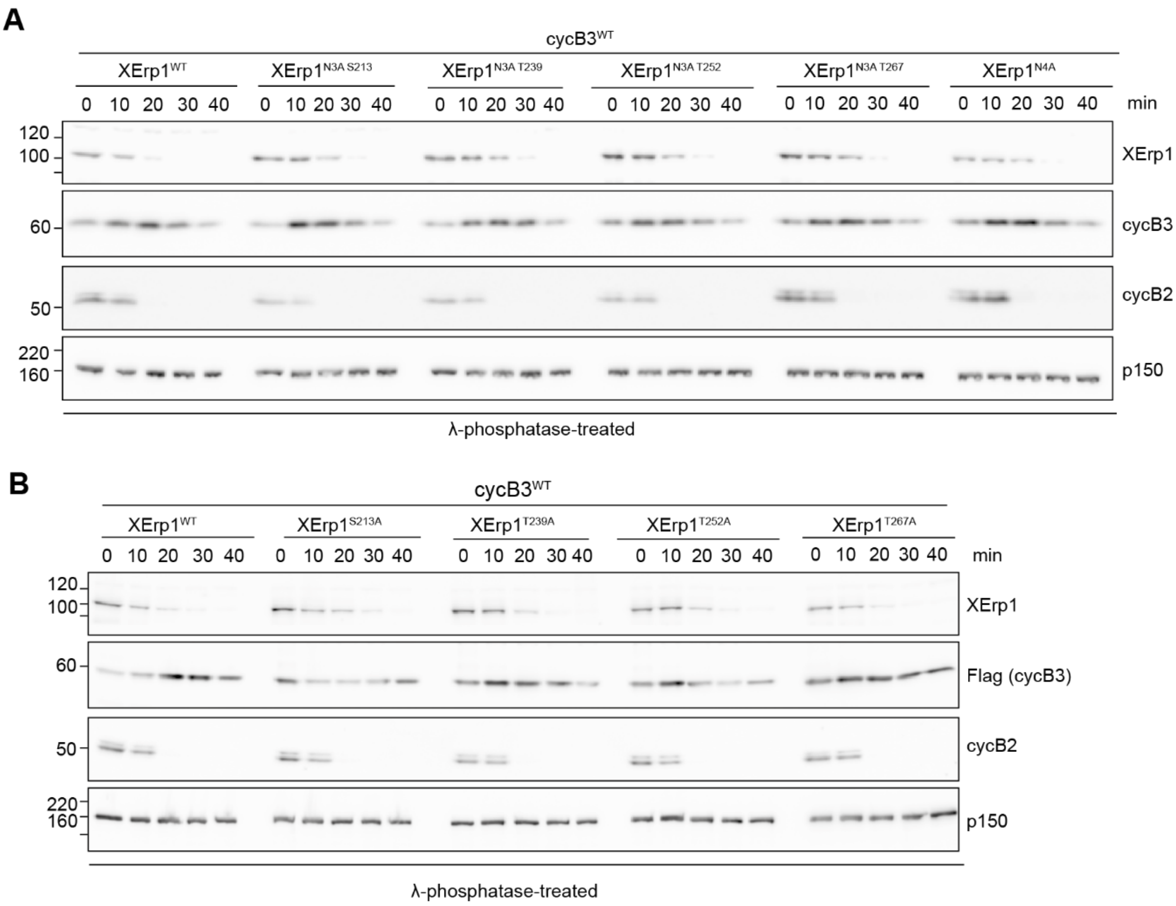

Figure 15: N-cluster phosphorylation contributes minor to XErp1 degradation. (A) XErp1 degradation assay with indicated Myc-XErp1 IVT constructs ectopically added to CSF extract. After a short incubation time, Flag-cycB3^{WT} IVT was added and the time course started. Samples were taken at indicated time points and directly treated with λ-phosphatase. Samples were analysed via SDS-PAGE and western blot. CycB2 serves as a cell cycle marker while p150 serves as a loading control. One representative experiment from two biological replicates is shown. **(B)** Same experiment as in (A) with indicated Myc-XErp1 constructs. One representative experiment from two biological replicates. Further replicates were presented in the master's thesis of Camilla Kleinhempel.

available, no difference in degradation between the constructs and the XErp1^{N4A} construct was observed (Fig. 15A). Only the XErp1 constructs with available S213 or T252 site seemed to be better degraded when time point 10 and 20 min were compared between these two and XErp1$^{N3A\ T239}$ and XERp1$^{N3A\ T267}$. Furthermore, mutations of single N-cluster phosphorylation sites only had a minor effect on XErp1 stability, as single alanine substitutions in the N-cluster revealed a weak stabilization of XErp1^{S213A} or XErp1^{T252A} and no stabilization of XErp1^{T239A} and XErp1^{T267A} compared to XErp1^{WT} at all (Fig. 15B). In summary, the XErp1 degradation assays indicated the necessity for all M-cluster sites and at least a few SP or TP sites in the N-cluster to allow XErp1^{WT} degradation kinetics. The phosphorylation of T97 is absolutely necessary for XErp1 degradation and no single mutation of the eight Cdk1 consensus sites revealed a stronger stabilization than T97A (master's thesis of Camilla Kleinhempel, Fig. 13B), but further phosphorylation is also indispensable for efficient XErp1 degradation. The further phosphorylation sites seem to be partially redundant as the pattern of different XErp1 alanine substitutions showed similar degradation behaviour, e.g. XErp1$^{N3A\ S213}$ and XErp1$^{N3A\ S252}$.

2.6. Efficient T97 phosphorylation depends on multisite phosphorylation

Phosphorylation of T97 is not sufficient to target XErp1 for degradation and efficient and fast degradation depends on multisite phosphorylation (Fig. 13-15). Multisite phosphorylation can have several effects to strengthen XErp1 degradation by either influencing T97 phosphorylation, like an internal positive feedback loop or by recruiting the kinase Plx1 phosphorylating the two degron motifs in XErp1. To clarify the role of multisite phosphorylation, first, several XErp1 variants for T97 phosphorylation in metaphase II arrested extract were tested. A second necessary phosphorylation for cycB3-mediated degradation of XErp1 is T170 (Bouftas et al., 2022). So far, the kinase for T170 phosphorylation has not been identified. Plx1 is the likeliest candidate for T170 phosphorylation as Isoda et al. showed direct phosphorylation of XErp1 T170 by Plk1 in an in vitro kinase assay (Isoda et al., 2011) creating its own docking motif via the polo-box domain (PBD). I also wanted to examine if T170 phosphorylation is indeed downstream of all M- and N-cluster phosphorylation. In Fig. 9F, T97 phosphorylation compared between cycB3^{WT} and cycB3^{TEM}, which also impaired multisite phosphorylation, was already investigated in vitro and no obvious different was detected. To evaluate T97 phosphorylation in CSF and its dependency on further sites like the M- and N-cluster sites as well as on T170 and Plx1 activity, different recombinant XErp1 constructs (1-350 aa) were added to CSF extract and incubated in the presence of cycB3^{WT} for 45 min. Flag-cycB3 constructs were added as mRNA and expressed for 20 min before MBP-XErp1$^{1\text{-}350}$-His addition. To achieve a maximum of XErp1 phosphorylation without degradation, CSF extract was arrested in metaphase II by the addition of MG262 and C-terminal XErp1 (see above). Metaphase II arrest was confirmed by the phosphorylation signal of Cdc27 in all conditions (Fig. 16A). To investigate the level of T97 phosphorylation, samples

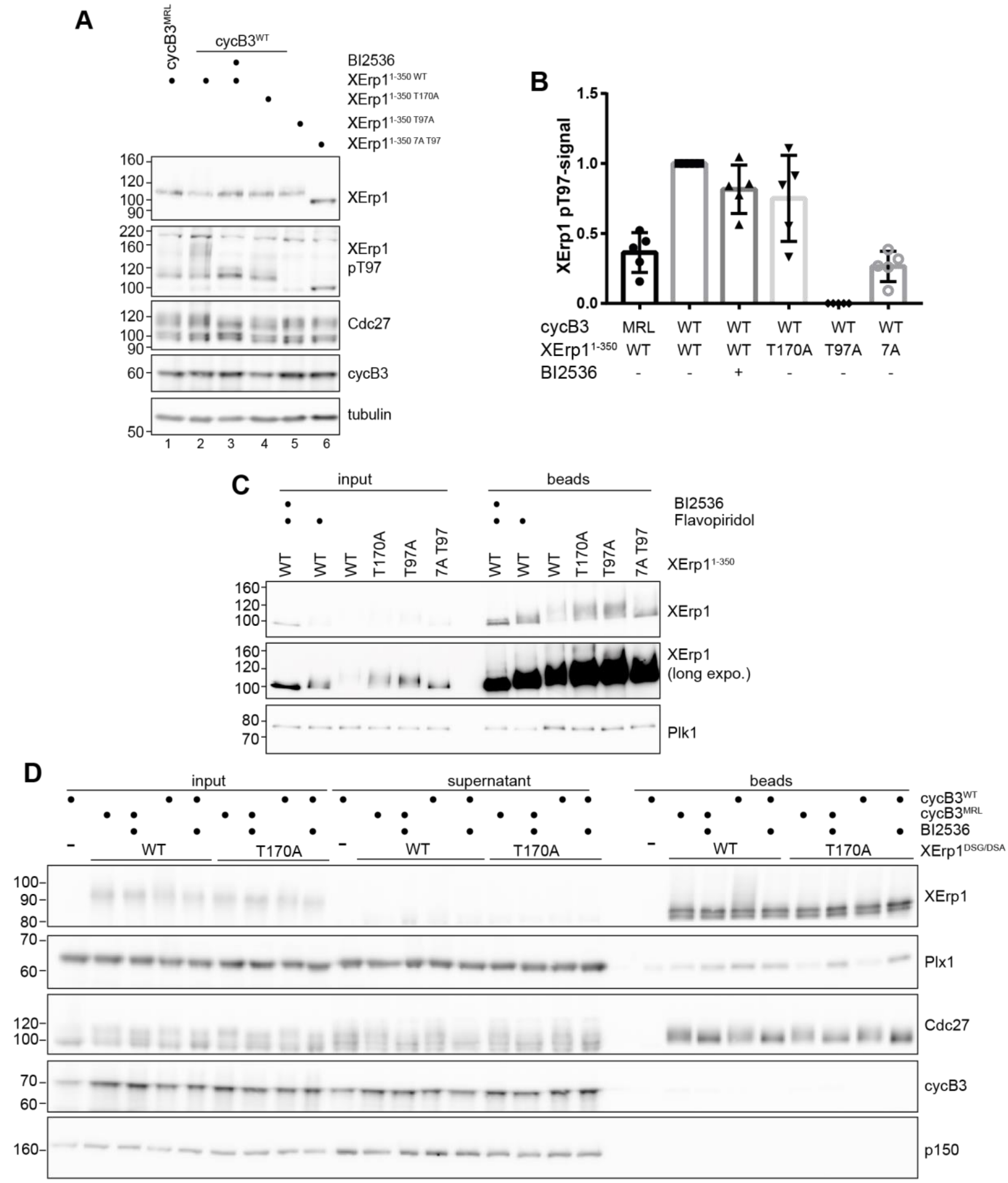

Figure 16: Effect of multisite phosphorylation on T97 phosphorylation and Plk1 binding. (A) CSF extract arrested in MII with MG262 and C-terminal XErp1 was supplemented with indicated Flag-cycB3 mRNA and incubated for 20 min before the addition of recombinant MBP-XErp1-His 1-350aa constructs. In one condition the Plk1 inhibitor BI2536 (20 µM) was supplemented as well. Phosphorylation occurred for 45 min and afterwards, samples were taken and analysed via SDS-PAGE and western blot. Tubulin serves as a loading control. One representative experiment from five biological replicates is shown. **(B)** Quantification of the experiment from (A) and the further replicates by analysing the pT97 signal (Mean ± SD). XErp1 pT97 signal was quantified and the signal in the cycB3^{WT} and XErp1$^{1\text{-}350\ WT}$ condition was set as 1 and the signal in cycB3^{WT} and XErp1$^{1\text{-}350\ T97A}$ condition as 0. **(C)** In vitro kinase assay and pull-down to observe Plk1 binding to different XErp1 constructs. Recombinant proteins were mixed and incubated for 1 h and 15 min in the presence of ATP. Beads bound to XErp1 antibody were used for immunoprecipitation of XErp1 from the reaction mix. IP was performed for 30 min at 6 °C. Samples were taken and analysed via SDS-PAGE and western blot. One representative experiment from two technical replicates. **(D)** Flag-IP of Flag-XErp1$^{DSG/DSA}$ constructs to analyse co-immunoprecipitation of Plx1. CSF extract was arrested with MG262 and C-terminal XErp1. CSF extract was supplemented with mRNA of the indicated Myc-cycB3 constructs. After 20 min incubation, Flag-XErp1$^{DSG/DSA}$ constructs and either BI2536 (20 µM) or DMSO were added. IP was performed in 1:4 dilutions in an IP buffer for 30 min at RT. Samples were taken and analysed via SDS-PAGE and western blot. One representative experiment from two biological replicates is shown. P150 serves as loading control.

were analysed via western blot with the phospho-T97 antibody (Fig. 16A). When T97 residue of XErp1$^{1-350}$ was mutated to alanine, all signal detected was supposed as background signal (Fig. 16A, lane 5, Fig. 16B as zero). To analyse, how much of the phosphorylation of T97 is mediated by cycB1/Cdk1 in the steady state of metaphase II, cycB3^{MRL} instead of cycB3^{WT} was supplemented. In the presence of cycB3^{WT}, the XErp1 pT97 signal increased to around three-fold compared to the cycB3^{MRL} condition (Fig. 16A, quantification 16B). To test the influence of Plx1 on T97 phosphorylation, the Plx1 inhibitor BI2536 was added in one condition. Furthermore, XErp1$^{1-350\ 170A}$ mutant was compared to XErp1$^{1-350\ WT}$, to analyse T97 phosphorylation in the absence of the possible PBD binding site of Plx1. In both conditions, only minor variations in the pT97 signal were detected (Fig. 16A and B, lanes 3 and 4 compared to 2). This suggests that the influence of Plx1 activity as well as T170 on T97 phosphorylation is negligible and both the T170 site and Plx1 fulfils a downstream function in XErp1 phosphorylation. In a further condition, a XErp1$^{1-350}$ version in which all M- and N-cluster sites except T97 were mutated to alanine (7A) was tested for T97 phosphorylation. This reduced T97 phosphorylation to the steady state level observed in MII in the absence of ectopic cycB3^{WT} (Fig. 16A and B, lane 6). Therefore, full T97 phosphorylation can only be achieved if additional M- and N-cluster Cdk1 sites beyond T97 are present in XErp1 which reveals a mutual dependency of T97 phosphorylation and the residual SP and TP sites in the M- and N-cluster in CSF extract. On the one hand, T97 phosphorylation is necessary for starting multisite phosphorylation of the M- and N-cluster sites, but on the other hand further phosphorylation of the M- and N-cluster sites also further enhances T97 phosphorylation.

Next, the influence of multisite phosphorylation on downstream Plx1 binding was investigated. To evaluate the impact of the different phosphorylation sites on Plx1 binding, an in vitro pull-down of recombinant XErp1 that was incubated with recombinant cycB3/Cdk1 and Plk1 (Plx1 is named Plk1 in all other vertebrates than *Xenopus laevis*) was performed. Both kinases were purified from Sf9 cells. CycB3^{WT}/Cdk1^{AFE} from *Xenopus laevis* and Plk1 from *Homo sapiens* were used as the concentration of the human Plk1 was higher than the concentration of the *Xenopus laevis* Plx1. As the structure of Plk1 is highly conserved (Lowery et al., 2005), there will be no difference in substrate phosphorylation between human Plk1 and *Xenopus laevis* Plx1. Different recombinant XErp1$^{1-350}$ constructs were incubated with recombinant cycB3^{WT}/Cdk1^{AFE} and Plk1. After an initial incubation to allow phosphorylation, all reactions were placed on Dynabeads bound to XErp1 antibody to pull out XErp1 and all possible binding partners. Input and bead fractions were analysed by SDS-PAGE and western blot. Full XErp1 phosphorylation was only achieved in the presence of both active Plk1 and Cdk1 as inhibitors for both kinases, BI2536 and Flavopiridol, respectively, drastically reduced phosphorylation shift of XErp1 in western blot analysis (Fig. 16C). Plk1 strongest bound to XErp1$^{1-350}$ in the XErp1$^{1-350\ WT}$ condition, while it barely bound to XErp1 either in the absence of Plk1 activity and/or Cdk1 activity (Fig. 16C). Thus, Plk1 bound strongest to XErp1$^{1-350\ WT}$, if it was previously phosphorylated by cycB3^{WT}/Cdk1^{AFE}. Without the activity of Cdk1, comparable loss of Plk1 binding as with inhibition of both kinases was observed, although Plk1 phosphorylation still occurred (phosphorylation shift in the second condition in bead and input, Fig. 16C). Therefore, Cdk1 phosphorylation is a prerequisite for Plk1 binding to XErp1. Comparing the different XErp1$^{1\text{-}350}$ mutants with XErp1$^{1\text{-}350\ WT}$ revealed that all tested mutations ranging from T170A to T97A and 7A reduced binding of Plk1 to a similar extent, but not as strong as the presence of the kinase inhibitors (Fig. 16C). This indicates that strong binding of Plk1 can only be achieved if multisite phosphorylation occurs as well as phosphorylation of the Plk1 binding site T170, but it might also lead to the conclusion that still not all possible phosphorylation sites responsible for strong Plk1 binding were identified as there was no condition which lacked Plk1 binding completely.

To further investigate the responsible phosphorylation sites for binding of Plx1 in the cycB3-induced XErp1 degradation pathway, immunoprecipitation of different stable Flag-XErp1$^{DSG/DSA}$ constructs was performed via Flag antibody from CSF extract in the presence of either Myc-cycB3^{WT} or Myc-cycB3^{MRL}. Bead samples were analysed for co-immunoprecipitated endogenous Plx1 (Fig. 16D). To test the dependency of Plx1 binding on Plx1 activity, the Plk1 inhibitor BI2536 was supplemented. The strongest binding of Plx1 to XErp1$^{DSG/DSA}$ was achieved with XErp1$^{DSG/DSA\ WT}$ (Fig. 16D). This binding was not influenced by the addition of BI2536 but strongly decreased upon T170A mutation in XErp1 (Fig. 16D). Binding of Plx1 also depended on cycB3/Cdk1 activity, as cycB3^{MRL} did not lead to strong binding of Plx1 to XErp1$^{DSG/DSA\ WT}$. In all conditions with or without BI2536, Plk1 binding increased upon the addition of BI2536 to the level of Plx1 binding found in the cycB3^{WT}/XErp1$^{DSG/DSA\ WT}$ condition, which is probably due to trapping the kinase with its substrate as BI2536 is an ATP-competitive inhibitor. This artificial tethering of Plk1 to XErp1 induced by the inhibitor did not allow any conclusion on the necessity of Plx1 activity for Plx1 binding to XErp1, but at least this experiment shows that T170 is important for Plx1 binding.

2.7. Different substrate specificity for cycB1 and cycB3

Although cycB1/Cdk1 activity is present in both, metaphase I and metaphase II, of meiosis only cycB3/Cdk1 can prevent premature XErp1 accumulation as well as induce artificial CSF-release. In the publication of Bouftas et al., the difference between cycB1 and cycB3 was explained by different substrate specificity toward the T97 phosphorylation site (Bouftas et al., 2022). To elucidate further differences between the two B-type cyclins, I first investigated whether cycB3 can bind to the same proteins as cycB1 in general as some of these interacting partners are known to be phosphate-binding pocket dependent, which might result in different binding behaviour due to the altered phosphate-binding pocket in cycB1 and cycB3 (Fig. 5). An IP of ectopically Flag-tag cycB1 and cycB3 IVT from CSF extract arrested in metaphase II by the addition of MG262 and okadaic acid was performed. With both cyclins, Cdk1 and Cks2 co-immunoprecipitated to a similar extent (Fig. 17A). Nevertheless, when analysing verified substrates of the phosphate-binding pocket of cycB1, like separase and Cdc27 (Yu et al., 2021) (Christian Heinzle's doctoral thesis), only binding to cycB1 and no binding to cycB3 was observed (Fig. 17A). This suggests that cycB3 and cycB1 differ in their substrate specificity, but this difference can be attributed to both the phosphate-binding pocket and further interacting sites in the

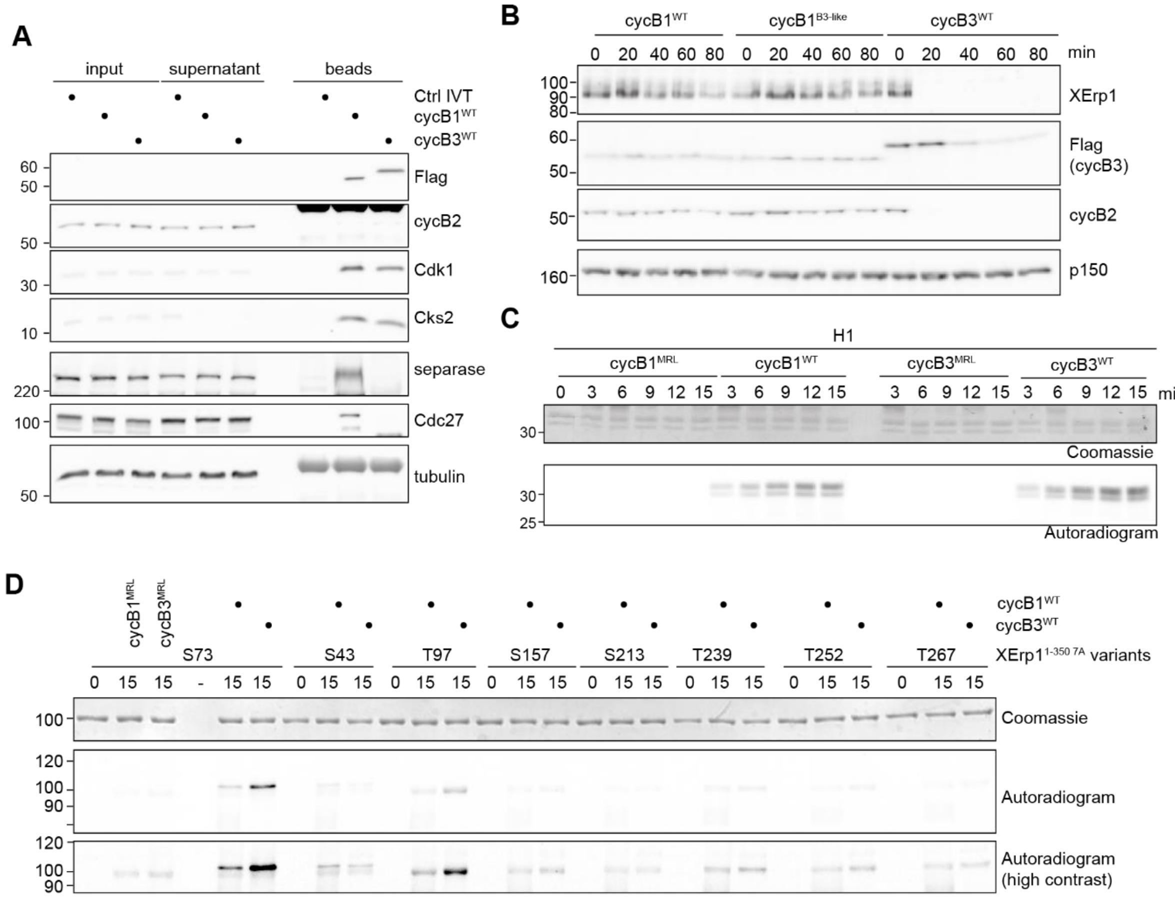

Figure 17: CycB3 increases Cdk1 activity toward XErp1. (A) Flag-IP of Flag-tag cycB1^{WT} compared to cycB3^{WT} IVT from CSF extract which was arrested in metaphase II by the addition of MG262 and okadaic acid (10 µM). Samples were analysed via SDS-PAGE and western blot. Tubulin serves as a loading control. One representative experiment from three independent biological replicates. **(B)** CSF time course with ectopically added IVT of Flag-tagged cycB1^{WT}, cycB1$^{B3\ like}$ or cycB3^{WT}. Samples were taken at indicated time points and analysed via SDS-PAGE and western blot. **(C)** In vitro H1 kinase with [γ-^{33}P]ATP and Flag-tag cycB1 or cycB3 variants expressed from mRNA in CSF extract and pulled out with anti-Flag antibody. Samples were taken at indicated time points and analysed via SDS-PAGE. Dried gel was used for the autoradiogram. One representative experiment from three independent biological replicates is shown. Adapted from Bouftas et al., 2022. **(D)** In vitro kinase assay with [γ-^{33}P]ATP and Flag-tag cycB1 or cycB3 variants expressed from mRNA in CSF extract and pulled out with anti-Flag antibody. Recombinant XErp1^{7A} was used as the substrate for the kinase assay. Samples were taken at indicated time points and analysed via SDS-PAGE. Dried gel was used for the autoradiogram.

cyclins. The finding only reinforces the hypothesis of major varieties between both cyclin/Cdk complexes influencing the phosphorylation of different substrates. Next, the amino acids of the cycB1 pocket and the surrounding residues, which might also influence binding to pT97, were mutated to the corresponding amino acids of the cycB3 pocket (all cycB1 mutations: H282L, K286R, Q173E, L176E, K179E, Q182H, L181N, L265Y). Then, the efficiency of XErp1 degradation upon addition to CSF extract was tested (Fig. 17B). As expected, cycB1^{WT} did not influence XErp1 stability during the time course while cycB3^{WT} addition led to strong and fast degradation of XErp1 (Fig. 17B). Addition of the mutated cycB1 version (cycB1$^{B3\text{-}like}$) did not increase XErp1 degradation in CSF extract, therefore mutations of the phosphate-biding pocket and proximal residues in cycB1 were not sufficient to mimic cycB3 (Fig. 17B). To further investigate the difference between cycB1 and cycB3, the activity of each cyclin-Cdk1 complex towards XErp1^{7A} constructs were tested. This setup allowed us to compare the phosphorylation efficiency of either cycB1/Cdk1 or cycB3/Cdk1 in all single XErp1 M-and N-cluster sites. Any side effects from multisite phosphorylation and phosphate-binding pocket-binding can be excluded as only single phosphorylation sites are available in the XErp1$^{1\text{-}350\ 7A}$ construct. Flag-cycB1 and Flag-cycB3 were expressed from mRNA in CSF extract and pulled-out by Dynabeads bound to Flag antibody. CycB bound to beads was then used for the kinase assay. This kinase assay revealed a weaker activity of cycB1/Cdk1 compared to cycB3/Cdk1 complex toward specific XErp1$^{1\text{-}350\ 7A}$ mutants: S73, T97, S157, T239 and T252 (Fig. 17D). For XErp1$^{7A\ S213}$ and XErp1$^{7A\ T267}$ no difference was detected and only for XErp1$^{7A\ S43}$ phosphorylation by cycB1/Cdk1 was stronger than phosphorylation by cycB3/Cdk1, although the overall signal was weaker than for the main phosphorylated sites S73 and T97 (Fig. 17D). H1, a generic cyclin/Cdk1 substrate was equally phosphorylated by cycB1^{WT}/Cdk1 and cycB3^{WT}/Cdk1 (Fig. 17C). Thus, I additionally identified further phosphorylation sites in the M- and N-cluster of XErp1, especially S73, beyond the known T97 phosphorylation site, which were stronger phosphorylated by cycB3/Cdk1 compared to cycB1/Cdk1. Besides, I also identified one site which was stronger phosphorylated by cycB1/Cdk1, S43 in XErp1. In conclusion, XErp1 is an overall better substrate for cycB3/Cdk1 than for cycB1/Cdk1, independently of the phosphate-binding pocket.

2.8. Identification of further cycB3 substrates

Finally, I wanted to explore further phosphate-binding pocket dependent substrates of cycB3 during meiosis to elucidate if cycB3 plays additional roles besides the regulation of XErp1. In an explorative experiment, cycB3 interacting proteins were searched in an unbiased way by expression of N-terminally Flag-tagged cycB3^{WT} or cycB3^{TEM} from mRNA in CSF extract and subsequent reisolation of cycB3 via the Flag-tag. Bead samples were collected and either loaded on SDS-PAGE for western blot analysis or prepared for mass spectrometry (MS) analysis (Fig. 18). Western blot analysis revealed in both cycB3 conditions strong immunoprecipitation of both Flag-cycB3 and co-immunoprecipitation of Cdk1 (Fig. 18A). The MS analysis showed an enrichment for several proteins in the cycB3^{WT} condition compared to the cycB3^{TEM} condition, while cycB3 levels were not enriched in between the two conditions. Significantly enriched between cycb3^{WT} and cycB3^{TEM} were only two proteins: etv6 (ETS variant transcription factor 6) and dnttip1 (deoxynucleotidyltransferase, terminal, interacting protein 1) (Fig. 18B/C). Both proteins are nuclear localized and DNA-binding with etv6 being a transcription factor and dnttip1 being a member of the steroid/thyroid receptor superfamily. One of the enriched but not significantly enriched proteins was XErp1 (fbxo43.S) (Fig. 18B) validating XErp1 as a cycB3 phosphate-binding pocket dependent substrate, shown in the experiments above (Fig. 9-11). Promising cell-cycle relevant proteins enriched by cycB3^{WT} are the subunit B55δ of the PP2A phosphatase (ppp2r2d) and the aurora kinase B (aurkb) (Fig. 18B/C). Interestingly, B55δ was also enriched in a cycB3 pull-down coupled to MS from oocytes 20 min after GVBD (data not shown). The MS-results revealed no significant difference in Cks2 levels between cycB3^{WT} and cycB3^{TEM} although Cks2.L and Cks2.S were slightly enriched in cycB3^{WT} (Fig. 18B). These results underline the critical function of the cycB3 phosphate-binding pocket in regulating XErp1 degradation and suggest additional cell cycle related function of cycB3 mediated by the phosphate-binding pocket.

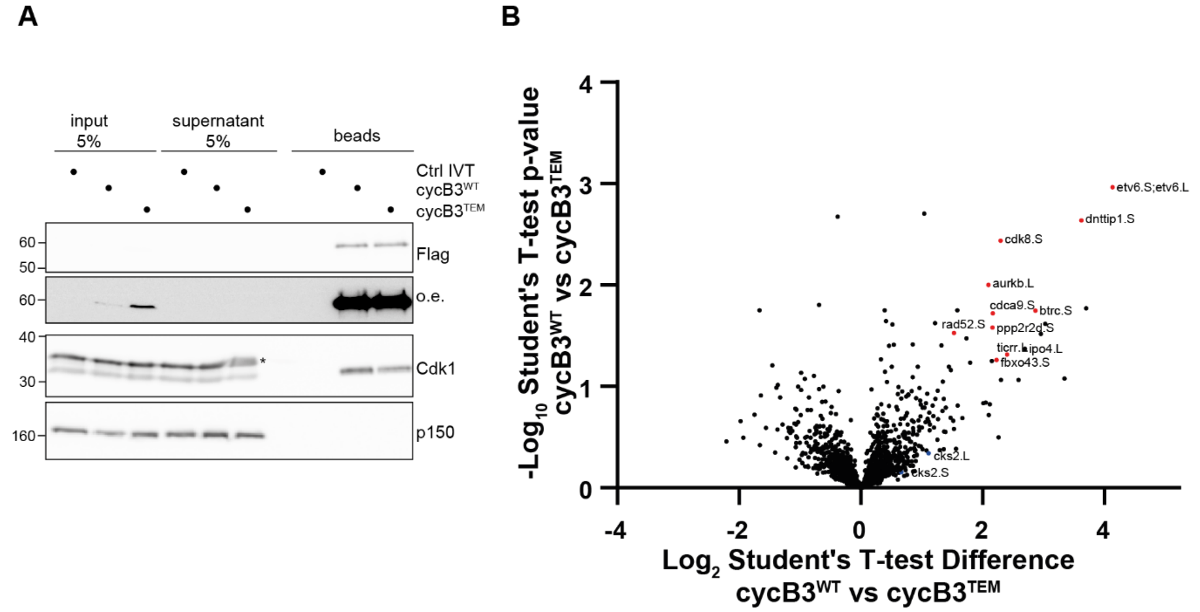

C

Gene symbol	Name	Function
etv6.S/etv6.L	ETS variant transcription factor 6	Transcription factor
dnttip1.S	deoxynucleotidyltransferase, terminal, interacting protein 1	Member of the steroid/thyroid receptor superfamily
cdk8.S	cyclin-dependent kinase 8	Cyclin C-dependent kinase CDK8
aurkb.L	aurora kinase B	Serine/threonine kinase
cdca9.S	cell division cycle associated 9	Component of the chromosomal passenger complex (CPC)
btrc.S	β-TrCP	F-box protein/ubiquitin protein ligase complex component
rad52.S	RAD52 homolog	DNA repair and recombination protein RAD52/RAD22
ppp2r2d.S	protein phosphatase 2 regulatory subunit B, delta	Serine/threonine protein phosphatase 2A, regulatory subunit
ticrr.L	TOPBP1-interacting checkpoint and replication regulator	DNA replication
fbxo43.S	F-box protein 43/XErp1	Required to prevent anaphase onset in cytostatic factor-arrested oocytes

Figure 18: IP of cycB3^{WT} and cycB3^{TEM} coupled to MS analysis. (A) Flag-cycB3 constructs were expressed from mRNA in CSF extract for 1 h. CSF extract was arrested in MII by the addition of MG262 and Myc-C-terminal XErp1 IVT. IP with Flag antibody was performed for 1 h at RT. Samples were analysed via SDS-PAGE and western blot. Bead samples were also analysed via MS in (B). One representative experiment of three independent biological replicates is shown. The star marks Myc-signal (form C-terminal XErp1 IVT) in western blot detected with Cdk1 antibody. P150 serves as loading control. **(B)** Volcano plot for cycB3^{WT} versus cycB3^{TEM} interacting proteins. Each dot represents one identified protein. Only etv6.S/etv6.L and dnttip1.S are significantly enriched according to statistical analysis with p-value <0.05. Red dots mark enriched protein with the respective protein name next to them, while blue dots depict Cks2.S and Cks2.L. Peter Heid performed MS analysis shown here. **(C)** Table of all proteins mark as red dots in (B) with the respective name and function. Proteins written in red were significantly enriched in the MS analysis of (B).

3. Discussion

3.1. Summary of findings

Cyclin B3 is indispensable for meiosis based on findings from several organisms ranging from *Drosophila* to mice (Deyter et al., 2010; Jacobs et al., 1998; Zhang et al., 2015). Here, I was able to reproduce in *Xenopus laevis* oocytes the phenotype of metaphase I arrest upon cycB3 depletion. Furthermore, a direct correlation between the phosphate-binding pocket and the cycB3 function in metaphase I was observed as only cycB3 with an intact phosphate-binding pocket could rescue the metaphase I arrest. The phosphate-binding pocket of cycB3 was identified from sequence alignments with cycB1 and a mutant with a deficient phosphate-binding pocket was unable to rescue MI arrest caused by cycB3 depletion (Fig. 7). I further narrowed down the binding site of the phosphate-binding pocket to pre-phosphorylated T97 of XErp1 (Fig. 10). Phosphorylation of T97 is a prerequisite for cycB3 mediated degradation (Fig. 13B). Binding to this site via the phosphate-binding pocket increase overall phosphorylation on XErp1 in a mutual manner, with phosphorylated T97 stimulating phosphorylation on the residual SP and TP sites in the M-and N-cluster in XErp1, while full pT97 is only achieved if the residual sites can be phosphorylated (Fig. 9F and 16A/B). T97 is conserved throughout vertebrates

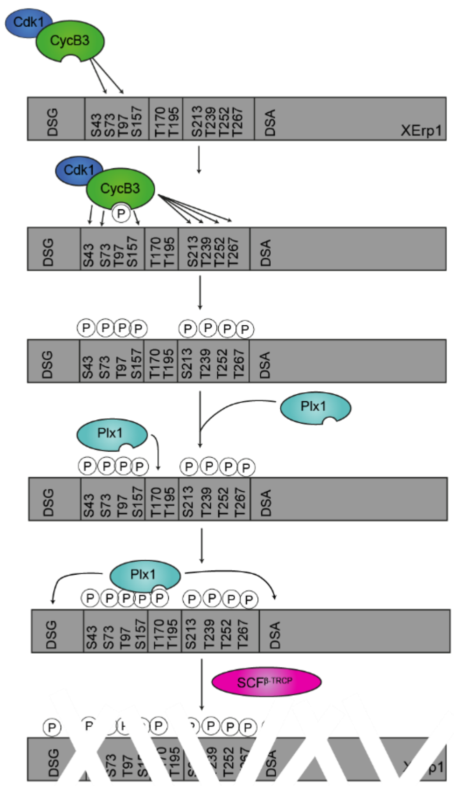

Figure 19: Scheme of cycB3 mediated XErp1 degradation. CycB3/Cdk1 first strongly phosphorylates XErp1 at pT97, creating its own phosphate-binding pocket dependent binding site. This site facilitates further downstream phosphorylation downstream in the M- and N-cluster of XErp1. Full phosphorylation of XErp1 leads to Plx1 binding, phosphorylation of T170 and strong binding of Plx1 to pT170. Plx1 can finally phosphorylate the DSG/DSA motifs, recruiting SCF$^{\beta\text{-TRCP}}$ and resulting in proteasome-dependent XErp1 degradation.

(Bouftas et al., 2022) and our results provide an explanation for the importance of this site in vertebrate oocytes. XErp1 phosphorylation on all M-cluster sites and several N-cluster sites by cycB3 is necessary for Plk1 binding and less phosphorylation is associated with weaker Plk1 binding (Fig. 16). Our data suggest that the order of phosphorylation events occurring on XErp1 begins with cycB3, which is then followed by phosphorylation of T170, probably by Plk1/Plx1 itself, and the phosphorylation of the DSG/DSA motifs by Plk1/Plx1 (Fig. 19). The phosphorylation of the DSG/DSA motifs finally leads to recruitment of $SCF^{\beta\text{-TRCP}}$ and degradation of XErp1 (Rauh et al., 2005; Schmidt et al., 2005; Tung et al., 2005). With these results, we gain further insights into the mechanism of how cycB3 enables XErp1 degradation and therefore prevents premature metaphase I arrest during oocyte maturation. In addition, for the first time a phosphate-binding pocket in another B-type cyclin, cycB3, was identified, thereby demonstrating that this pocket is not restricted to cycB1.

3.2. The phosphate-binding pocket is a speciality of B-type cyclins

The phosphate-binding pocket was just recently identified in cycB1 functioning in mitosis as an additional inhibitory mechanism for separase (Yu et al., 2021). This phosphate-binding pocket is a unique B-type cyclin feature adding a further layer of substrate recognition beside the SLiM motifs for the different cyclins (see Introduction 1.2.1.) and Cks mediated substrate docking. The minimal consensus motif of Cdk is serine or threonine followed by a proline (Brown et al., 1999) and this consensus motif is shared by further proline-directed kinases, like MAPKs and GSK3 (glycogen synthase kinase 3) (Hardt & Sadoshima, 2002; Hutti et al., 2004; Songyang et al., 1996). Although the different kinases share the same minimal consensus motif, they all phosphorylate specific substrates. This substrate specificity is on the one hand mediated by extended consensus motifs like the preference of Cdk for a positive charge in the +3 position and on the other hand by specific interfaces between kinase and substrate for substrate recognition. For the MAPK family, substrate recognition is therefore mediated by SLiMs like the D-site or the DEF-docking motif (Chang et al., 2002; Jacobs et al., 1999; Murphy et al., 2002; Tanoue et al., 2000). There are also differences in the recognition motifs inside the MAPK family, for example, Erk and p38/MAPK prefer different specific amino acids in these motifs to guarantee substrate specificity (Sheridan et al., 2008). GSK3 prefers helical peptides for recognition (Bax et al., 2001; Dajani et al., 2003). An α-helix together with an extended loop in GSK3β forms a hydrophobic binding channel for an α-helix in axin leading to kinase-substrate binding (Dajani et al., 2003). For cycB/Cdk complexes, the phosphate-binding pocket builds a unique substrate recognition interface, which allows B-type cyclins to direct Cdk1 to specific pre-phosphorylated substrates. Pre-phosphorylation can either occur by other kinases or by Cdk itself. This recruitment via the phosphate-binding pocket might result in the phosphorylation of suboptimal phosphorylation sites or even non-consensus sites and also in multisite phosphorylation. This allows a complex order of phosphorylation events for example in the cell cycle.

3.3. The phosphate-binding pocket in different B-type cyclins

Interestingly, the phosphate-binding pockets of cycB1, as well as of cycB2, 4 and 5 (in *Xenopus laevis*), contained different amino acids (RHK) than the phosphate-binding pocket of cycB3 (RLR) (Fig. 5). The most drastic change in amino acid sequence in the three amino acids which build the phosphate-binding pocket is the difference in the second amino acid from histidine in cycB1 to leucine in cycB3. Leucine is not positively charged which results in a lower positive surface charge of the phosphate-binding pocket of cycB3 compared to cycB1. In cycB3 further amino acids might be important for substrate binding both in the phosphate-binding pocket and in other parts of cycB3. AlphaFold prediction revealed two further amino acids which might be involved in the structure of the phosphate-binding pocket, Y292 and H209 in cycB3, which also build hydrogen bonds with XErp1 either with T97 itself or the backbone in the T97 region. Furthermore, the first helix of the helices bundle building the cyclin fold in cycB3 builds a negatively charged surface corresponding to positively charged amino acids downstream of T97 (Fig. 20). Structural features together with the difference in the phosphate-binding pocket might lead to the different substrate binding between cycB1 and cycB3 (Fig. 17C). As demonstrated in this thesis, XErp1 as a cycB3 phosphate-binding pocket dependent substrate is a strong binding partner for cycB3 but not for cycB1 (master's thesis of Michael Schäfer, Fig. 10A).

For cycB1 and cycB2 it was shown that although they differ in expression pattern, deletion of one of each can be rescued by overexpression of the other B-type cyclin in mouse oocytes (Daldello et al., 2019; Li et al., 2018). For cycB3 knock-down in mice, the phenotype of MI arrest during oocyte maturation could not be rescued by the expression of cycB1 but by the expression of cycB3 from different species (Karasu et al., 2019), underlining the uniqueness of cycB3. This unique and conserved feature of cycB3, to prevent premature accumulation of XErp1, is completely dependent on an intact phosphate-binding pocket (Fig. 7-8). Strikingly, a higher cycB3/Cdk1 activity compared to cycB1/Cdk1 activity toward XErp1 in single phosphorylation sites in the M- and N-cluster of XErp1, especially for S73 and T97, which were phosphate-binding pocket independent, was shown. This is in line with stronger T97 phosphorylation mediated by cycB3 compared to cycB1, described in Bouftas et al. 2022. CycB1/Cdk1 showed stronger activity toward only one site in the M-and N-cluster, S43, (Fig. 17D). This observation revealed that apart from the difference in the phosphate-binding pocket between cycB1 and cycB3 further features must differ between these B-type cyclins. I failed in mimicking the cycB3-induced release from MII with cycB1 mutated to the corresponding amino acids of cycB3 in the region of the phosphate-binding pocket (Fig. 17B), underlining the fact that the phosphate-binding pocket is not the only difference between cycB1 and cycB3 and more than the mutated residues might be important for a functional pocket. It is possible that besides the phosphate-binding pocket, cycB3 exploits further binding motifs on XErp1 like SLiMs. As cycB3 shows sequence similarity to both B-type cyclins and A-type cyclins two SLiMs for binding could be possible, the LxF motif and the RxL motif respectively (Örd et al., 2019). Both SLiMs variants are present in XErp1 and although the hydrophobic patch responsible for binding the motifs in cycB3 is more similar to cycA, the RxL motifs in XErp1 only mildly influenced XErp1 degradation by cycB3 which was tested by mutation of RxL to AxA (data not shown). Mutation of the LxF motifs in XErp1 will answer the question if cycB3 binds this motif.

Alignment of the T97 region from different vertebrate species reveals strong conservation of a negatively charged glutamate in -1 position, a positively charged lysine in position +5 and a positively charged stretch downstream of the T97 phosphorylation site (Fig. 20). The strong conservation of these residues might indicate a functional role of these amino acids. Two of these arginine residues from the positive stretch where part of the mutated RxL motifs and thus do not seem to be important for cycB3 binding. Alternatively, it might be essential to mutate all three arginines in this stretch simultaneously to abrogate the interaction with cycB3. Mutations of these conserved amino acids either simultaneously or one by one might elucidate the interaction mode between cycB3 and XErp1 in more detail, especially as the positive stretch binds to negatively charged amino acids located in and next to the hydrophobic patch in the AlphaFold2 prediction of the complex formed by cycB3/Cdk1/Cks2 and XErp1 shown in Fig. 10C. Insights into the structure of cycB3 with or without XErp1 by cryo-EM or crystallography might resolve the specific features in cycB3 and either confirm or disprove the AF2 model. This will then shed light on the structural differences between cycB1 and cycB3 to explain the observed differences in substrate specificities.

XErp1/Emi2 T97-region

Xenopus laevis	90	QLAPLYETPRVGKKEFSLRRRLLI	113
Danio rerio	64	PALTWCETPKLGRKNTSLRRRLLV	87
Mus musculus	79	KSPELCETPKLRRKKCTLRRRLDF	102
Homo sapiens	137	KTPELCETPKISGKKCLPRRRLNV	160
Gallus gallus	101	KSTYFFETPKAGRKGFSLRRRLLL	124

Figure 20: Alignment of XErp1/Emi2 T97 region from different vertebrate species. In red threonine 97 of XErp1 from *Xenopus laevis* and the corresponding residues in the different species are highlighted. In orange, all highly conserved residues around the T97 sites are marked, while in green similar but not completely conserved residues are denoted.

3.4. Tethering only partially rescues the phosphate-binding pocket

Circumventing binding of the cycB3 phosphate-binding pocket to XErp1 by tethering the cycB3 mutant to XErp1, rescued the failure of the cycB3 phosphate-binding pocket mutant to induce XErp1 degradation in CSF extract (Fig. 12). The fusion protein XErp1$^{1\text{-}350}$-cycB3^{TEM} led to significant more degradation than observed on endogenous XErp1 after addition of cycB3^{TEM} (comparison of Fig. 12A with 8). However, the fusion of XErp1$^{1-350}$ and cycB3^{WT} was still degraded with faster kinetics than the cycB3^{TEM} fusion protein. This observation could be explained by the fact that the phosphate-binding pocket still facilitates the correct positioning of the cycB3/Cdk1 complex on XErp1 by binding to phosphorylated XErp1 in the WT condition compared to the phosphate-binding pocket-mutant.

This assumption is strengthened by the fact that degradation of endogenous XErp1 was observed by the addition of XErp1$^{1-350\ T97A}$-cycB3^{WT} fusion but not XErp1$^{1-350\ T97A}$-cycB3^{TEM} fusion, which led to the necessity of supplementing C-terminal XErp1 fragment to CSF extract in this experiment to ensure MII state in all conditions (Fig. 12B). Therefore, cycB3^{WT} in the fusion protein was able to phosphorylate XErp1 both in cis (the fused XErp1) as well as in trans (endogenous XErp1). The binding of the phosphate-binding pocket to the available target site in endogenous XErp1 could therefore compete with the tethering effect of the fusion construct, especially in the case when the target site is missing in cis in the XErp1$^{1-350\ T97A}$-cycB3^{WT} fusion protein. This also explains the bigger difference in degradation kinetics between XErp1$^{1-350}$-cycB3^{WT} and XErp1$^{1-350}$-cycB3^{TEM} compared to XErp1$^{1-350\ T97A}$-cycB3^{WT} and XErp1$^{1-350\ T97A}$-cycB3^{TEM} (Fig. 12A vs 12B), as in the former case less competition with endogenous XErp1 occurs. This leads to the assumption that binding to phosphorylated T97 strengthens the correct positioning of cycB3/Cdk1 on XErp1 facilitating multisite phosphorylation.

3.5. The role of Cks in cycB3-mediated XErp1 degradation

Besides the phosphate-binding pocket of cycB, Cdk uses Cks as another external phosphate adaptor that has been shown to have tremendous roles in the cell cycle (see Introduction 1.2.4.). During this thesis, the question appeared if Cks1 or 2 might be also involved in targeting cycB3/Cdk1 to XErp1. In *Xenopus laevis*, only p9 corresponding to Cks2 has been described so far (Patra & Dunphy, 1996). In mice, the untimely expression of Cks1 during meiosis and embryonic divisions is lethal (Ellederova et al., 2019). I therefore postulate Cks2 to be the main functioning Cks protein in meiosis. This hypothesis is supported by the fact that Cks2 was also the only Cks protein identified via MS in IPs of cycB3^{WT} and cycB3^{TEM} from CSF extract (Fig. 18) and detected in CSF samples via western blot with antibodies created against Cks1 or Cks2 specific peptides. In the MS analysis, the levels of Cks2 were slightly enriched in cycB3^{WT} compared to cycB3^{TEM} and western blot analysis often showed less Cks2 co-immunoprecipitated with cycB3^{TEM}, as well. If the difference in Cks2 levels detected in most of the western blots was correct, this might raise the possibility that XErp1 is more stable upon treatment with cycB3^{TEM} because it interacts less efficiently with the phosphate adaptor Cks2. However, the depletion of Cks2 from CSF extract revealed that in its absence cycB3 was still efficiently inducing XErp1 degradation (Fig. 11), excluding Cks2 from a significant role in cycB3-mediated XErp1 degradation. A further argument for a Cks2 independent mechanism was the equal binding of Cks2 to both cycB1 and cycB3 (Fig. 17A). If Cks2 would be the main driver of XErp1 binding for cycB/Cdk1 complexes, we would expect similar affinity of cycB1 and cycB3 to XErp1, which was not the case for full-length XErp1 as well as for a phosphorylated T97 peptide, which is the main docking site for the phosphate-binding pocket (master's thesis of Elijah Johannes and Michael Schäfer). In addition, multisite phosphorylation of XErp1 with recombinant cycB3/Cdk1^{AFE} complexes purified without Cks1 or 2 was achieved (Fig. 9F). Together these results suggest a Cks2 independent mechanism for cycB3 mediated XErp1 degradation. However, due to the failure in detecting Cks1, I cannot completely exclude a possible role of this phosphate adaptor protein for the function of cycB3 in meiosis.

3.6. The phosphate-binding pocket in the context of different species

The phosphate-binding pocket of cycB3 is conserved in vertebrates as well as in *Drosophila melanogaster*, *Caenorhabditis elegans* and *Clytia heimispherica*. In vertebrates, the mechanism of CSF-arrest with XErp1/Emi2 as the main factor to establish the arrest is conserved (Liu et al., 2007; Maller et al., 2002). The kinase Mos and its downstream effectors MAPK and p90^{Rsk} are also essential for CSF-arrest. However, p90^{Rsk} is dispensable for metaphase II arrest in mice (Dumont et al., 2005), highlighting XErp1/Emi2 as one of the main downstream proteins responsible for CSF-arrest. Vertebrate cycB3 therefore ensures correct accumulation of XErp1/Emi2 exclusively in metaphase II not only in mice and *Xenopus laevis* but most probably also in other vertebrates. The conservation of the phosphate-binding pocket suggests a conserved substrate recognition of XErp1/Emi2 by cycB3 followed by phosphate-binding pocket dependent degradation. Interestingly, species without a metaphase II arrest like starfish, jellyfish and fruit fly, do not have a XErp1/Emi2 related protein but contain a cycB3 phosphate-binding pocket. From an evolutionary point of view maintaining a substrate recognition site only brings an advantage if the substrate is present, otherwise, the recognition site would probably be lost in the same manner as the substrate. One example of co-evolution of substrate recognition site and substrate is the Mad2-interaction motif in Mad1 and Cdc20, which co-evolved with Mad2 (van Hooff et al., 2017). The circumstance that there are species with a functional phosphate-binding pocket, but without the substrate XErp1/Emi2, leads to the conclusion that there must be another main cycB3 phosphate-binding pocket substrate. Interestingly, B55, one of the regulatory subunits of PP2A, was identified as a potential phosphate-binding pocket dependent substrate in this thesis as well as found as a cycB3 interacting protein in *Drosophila melanogaster* (Garrido et al., 2020). It would be worthwhile to elucidate the relationship between cycB3 and B55 in meiosis in further research. In *Drosophila*, it was speculated that PP2A-B55 might be important for the dephosphorylation of Cdc20 and therefore for the activation of APC/C^{Cdc20} upon metaphase exit (Garrido et al., 2020). Another finding from Garrido et al. in *Drosophila* is a direct interaction of cycB3 and the APC/C leading to its phosphorylation (Garrido et al., 2020). This finding could not be reproduced for *Xenopus laevis* in this study as no interaction with Cdc27, the same APC/C subunit investigated by Garrido et al., and cycB3^{WT} was found in co-immunoprecipitation experiments (Fig. 17A and 18). Nevertheless, the final outcome of APC/C activation in the presence of cycB3 seems to be conserved throughout these species. However, in *Xenopus laevis* the role of cycB3 seems to be restricted to meiosis while in *Drosophila* cycB3 influences the APC/C activity in both meiosis and mitosis (Garrido et al., 2020; Yuan & O'Farrell, 2015). To investigate the direct and indirect effects of cycB3 on the APC/C and the contribution of the phosphate-binding pocket to this mechanism will be interesting research questions to address in the future. Especially findings on cycB3 and its interacting proteins in different species outside from vertebrates will give helpful insight in the evolution of cycB3 in meiosis.

3.7. XErp1 stability in different contexts

XErp1 is a component of the CSF, leading to metaphase II arrest in vertebrates. The regulation of XErp1 stability in meiosis was intensively investigated in previous publications, both during steady state in metaphase II as well as the degradation upon metaphase II exit (Isoda et al., 2011; Rauh et al., 2005; Schmidt et al., 2005; Schmidt et al., 2006; J. Q. Wu et al., 2007). The mechanism of XErp1 degradation upon metaphase II exit involves the CaMKII as the driving force for destabilization of XErp1, although the downstream events are similar to the proposed cycB3 mediated mechanism with Plx1/Plk1 being recruited to XErp1 and phosphorylating the degron motif (Rauh et al., 2005; Schmidt et al., 2005; Schmidt et al., 2006). In the steady state of metaphase II arrest, the mechanism of constant XErp1 destabilization by cycB1/Cdk1 resembles the cycB3/Cdk1 mediated mechanism by exploiting similar phosphorylation sites, with the significant difference of an effective and fast XErp1 degradation induced by cycB3/Cdk1, compared to a very slow turn-over induced by cycB1/Cdk1. Our data suggest that the difference between the B-type cyclins is driven by alterations in the phosphate-binding pocket as well as in the overall activation of Cdk1 toward XErp1 as a substrate (see discussion above). A closer comparison between the steady state level of XErp1 in metaphase II (see Introduction 1.1.3.) and the prevention of XErp1 accumulation in meiosis I by cycB3, also revealed differences in Plx1/Plk1 binding. In the study of Isoda et al., it was found that both T195 and T170 in XErp1 are responsible for Plx1/Plk1 binding and only mutating both led to a strong reduction of Plx1 binding to XErp1 (Isoda et al., 2011). Here, I showed that in the case of cycB3-mediated degradation mutation of XErp1 T170 alone was already sufficient to lose binding of Plx1/Plk1 both in vitro as well as in CSF (Fig. 16). This is in line with the findings from Bouftas et al., describing strong stabilization of the XErp1 T170A mutant, but no effect of the T195A mutation in case of cycB3 addition to CSF extract (Bouftas et al. 2022). Within this thesis, I was not able to find out which kinase phosphorylates T170. Testing Plx1/Plk1 by inhibition with BI2536 was inconclusive as inhibition of Plx1/Plk1 always leads to artificial binding of Plx1/Plk1 to XErp1, which was independent of its pre-phosphorylation state both in vitro as well as in CSF extract (Fig. 16D, in vitro data not shown). Nevertheless, I propose that Plx1/Plk1 is still the likeliest candidate for T170 phosphorylation as Isoda et al. showed that Plk1 is able to phosphorylate T170. It was shown that Plx1/Plk1 binding to XErp1 is stimulated by cycB3/Cdk1 activity as without Cdk1 activity both in vitro and in CSF extract less Plx1/Plk1 binding occurred (Fig. 16C/D). This result underlines that cycB3/Cdk1 is needed as the primary kinase to phosphorylate XErp1. Plx1/Plk1 recruitment also depended on multisite phosphorylation of the M-and N-cluster sites as reduced binding of Plk1 to $XErp1^{1\text{-}350\ 7A\ T97}$ and $XErp1^{1\text{-}350\ T97A}$, both impaired in multisite phosphorylation, occurred (Fig. 16C). This is in line with the experiments from Isoda et al., showing reduced Plk1 binding to $XErp1^{8A}$ mutant, with all eight M-and N-cluster sites mutated to alanine. Likely, the amount of phosphorylation in the M-and N-cluster and not the positioning of phosphorylation (except for T97) is relevant for degradation as mutations of different single phosphorylation sites reveal that at least all M-cluster sites and several N-cluster sites have to be present for effective XErp1 degradation (Fig. 15, master’s thesis of Camila Kleinhempel). The amount and not the exact positioning of the sites seems to be more relevant as several constructs containing distinct mutations but with the same amount of unmutated phosphorylation sites were degraded with the same kinetics (Fig. 14 & 15).

The necessity of multisite phosphorylation is a known phenomenon in the cell cycle as other proteins like Ndd1 as well as CPEB1 also depend on multisite phosphorylation (Asfaha et al., 2022; Setoyama et al., 2007). Especially the degradation mechanism of CPEB1 described by Setoyama et al. resembles the cycB3-mediated XErp1 degradation. CPEB1 is sequentially phosphorylated by Cdk1 and Plx1 with the former creating a binding site for the latter, followed by phosphorylation of a degron motif by Plx1 and finally the ubiquitination of CPEB1 by $SCF^{\beta\text{-}TRCP}$ (Setoyama et al., 2007). For full CPEB1 degradation, more than one Cdk1 phosphorylation event was necessary and rather the amount than the positioning of phosphorylation events contributed to efficient degradation, the same as for XErp1 in the cycB3/Cdk mediated degradation.

XErp1 also plays an essential role in the early embryonic cell cycle in *Xenopus laevis* by counteracting APC/C activity (Tischer et al., 2012). In the early embryonic cell cycle, XErp1 accumulates right after fertilization and is present until mid-blastula transition (MBT), where the embryo starts to produce its own mRNA and is cleared from maternal mRNA (Inoue et al., 2007; Tischer et al., 2012). Until now it is not clear how XErp1 is degraded at MBT and it is tempting to speculate that maybe cycB3 is resynthesized at this time point to initiate the degradation of XErp1.

4. Conclusion

In this study, I describe a phosphate-binding pocket in cycB3 and show that it is, necessary for cycB3 function in meiosis. The phosphate-binding pocket was characterised as a docking interface of cycB3/Cdk1 for XErp1 pre-phosphorylated on residue T97. This binding mechanism leads to further downstream phosphorylation on XErp1 by cycB3/Cdk1 and Plx1 recruitment and ultimately results in XErp1 degradation. The phosphate-binding pocket is therefore an essential feature of cycB3 for preventing premature accumulation of XErp1 in meiosis I. The cycB3 phosphate-binding pocket differs from the phosphate-binding pocket of other B-type cyclins, represented by cycB1, which might lead together with yet unidentified structural differences to different substrate recognition, as substrates recognized by cycB1 were not bound by cycB3. Furthermore, the order of phosphorylation events in cycB3-mediated XErp1 degradation was resolved by in vitro phosphorylation assays with recombinant components.

In the future, structural studies as well as the analysis of potential new phosphate-binding pocket dependent substrates identified in this study will result in a clearer understanding of the specificity and function of cycB3's phosphate-binding pocket.

5. Contributions

In this thesis, several purified proteins were used, which were not purified by me. Martina Baack made a great effort to purify sufficient and pure $cycB3^{WT}$ and $cycB3^{TEM}/Cdk^{AFE}$ complex by continuously optimizing the purification protocol. Christian Heinzle purified the human Plk1 protein, which was used, as the *Xenopus laevis* protein purified by me was less concentrated. Tatjana List helped with the purification of the $XErp1^{1A}$ constructs.

The work of Michael Schäfer was a great help for this thesis by contributing to the understanding of the binding site of the phosphate-binding pocket. Under my supervision during his master's thesis in Prof. Dr. T.U. Mayer´s laboratory, he performed the pT97-peptide pull-downs shown in **Fig. 10B**. He also performed two replicates of the experiment shown in **Fig. 10A**.

Fig. 17C was taken from the publication by Bouftas et al., 2022.

Peter Heid from Prof. Dr. Florian Stengel's laboratory performed the MS analysis of the IP from CSF extract and oocytes shown in **Fig. 18**.

6. Material and Methods

6.1. Purification of recombinant proteins

6.1.1. Recombinant cycB3/Cdk1^{AFE}

For recombinant cycB3/Cdk1 complexes, genes were cloned into the pMACS backbone with either N-terminal Strep-tag (cycB3) or N-terminal His-tag (Cdk1). Transposition was performed according to Bac-to-Bac® Baculovirus Expression Systems (Invitrogen) and transfection with Cellfectin^{TM} II according to the protocol of Invitrogen. For the creation of P1, 500 µl P0 was added to 100-200 ml Sf9 cells (500,000 cells/ml) and incubated until all cells were infected, apparent from GFP signal in cells, in general after 3-4 days. Sf9 cells were then co-infected with P1 baculoviruses of cycB3 and Cdk1 variants and were harvested 48-52 h post-infection by centrifugation at 1000xg, 4 °C for 15 min. Cells were resuspended with lysis buffer (PBS, 0.5 M NaCl, and 1x Protease-Inhibitors (complete tablets w/o EDTA (Roche)). After freezing the thawed pellet was sonicated with a Branson sonicator (5 min w/o pulse). Lysate was cleared by two centrifugations each for 15 min at 50,000xg and 4 °C. Triton-X-100 was added to the supernatant to a final concentration of 0.25 %. After filtration (0.45 µm) Nuclease was added (1: 10,000 Universal Nuclease Pierce final 25 E/ml) and the lysate was incubated for 4 h with StrepTactin Superflow (IBA) beads. Beads were washed six times with PBS/0.5M NaCl (two times in batch and four times in column) and once with PBS. The cycB3/Cdk complex was eluted with PBS containing 10 mM Desthiobiotin.

6.1.2. Recombinant XErp1 constructs

For purification of XErp1 1-350aa fragments, XErp1 mutants were cloned into a pMALvector with N-terminal MBP tag and C-terminal His-tag as well as two TEV cleavage sites after the MBP-tag. Expression took place in BL21 DE3 RIL *E. coli* induced with 500 µM IPTGat an OD600 of 0.5 for 3-4 h at 37 °C. Bacteria were centrifuged for 10 min at 3,000xg and the pellet was resuspended in 20 ml Lysis buffer (20 mM Tris-HCl pH 8.0, 300 mM NaCl, 5 Mm Imidazole and 1x Protease Inhibitor). After snap-frozen in liquid nitrogen cell pellets were stored at -80 °C until purification. For purification thawed bacteria pellet solution was lysed with the Emulsi-Flex-C3. Lysate was cleared by centrifugation at 20,000xg, 4 °C for 30 min. The supernatant was mixed with 1 ml Ni-NTA beads (Qiagen), and washed with 10 ml PBS before use. Beads and lysate were incubated for 2 h at 4 °C rotating. Beads were washed three times with washing buffer (20 Mm Tris HCl pH 8, 300 mM NaCl, 20 mM Imidazole, 0.1 % Triton-X-100) containing 1 mM ATP and 1 mM $MgCl_2$ and three times with washing buffer. Elution took place with elution buffer (20 mM Tris HCl pH 8, 300 mM NaCl and 200 mM Imidazole) in 10 fractions. Peak fractions were identified via Coomassie, pooled and dialysed with PBS containing 10 % Glycerol o/n 4 °C. For storage dialysed protein was aliquoted, snap frozen and kept at -80 °C.

6.1.3. Recombinant polo-like kinase

Plx1 or Plk1 was cloned into a pMACS backbone with an N-terminal His-tag and transposition as well as transfection was performed as mentioned above. For expression of Plx1 WT or KD, Sf9 cells were infected with P1 and incubated for 48 h at 27 °C and 3 h before harvesting cells were treated with 100 nM okadaic acid. Cells were harvested by centrifugation at 1000xg for 5 min. Cell pellets were snap-frozen until purification. For purification, cell pellets were resuspended in 1 ml Lysis buffer (10 mM HEPES pH 7.5, 20 mM β-Glycerophosphate, 1 mM EGTA, 5 mM β-Mercaptoethanol, 0.1 mM Na-Vanadate, 2x Protease-Inhibitor cOmplete (Roche), 150 mM NaCl, 1 % CHAPS, 20 mM Imidazole) per $2*10^7$ cells. Cell lysate was cleared by centrifugation at 4 °C 23,500 rpm for 30 min followed by filtration (0.45 µm). Lysate was incubated for 2 h with Ni-NTA beads (Qiagen) previously washed with Lysisbuffer (200µl beads per 5ml Lysate). Beads were washed with around 50 to 75 column volumes washing buffer (10 mM HEPES pH 7.5, 0.1 mM Na-Vanadate, 20 mM β-Glycerophosphate, 1 mM EGTA, 5 mM β-Mercaptoethanol, 500 mM NaCl, 0.1 % CHAPS, 1x Protease-Inhibitor cOmplete (Roche), 20 mM Imidazole). Protein was eluted in 10 fractions with Elution buffer (10 mM HEPES pH 7.5, 25 mM NaCl, 2 mM $MgCl_2$, 1 mM EGTA, 50 mM Sucrose, 5 mM β-Mercaptoethanol, 200 mM Imidazole). Fractions with similar protein concentrations were pooled and dialysed against 10 mM HEPES pH 7.5, 150 mM NaCl, 1 mM DTT, 200 mM Imidazole, 10 % Glycerol, and 1 mM EDTA. After dialysis Glycerol was added to a final concentration of 25 % and samples were aliquoted, snap frozen in liquid nitrogen and stored at -80 °C.

6.2. In vitro assay

For in-vitro phosphorylation assay, 8.4 to 15 ng/µl cycB3/Cdk1^{AFE} and 50 ng/µl Plk1 (human) were used to phosphorylate 10 to 20 ng/µl XErp1 1-350aa variants. The reaction buffer, PB-buffer, contains PBS with 1 % Glycerol, 20 mM EGTA, 15 mM $MgCl_2$, 1 mM DTT, 1x Protease inhibitor (complete w/o EDTA), 1x PhosStop (Roche) and 0.5 mM ATP. The phosphorylation reaction took place at 25 °C for 1-1.5 h. The phosphorylation reaction was stopped by dilution of 1:10 into 1.5x Lämmli (sample buffer).

6.3. Radioactive kinase assay

Radioactive kinase assays were performed to test the activity of purified cycB3/Cdk1^{AFE} against either histone H1 or XErp1 1-350aa constructs. Around 8 to 17 ng/µl cycB3/cdk1^{AFE} were incubated with 40 ng/µl Histone H1 or 80 ng/µl XErp1, 50 µM ATP and 0.22 µCi/µl in PB-buffer (PBS with 1 % Glycerol, 20 mM EGTA, 15 mM $MgCl_2$, 1 mM DTT, 1x Protease inhibitor (complete w/o EDTA), 1x PhosStop (Roche)). The reaction took place at 25 °C and 1400 rpm shaking. Samples were taken at indicated time points and directly diluted in 3x Lämmli to a final concentration of 1x Lämmli.

6.4. Xenopus laevis methods

6.4.1. Husbandry and handling of frogs

Frogs were kept in the animal facility (TFA) at the university of Konstanz. Handling and experiments with the frogs were performed according to the animal welfare regulation approved by the Regional Commission in Freiburg (Germany).

6.4.2. Preparation of stage VI oocytes

Ovaries were surgically removed from adult female *Xenopus laevis* and maintained in MBS buffer. For separating single oocytes, ovaries were picked in smaller pieces and treated with Liberase (50 µg/ml) for 1.5 h. After washing Liberase-treated oocytes 3 to 4 times with MBS buffer, stage VI oocytes were sorted by hand after Dumont (Dumont, 1972).

6.4.3. CycB3^{WT} or cycB3^{TEM} meiosis I arrest rescue

Xenopus laevis stage VI oocytes were injected with codon-optimized Flag-Trim21 mRNA (7 ng/oocyte), cycB3 antibody (against aa 6-22) or control IgG (29 ng/oocyte) and IVT of cycB3$^{WT\Delta15}$, cycB3$^{TEM\Delta15}$ or control IVT respectively (1.5 nl to 5.55 nl/oocyte). In total a volume of 18.4 nl was injected per oocyte. After incubation for 14-16 h at 19 °C in MBS-buffer a progesterone (5 µg/ml in OR2) time course was started and samples were taken at indicated time points by removing buffer and snap-frozen in liquid nitrogen.

6.4.4. Lysis of oocytes

Oocytes were taken at specific time points and stored at -80 °C until oocyte lysis for western blot analysis. For lysis, oocytes were supplemented with 5.48 µl/oocyte fresh prepared oocyte lysis buffer (4.73 µl PE-LB, 0.5 µl 0.5 M NaF, 0.05 µl 0.5 M β-Glycerophosphate, 0.2 µl 25x Protease-Inhibitor) and scratched until all oocytes were completely lysed. Then oocytes were centrifuged for 10 min at 4 °C and full speed. The clear lysate was removed from cell debris (5 µl/lysed oocyte) and resuspended with an equal amount of 3x Lämmli. If oocytes were treated with λ-Phosphatase, oocytes were lysed with buffer without NaF and β-Glycerophosphate (see λ-Phosphatase treatment).

6.4.5. Immunofluorescence staining (IF)

For immunofluorescence staining oocytes were fixed at desired time points in 100 mM KCl, 3 mM $MgCl_2$, 10 mM K-HEPES pH7.8, 3.7 % Formaldehyde, 0.1 % Glutaraldehyde and 0.1 % Triton X-100, overnight at 4 °C shaking. Oocytes were bleached in 10 °% H_2O_2 in MeOH at RT exposed to light for one day. After bleaching oocytes were blocked three times with AbDil (2 % BSA, 0.1 % NaN_3 and 0.1 °% Triton X-100 in PBS) for 1 h at 4 °C on a shaker. For antibody staining, FITC-labelled anti-tubulin antibody was diluted to a final concentration of 1 µg/ml and for DNA staining Hoechst 33342 was added to a final concentration of 1 µg/ml in AbDil. Oocytes were then incubated for at least 48 h to

72 h at 4 °C in the dark on a shaker. After staining oocytes were washed three to four times with PBST. Mounting took place at slides with holes in a diameter of 1.2 µm -1.3 µm with the vacuum grease ring method.

6.4.6. CSF preparation

Xenopus laevis female adults were primed for extract preparation with hCG (chorionic gonadotropin, human, Sigma, 50 U) into the dorsal lymph sack of females. Primed frogs were used after at least two days' rest until 14 days after priming. For induction of egg laying frogs were injected with 500 U hCG around 18-26 h before egg collection. For egg-laying frogs were separated in tanks containing MMR-buffer. Laid eggs were washed with MMR and apoptotic or malformed eggs were removed. For removal of the jelly coat, eggs were treated with a de-jellying solution for up to 7 min and washed afterwards with CSF-XB. For egg lysis, they were transferred into centrifugation tubes with 750 µl CSF-XB supplemented with 0.1 mg/ml cytochalasin B. Eggs were compacted by centrifugation for 1 min with 200xg followed by 1 min at 650xg. The excess of buffer and apoptotic eggs were removed before the final centrifugation step of 16,500xg for 10 min. All centrifugation steps were performed at 4 °C. After the final centrifugation step the middle layer containing the cytoplasmic extract was removed by puncturing the tube. CSF extract was supplemented with 10 µg/ml cytochalasin B and tested for integrity with 600 µM $CaCl_2$ and sperm nuclei.

6.5. Immunoprecipitation (IP)

For all immunoprecipitation experiments, Dynabeads™ Protein G (invitrogen™) were used and the amount of beads was calculated according to the binding capacity indicated by the producer. Dynabeads were washed three times with PBST and once with PBS before the addition of the antibody, as well as after antibody binding. Antibody binding took place for 1 h at room temperature or overnight at 6 °C.

6.5.1. IP of XErp1 variants from CSF extract

For each condition, CSF extract was supplemented with 1:20 C-terminal XErp1 and MG262 (100 µM) to arrest CSF extract in meiosis II. For cycB3 expression, mRNA was added to a final concentration of 0.04 µg/µl. After incubation for 20 min at 20 °C to allow mRNA translation, Plk1 inhibitor BI2536 (final conc. 20 µM) or solvent control (DMSO) and Flag-XErp1 IVT variants (1:20) were supplemented to the extract and incubated again for 10 min at 20 °C. Before the IP CSF extract was diluted 1:4 in IP-buffer (20 mM Tris-HCl, 100 mM NaCl, 10 mM EDTA, 5 mM NaF, 1 mM NaVO3, 1 mM DTT, 1x Protease Inhibitor, 1x PhosStop) and added to Flag-antibody bound Dynabeads (binding was performed as described above). For 2 µl XErp1 IVT 4 µg Flag-antibody were bound to beads. IP was performed for 30 min at RT. After IP, the supernatant sample was taken and beads were washed two times with PBS containing 0.025 % Tween20 and two times with PBS. For western blot analysis beads were supplemented with 1.5x sample buffer.

6.5.2. IP of cycB3 from CSF extract

Flag-IP of Flag-cycB3^{WT} or Flag-cycB3^{TEM} was performed in CSF extract arrested with 1:20 C-terminal XErp1 and MG262 (100 µM) in metaphase II. IVT of cycB3 (1:20 – 1:24) and XErp1 variants (1:20) was added and incubated for 10 min at 20 °C. An input sample (1:10 diluted in 1.5x Lämmli) was taken and CSF extract was added to washed beads. Dynabeads were previously bound with 4 µg Flag-antibody for 2 µl IVT to pull-down as described in producer protocol. IP was performed for 30 min at RT. A supernatant sample (1:10 diluted in 1.5x Lämmli) was taken and beads were washed two times with PBST and once with PBS. Afterwards, beads were treated with one-half of the IP volume λ-phosphatase mix and incubated for 50 min at 30 °C. To stop the λ-phosphatase reaction the other half of IP volume of 3x Lämmli was added. The bead samples were therefore 10-fold more concentrated than the input and supernatant samples.

6.5.3. IP of cycB3 and cycB1 from CSF extract

For the comparison of binding partners of cycB1 and cycB3, CSF extract was supplemented with 100 µM MG262 and 10 µM okadaic acid to maintain the extract in metaphase II with an active APC/C. CSF was distributed and either control IVT or Flag-tag cycB1 or cycB3 was added (1:10-1:20) and the extract was incubated at 20 °C for 15 min. Dynabeads previously bound to 1 µg antibody per 10 µl extract where washed and prepared for the extract addition. After the input sample was taken (1:10 diluted in 1.5 x Lämmli), IP was performed with 60 µl extract for 1 h at RT on a spinning wheel. The supernatant sample was taken and beads were washed three times with PBS with 0.025 % Tween 20. Beads were resuspended in 20 µl 1.5 x Lämmli and 10 µl were loaded for analysis on SDS-PAGE.

6.5.4. IP for Cks2 depletion from CSF extract

For Cks2 depletion from CSF extract, 6 µg of Cks2 antibody for 70 µl CSF extract were bound to beads. Depletion took place over three rounds of Cks2 pull-down for 30 min at RT. After depletion, the supernatant extract was used for time course experiments.

6.6. XErp1 degradation assay in CSF

For investigation of the degradation behaviour of different XErp1 mutants, CSF extract was incubated with 1:20 to 1:40 µl XErp IVT for 5-10min at 20 °C. The time course was started by the addition of cycB3 IVT (1:13 to 1:20). At the respective time points samples were taken and either directly diluted 1:10 in 1.5x Lämmli or added to the same amount of λ-Phosphatase mix and dephosphorylated. For comparison of cycB3^{WT} and cycB3^{TEM}, no ectopic XErp1 construct was supplemented.

6.7. λ-Phosphatase treatment

For the dephosphorylation of CSF extract samples, two phosphatase mixes were used depending on whether the sample was loaded with non-λ-phosphatase-treated samples or not. If only CSF samples were compared via SDS-PAGE and immunoblot, CSF extract was mixed 1:2 with λ-phosphatase mix, containing 1 volume of λ-Phosphatase (NEB) with 1 volume of water, 10 volumes 10 mM $MnCl_2$ and 10 volumes of 10x PMP buffer (NEB). The phosphatase mix for comparing untreated with treated samples contained 1:20 λ-phosphatase in 1 mM $MnCl_2$ and 1x PMP-buffer, CSF extract was diluted 1:5 with the phosphatase mix.

For dephosphorylation of oocyte lysate, oocytes were lysed without NaF and β-Glycerophosphate and incubated with 1:4 λ-Phosphatase mix, containing 1 volume λ-Phosphatase with 2 volumes 10x PMP buffer and 2 volumes 10 mM $MnCl_2$, after lysis. Samples were incubated for 30-45 min at 30 °C. The dephosphorylation reaction was stopped by the addition of Lämmli, either 1:5 or 1:2 for CSF extract or 1:3 for oocyte lysate.

6.8. SDS-PAGE

Samples were loaded on SDS-gels for analysis, either conventional SDS-PAGE or Tricine-SDS-PAGE (Haider et al., 2012) was used. The percentage of acrylamide varied from 8 to 12 % per gel. Each gel was loaded with 5 µl of BenchMark ™ Protein Ladder (Invitrogen) and 5 µl of the samples. Samples were heated at 95 °C for 5 min previous to loading. Small and big gels were run at 30 mA or 60 mA respectively. Tricine gels were run at 180 to 200 V.

6.9. Western blot

For the transfer of the separated proteins from SDS-gel to a nitrocellulose or PVDF membrane, a western blot was performed using the wet transfer method. Small gels were blotted for 1 h at 120 V while large gels were transferred for 2 h at 120 V. After the transfer, the membrane was stained with Ponceau solution to mark BenchMark and blocked with 3-5 % milk in PBST for at least 30 min at room temperature. To detect proteins, the membrane was incubated overnight with the primary antibody. On the next day, the membrane was washed three times with PBST and incubated with the secondary antibody for 1 h at room temperature. Before detection with ECL solution, the membrane was washed again three times in PBST. For detection, the membrane was laid in sufficient SuperSignal West Pico PLUS (Thermo Fisher) solution and then imagined on the LAS-3000 (Fujifilm).

6.10. Coomassie staining

For staining SDS-gels in Coomassie, they were put into 1 to 5 diluted Coomassie solution and heated for around 2 to 3 min in the microwave. Staining took place for around 20 min at moderate shaking at room temperature. Afterwards, the Coomassie solution was discarded and gels were destained with Destain solution for around 1 h at room temperature while moderate shaking. The destain solution was exchanged at least once during this time.

6.11. Molecular Cloning

All plasmids were cloned via insertion of the gene of interest in the multiple cloning site with FseI and AscI. Primers were always designed to insert the gene of interest in frame to N- or C-terminal tags. For XErp1-cycB3 fusion constructs, cycB3 was inserted via the AscI cutting site at the 3’ end of XErp1, therefore primer containing an AscI cutting site at the 5’ and 3’ end where used for cycB3 amplification.

6.11.1. Polymerase chain reaction (PCR) for amplifying

For amplification of genes, PCR was performed with 10 ng template DNA, 0.2875 µM forward and reverse primer, 200 µM dNTPs, 3 %DMSO, 1x Phusion buffer and 2 U/50 µl PCR reaction Phusion® High-Fidelity DNA Polymerase (NEB). PCR program was used as described in the producer protocol with three different annealing temperatures ranging from 55 °C to 70 °C and elongation time varying from 30 s to 1 min per 1000 bp. Afterwards, DNA was separated on a 1 % Agarose gel at 120 V in a TBE buffer. DNA with the correct size was cut out and purified via NucleoSpin Gel and PCR Clean-up kit (Macherey-Nagel).

6.11.2. PCR for mutagenesis

For mutation of single base pairs primers containing mutation were designed with at least 12 bases unaltered to 3’ and 5’ end. Both forward and reverse primers contained mutation. PCR was performed with the same composition and program as above. After PCR, DNA was digested with DpnI (1.18 U/µl) for 2 h at 37 °C.

6.11.3. Digestion with restriction enzymes

For digestion, desired DNA was supplemented with CutSmart (NEB) and 0.1 U/µl restriction enzyme for 1 h at 37 °C. Backbone digestions were separated on a 1 % Agarose gel while inserts were cleaned from the digestion mix via NucleoSpin Gel and PCR Clean-up kit (Macherey-Nagel).

6.11.4. Ligation

For ligation backbone and insert were mixed in a ratio of 1:3 and incubated with 1x T4 Ligase buffer and 20 U/µl T4 Ligase (NEB) for at least 20 min at room temperature.

6.11.5. Transformation

Ligated DNA was transformed into NEB® Turbo Competent *E. coli*. For 10 µl ligation mix, 100 µl bacteria and for mutagenesis mix, 200 µl per mutagenesis PCR reaction were used. First thawed bacteria were mixed with DNA and kept for 30 min on ice. Then a heat shock was performed for 45 s at 42 °C. For transformation with DNA from a mutagenesis PCR bacteria were recovered with 1 ml SOC medium for 1 h at 37 °C and then plated on Agarose plates containing the specific antibiotics for selection, while for transformation of ligation, bacteria were directly plated on Agarose plates after heat shock.

6.11.6. Mini-Prep

To screen colonies for correct plasmid, 2 ml cultures with TB+ medium were cultivated with single colonies for 5-7 h at 37 °C and 180 rpm. Cells were harvested by centrifugation for 2 min at 2000 g and DNA was isolated with NucleoSpin Plasmid kit (Macherey-Nagel). For testing correct ligation, test digestion was performed while mutagenesis PCR plasmids were sent for sequencing.

6.11.7. Midi-Prep

To obtain a large amount of plasmid DNA, a 50 ml culture of bacteria with the desired plasmid was grown overnight at 37 °C 180 rpm. Cells were harvested at 3000 g for 15 min and purified with a NucleoBond Xtra Midi kit (Macherey-Nagel). All DNA received via Midi-Prep were sequenced to verify the intact gene of interest as well as the transition into the backbone.

6.12. Synthesis of mRNA

For mRNA synthesis, the plasmid containing the gene of interest (pCS2 backbone) was linearized with a restriction enzyme, either XbaI or AscI, for 5 to 6 h. In total 10 µg DNA was digested with 0.8 U/µl enzyme in 50 µl reaction volume. DNA was precipitated by the addition of 2.5 µl 0.5 M EDTA, 5 µl 5 M ammonium acetate and 100 µl 100 % EtOH for at least 1h at -20 °C.

Precipitated DNA was centrifuged for 30 min at full speed at 4 °C and the dry pellet was solved in water. For in-vitro transcription, the mMESSAGE mMACHINE™ T7 ULTRA transcription kit (Invitrogen) was used. All incubation steps were performed at 37 °C and work was performed RNase-free. Transcription was performed with 1 µg linearized DNA supplemented with 10 µl NTP/ARCA buffer, 2 µl 10x T7 reaction buffer, 2 µl T7 enzyme mix, 1 µl RNAsin and filled up to 20 µl with water. The reaction mix was incubated for 2.5 h. For poly-A-tailing, first DNA was digested by the addition of 1 µl TURBO DNase for 15 min, then 36 µl water, 20 µl E-PAP buffer, 10 µl 25 mM $MnCl_2$, 10 µl ATP solution and 4 µl E-PAP was added. After incubation for 1 h mRNA was precipitated by the addition of 50 µl $LiCl_2$. For full precipitation, the mix was incubated overnight at -20 °C and centrifuged for 30 min at full speed at 4 °C on the following day. mRNA pellet was washed once with 200 µl 70 % EtOH, dried at 37 °C for 10 to 15 min and solved in water. After adjusting mRNA concentration to 1-1.7 µg/µl, aliquots were snap frozen in liquid nitrogen and stored at -80 °C.

6.13. In vitro transcription and translation

For the production of in vitro transcribed and translated proteins (IVT), TNT® SP6 High-Yield Wheat Germ Protein Expression System (Promega) was used. For a reaction volume of in total 50 µl, 10 µg plasmid containing the gene of interest (in a pCS2 vector) was mixed with 30 µl wheat germ extract and filled up with water (MiliQ) to 50 µl. The reaction mix was incubated for 2.5 h and afterwards aliquoted, snap-frozen in liquid nitrogen and stored at -80 °C.

6.14. Primary Antibodies

Antigen	Species	Producer	Final concentration/ dilution (WB)
Xl_Cks2	rabbit	Self-made (PSL against CLFRRPLPKEQQK and CLFRRPLPKDQQK peptide)	1 µg/ml
Xl_cycB2	mouse	Santa Cruz (sc-53239)	0.4 µg/ml
Xl_cycB3	rabbit	Self-made (purified against n-terminal CycB3 aa1-110)	0.15 ng/ml
Xl_cycB3	rabbit	Self-made (PSL against aa6-22: RPSRPVASKLPKLGKPVC peptide)	Used for Trim-away approach
Hs_Cdk1	mouse	Santa Cruz (sc-54)	1 µg/ml
Hs_ppCdk1	mouse	Gift from Tim Hunt	1:1000
Xl_Cdc27	rabbit	Self-made	0.5 µg/ml
Flag	mouse	Sigma-Aldrich F1804	1 µg/ml
Flag	rabbit	Self-made against Flag-peptide	1:1000
tubulin	mouse	Monoclonal antibody clone AA4.3	1:100
FITC-anti-tubulin	mouse	Sigma (F2168)	1:500 for IF
Hs_Plk1	mouse	Origene	3.17 µg/ml
Xl_Plx1	rabbit	Self-made	0.12ng/µl
P150	mouse	BD Transduction Laboratories (610473)	0.25 µg/ml
Xl_XErp1	rabbit	Self-made form rabbit 1694	0.53 µg/ml
Xl_XErp1 pT97	rabbit	Self-made against pT97 peptide (PSL)	1 µg/ml
Xl_XErp1 pT170	rabbit	Self-made against pT170 peptide (PSL)	1-2 µg/ml

6.15. Secondary antibodies

All secondary antibodies were coupled to horseradish peroxidase (HRP).

	Species	Producer	Dilution
Anti-rabbit	goat	Jackson Immuno Research Laboratories	1:5,000 -1:10,000 (0.16 -0.08 µg/ml)
Anti-mouse	goat	Jackson Immuno Research Laboratories	1:5,000 -1:10,000 (0.16 -0.08 µg/ml)
Anti-rabbit (confirmation specific)	mouse	Cell Signaling Technology	1:5,000

6.16. Chemicals

Name	Stock concentration	Final concentration
Ampicillin	100 mg/ml	100 µg/ml
APS	10 %	
ATP	100 mM/10 mM	50 µM-500 µM
BI2536	10 mM or 4 mM	20 µM
Cytochalasin B	10 mg/ml in DMSO	0.01 mg/ml
Chloramphenicol	34 mg/ml	34 µg/ml
cOmplete Protease inhibitor cocktail (Roche)	25x	1x
Flavopiridol	100 mM, pre-dilution 1:4 (in DMSO)	10 µM
Höchst 33342	1 mg/ml	1 µg/ml
MG262	10 mM	100 µM
Okadaic acid	1 mM, pre-dilution 1:5 (in DMSO)	1-10 µM
Progesterone	5 mg/ml in EtOH (16 mM)	5 µg/ml

6.17. Buffer

CSF extract /Stage VI buffer	
MMR-buffer	5 mM HEPES, 0.1 mM EDTA, 100 mM NaCl, 2 mM KCl, 1 mM $MgCl_2$, 2 mM $CaCl_2$, pH 7.6
CSF-XB buffer	100 mM KCl, 2 mM $MgCl_2$, 0.1 mM $CaCl_2$, 50 mM Sucrose, 10 mM HEPES, 5 mM EGTA, pH 7.7 with KOH
De-jellying solution	100 mM KCl, 1 mM $MgCl_2$, 0.1 mM $CaCl_2$, 2 % (w/v) L-cysteine (Sigma), pH 7.8 with NaOH
MBS-buffer	88 mM NaCl, 10 mM KCl, 10 mM $MgSO_4$, 25 mM $NaHCO_3$, 0.7 mM $CaCl_2$, 50 mM HEPES pH 7.8
OR2 buffer	82.5 mM NaCl, 2.5 mM KCl, 1 mM $CaCl_2$, 1 mM $MgCl_2$, 1 mM Na_2HPO_4, 5 mM HEPES pH 7.8
Oocyte lysis buffer	46 µM NaF, 4.6 µM β-Glycerophosphate and 0.912x cOmplete Protease-inhibitor in PE-LB (PE LB™ for Mammalian Cell G-Biosciences)
Buffer for SDS-PAGE/western blot/Coomassie	
3x Lämmli (sample buffer)	180 mM Tris HCl pH 6.8, 10 % SDS (w/v), 30 % Glycerol, 15 % β-Mercaptoethanol (w/v), Bromphenolblue
Running buffer	25 mM Tris, 190 mM Glycine, 0.05 % SDS
Western blot transfer buffer	25 mM Tris, 190 mM Glycine, 0.01 % SDS, 20 % MeOH
Coomassie	45 % EtOH, 10 % Acetic acid, 0.25 % Brilliant blue R in H_2O
Destain solution (for Coomassie)	25 % EtOH, 7 % Acetic acid in H_2O
Ponceau	0.2 % Ponceau S, 1 % Acetic acid
SDS-PAGE lower buffer	1.5 M Tris, 20 % SDS
Other buffers	
PBS	137 mM NaCl, 2.7 mM KCl, 10 mM Na2HPO4, 2 mM KH2PO4 pH 7.4
IP-buffer	20 mM Tris-HCl, 100 mM NaCl, 10 mM EDTA, 5 mM NaF, 1 mM NaVO3, 1 mM DTT, 1x Protease Inhibitor, 1x PhosStop (Nach Isoda et al.)

PB-buffer (kinase assay buffer)	1 % Glycerol, 20 mM EGTA, 15 mM MgCl2, 1 mM DTT, 1x PhosStop, 1x Complete in PBS (137 mM NaCl, 2,7 mM KCl, 10 mM Na_2HPO_4, 2 mM KH_2PO_4) (stand 25.11.22)
TBE buffer	89 mM Tris-borate, 89 mM boric acid, 2 mM EDTA pH 8.3

7. Abbreviations

aa	amino acid
AB	antibody
APC/C	anaphase-promoting complex/cyclosome
APS	ammonium peroxodisulfate
Arpp19	cAMP-regulated phosphoprotein 19
ATP	adenosine triphosphate
CaMKII	calcium/calmodulin-dependent kinase II
cAMP	cyclic adenosine monophosphate
CAK	Cdk-activating kinase
CaN	Calcineurin
Cdc	cell division cycle
Cdc27	cell division cycle 27 or APC3
Cdk	cyclin-dependent kinase
C. elegans	*Caenorhabditis elegans*
CK	casein kinase
CPEB	cytoplasmic polyadenylation element binding protein
CSF	cytostatic factor
cyc	cyclin
D. melanogaster	*Drosophila melanogaster*
D. rerio	*Danio rerio*
DMSO	dimethyl sulfoxide
DNA	deoxyribonucleic acid
DNase	deoxyribonuclease
dNTP	deoxynucleoside triphosphate
DTT	dithiothreitol
E. coli	*Escherichia coli*
EDTA	ethylenediaminetetraacetic acid
EGTA	ethylene glycol-bis(2-aminoethyl ether)-N,N,N′,N′-tetraacetic acid
Emi1	early mitotic inhibitor 1
EtOH	ethanol
FITC	Fluorescein
FL	Flavopiridol
Flag	3x FLAG-epitope tag
G. gallus	*Gallus gallus*
GSK3	glycogen synthase kinase 3
GVBD	germinal vesicle breakdown
Gwl	Greatwall
h	hour(s)
H1	Histone H1
hCG	human chorionic gonadotropin
HEPES	2-[4-(2-hydroxyethyl)piperazin-1-yl]ethanesulfonic acid
His	6x Histidine-tag
H. sapiens	*Homo sapiens*
IP	immunoprecipitation
IPTG	isopropyl-beta-D-thiogalactopyranoside
IVT	in vitro transcribed and translated protein
MI	first meiotic division
MII	second meiotic division
MAPK	mitogen-activated protein kinase

MBT	midblastula transition
MBP	maltose-binding protein
MeOH	Methanol
min	minute(s)
MIH	maturation-inducing hormone
M. musculus	*Mus musculus*
Mos	proto-oncogene c-Mos
MPF	maturation-promoting factor
mRNA	messenger RNA
Myc	6x Myc-epitope tag
Myt1	membrane-associated, tyrosine- and threonine-specific Cdk1 inhibitory kinase
Ni-NTA	Nickel-Nitrolotriacetic acid
OD600	optical density at 600 nm
o/n	overnight
$p90^{Rsk}$	90 kDa ribosomal protein S6 kinase
PBD	polo-box domain
PBS	phosphate-buffered saline
PCR	polymerase chain reaction
PG	progesterone
PKA	protein kinase A
Plk1	polo-like kinase 1
Plx1	*Xenopus laevis* polo-like kinase 1
PPX	protein phosphatase X (X is a number)
pT97	phosphorylated T97 in XErp1
RINGO	rapid inducer of G(2)/M transition in oocytes or Speedy
RNA	Ribonucleic acid
rpm	rounds per minute
RT	room temperature
s	second(s)
SDS-PAGE	sodium dodecyl sulfate-polyacrylamide gel electrophoresis
$SCF^{\beta\text{-TRCP}}$	SCF complex with the F-Box protein beta-transducin repeat-containing protein
Tris	2-amino-2-(hydroxymethyl)propane-1,3-diol
WB	western blot
Wee1	Wee1-like protein
WT	wild-type
XErp1	*Xenopus laevis* Emi1 related protein 1 or Emi2
X. laevis	*Xenopus laevis*

8. References

Abrieu, A., Brassac, T., Galas, S., Fisher, D., Labbé, J. C., & Dorée, M. (1998). The Polo-like kinase Plx1 is a component of the MPF amplification loop at the G2/M-phase transition of the cell cycle in Xenopus eggs. *J Cell Sci, 111 (Pt 12)*, 1751-1757. doi:10.1242/jcs.111.12.1751

Al-Rawi, A., Kaye, E., Korolchuk, S., Endicott, J. A., & Ly, T. (2023). Cyclin A and Cks1 promote kinase consensus switching to non-proline-directed CDK1 phosphorylation. *Cell Rep, 42*(3), 112139. doi:10.1016/j.celrep.2023.112139

Archambault, V., & Carmena, M. (2012). Polo-like kinase-activating kinases: Aurora A, Aurora B and what else? *Cell Cycle, 11*(8), 1490-1495. doi:10.4161/cc.19724

Asfaha, J. B., Örd, M., Carlson, C. R., Faustova, I., Loog, M., & Morgan, D. O. (2022). Multisite phosphorylation by Cdk1 initiates delayed negative feedback to control mitotic transcription. *Current Biology, 32*(1), 256-263.e254. doi:10.1016/j.cub.2021.11.001

Avilov, I., Horokhovskyi, Y., Cai, M., Orzechowski, A., Welp, L., Urlaub, H., Liepe, J., & Lenart, P. (2023). Phosphoproteomics identifies targets of Mos-MAPK regulating translation and spindle organization in oocyte meiosis. *bioRxiv*, 2023.2011.2027.568807. doi:10.1101/2023.11.27.568807

Bandyopadhyay, S., Bhaduri, S., Örd, M., Davey, N. E., Loog, M., & Pryciak, P. M. (2020). Comprehensive Analysis of G1 Cyclin Docking Motif Sequences that Control CDK Regulatory Potency In Vivo. *Current Biology, 30*(22), 4454-4466.e4455. doi:10.1016/j.cub.2020.08.099

Bax, B., Carter, P. S., Lewis, C., Guy, A. R., Bridges, A., Tanner, R., Pettman, G., Mannix, C., Culbert, A. A., Brown, M. J., Smith, D. G., & Reith, A. D. (2001). The structure of phosphorylated GSK-3beta complexed with a peptide, FRATtide, that inhibits beta-catenin phosphorylation. *Structure, 9*(12), 1143-1152. doi:10.1016/s0969-2126(01)00679-7

Bhaduri, S., & Pryciak, P. M. (2011). Cyclin-specific docking motifs promote phosphorylation of yeast signaling proteins by G1/S Cdk complexes. *Curr Biol, 21*(19), 1615-1623. doi:10.1016/j.cub.2011.08.033

Blengini, C. S., Ibrahimian, P., Vaskovicova, M., Drutovic, D., Solc, P., & Schindler, K. (2021). Aurora kinase A is essential for meiosis in mouse oocytes. *PLOS Genetics, 17*(4), e1009327. doi:10.1371/journal.pgen.1009327

Booher, R. N., Holman, P. S., & Fattaey, A. (1997). Human Myt1 is a cell cycle-regulated kinase that inhibits Cdc2 but not Cdk2 activity. *J Biol Chem, 272*(35), 22300-22306. doi:10.1074/jbc.272.35.22300

Bouftas, N., Schneider, L., Halder, M., Demmig, R., Baack, M., Cladière, D., Walter, M., Al Abdallah, H., Kleinhempel, C., Messaritaki, R., Müller, J., Passarelli, F., Wehrle, P., Heim, A., Wassmann, K., & Mayer, T. U. (2022). Cyclin B3 implements timely vertebrate oocyte arrest for fertilization. *Developmental Cell*. doi:10.1016/j.devcel.2022.09.005

Bourne, Y., Watson, M. H., Hickey, M. J., Holmes, W., Rocque, W., Reed, S. I., & Tainer, J. A. (1996). Crystal structure and mutational analysis of the human CDK2 kinase complex with cell cycle-regulatory protein CksHs1. *Cell, 84*(6), 863-874. doi:10.1016/s0092-8674(00)81065-x

Brown, N. R., Korolchuk, S., Martin, M. P., Stanley, W. A., Moukhametzianov, R., Noble, M. E. M., & Endicott, J. A. (2015). CDK1 structures reveal conserved and unique features of the essential cell cycle CDK. *Nat Commun, 6*, 6769. doi:10.1038/ncomms7769

Brown, N. R., Lowe, E. D., Petri, E., Skamnaki, V., Antrobus, R., & Johnson, L. N. (2007). Cyclin B and cyclin A confer different substrate recognition properties on CDK2. *Cell Cycle, 6*(11), 1350-1359. doi:10.4161/cc.6.11.4278

Brown, N. R., Noble, M. E., Endicott, J. A., & Johnson, L. N. (1999). The structural basis for specificity of substrate and recruitment peptides for cyclin-dependent kinases. *Nat Cell Biol, 1*(7), 438-443. doi:10.1038/15674

Busa, W. B., & Nuccitelli, R. (1985). An elevated free cytosolic Ca2+ wave follows fertilization in eggs of the frog, Xenopus laevis. *J Cell Biol, 100*(4), 1325-1329. doi:10.1083/jcb.100.4.1325

Castilho, P. V., Williams, B. C., Mochida, S., Zhao, Y., & Goldberg, M. L. (2009). The M phase kinase Greatwall (Gwl) promotes inactivation of PP2A/B55delta, a phosphatase directed against CDK phosphosites. *Mol Biol Cell, 20*(22), 4777-4789. doi:10.1091/mbc.e09-07-0643

Castro, A., Peter, M., Magnaghi-Jaulin, L., Vigneron, S., Galas, S., Lorca, T., & Labbé, J.-C. (2001). Cyclin B/cdc2 Induces c-Mos Stability by Direct Phosphorylation in Xenopus Oocytes. *Molecular Biology of the Cell, 12*(9), 2660-2671. doi:10.1091/mbc.12.9.2660

Chang, C. I., Xu, B. E., Akella, R., Cobb, M. H., & Goldsmith, E. J. (2002). Crystal structures of MAP kinase p38 complexed to the docking sites on its nuclear substrate MEF2A and activator MKK3b. *Mol Cell, 9*(6), 1241-1249. doi:10.1016/s1097-2765(02)00525-7

Cheng, K. Y., Noble, M. E., Skamnaki, V., Brown, N. R., Lowe, E. D., Kontogiannis, L., Shen, K., Cole, P. A., Siligardi, G., & Johnson, L. N. (2006). The role of the phospho-CDK2/cyclin A recruitment site in substrate recognition. *J Biol Chem, 281*(32), 23167-23179. doi:10.1074/jbc.M600480200

Coudreuse, D., & Nurse, P. (2010). Driving the cell cycle with a minimal CDK control network. *Nature, 468*(7327), 1074-1079. doi:10.1038/nature09543

Coverley, D., Laman, H., & Laskey, R. A. (2002). Distinct roles for cyclins E and A during DNA replication complex assembly and activation. *Nat Cell Biol, 4*(7), 523-528. doi:10.1038/ncb813

Dajani, R., Fraser, E., Roe, S. M., Yeo, M., Good, V. M., Thompson, V., Dale, T. C., & Pearl, L. H. (2003). Structural basis for recruitment of glycogen synthase kinase 3beta to the axin-APC scaffold complex. *Embo j, 22*(3), 494-501. doi:10.1093/emboj/cdg068

Daldello, E. M., Luong, X. G., Yang, C.-R., Kuhn, J., & Conti, M. (2019). Cyclin B2 is required for progression through meiosis in mouse oocytes. *Development, 146*(8), dev172734. doi:10.1242/dev.172734

Deyter, G. M. R., Furuta, T., Kurasawa, Y., & Schumacher, J. M. (2010). Caenorhabditis elegans Cyclin B3 Is Required for Multiple Mitotic Processes Including Alleviation of a Spindle Checkpoint–Dependent Block in Anaphase Chromosome Segregation. *PLOS Genetics, 6*(11), e1001218. doi:10.1371/journal.pgen.1001218

Duckworth, B. C., Weaver, J. S., & Ruderman, J. V. (2002). G2 arrest in Xenopus oocytes depends on phosphorylation of cdc25 by protein kinase A. *Proc Natl Acad Sci U S A, 99*(26), 16794-16799. doi:10.1073/pnas.222661299

Ducommun, B., Brambilla, P., Félix, M. A., Franza, B. R., Jr., Karsenti, E., & Draetta, G. (1991). cdc2 phosphorylation is required for its interaction with cyclin. *Embo j, 10*(11), 3311-3319. doi:10.1002/j.1460-2075.1991.tb04895.x

Dumont, J., Umbhauer, M., Rassinier, P., Hanauer, A., & Verlhac, M. H. (2005). p90Rsk is not involved in cytostatic factor arrest in mouse oocytes. *J Cell Biol, 169*(2), 227-231. doi:10.1083/jcb.200501027

Dumont, J. N. (1972). Oogenesis in Xenopus laevis (Daudin). I. Stages of oocyte development in laboratory maintained animals. *Journal of Morphology, 136*(2), 153-179. doi:10.1002/jmor.1051360203

Duncan, F. E., Schindler, K., Schultz, R. M., Blengini, C. S., Stein, P., Stricker, S. A., Wessel, G. M., & Williams, C. J. (2020). Unscrambling the oocyte and the egg: clarifying terminology of the female gamete in mammals. *Molecular Human Reproduction, 26*(11), 797-800. doi:10.1093/molehr/gaaa066

Dupré, A., Buffin, E., Roustan, C., Nairn, A. C., Jessus, C., & Haccard, O. (2013). The phosphorylation of ARPP19 by Greatwall renders the auto-amplification of MPF independently of PKA in Xenopus oocytes. *J Cell Sci, 126*(Pt 17), 3916-3926. doi:10.1242/jcs.126599

Dupré, A., Daldello, E. M., Nairn, A. C., Jessus, C., & Haccard, O. (2014). Phosphorylation of ARPP19 by protein kinase A prevents meiosis resumption in Xenopus oocytes. *Nat Commun, 5*, 3318. doi:10.1038/ncomms4318

Dupré, A., Jessus, C., Ozon, R., & Haccard, O. (2002). Mos is not required for the initiation of meiotic maturation in Xenopus oocytes. *Embo j, 21*(15), 4026-4036. doi:10.1093/emboj/cdf400

Ellederova, Z., del Rincon, S., Koncicka, M., Susor, A., Kubelka, M., Sun, D., & Spruck, C. (2019). CKS1 Germ Line Exclusion Is Essential for the Transition from Meiosis to Early Embryonic

Development. *Molecular and Cellular Biology, 39*(13), e00590-00518. doi:10.1128/MCB.00590-18

Evans, T., Rosenthal, E. T., Youngblom, J., Distel, D., & Hunt, T. (1983). Cyclin: a protein specified by maternal mRNA in sea urchin eggs that is destroyed at each cleavage division. *Cell, 33*(2), 389-396. doi:10.1016/0092-8674(83)90420-8

Fatemi, N., Salehi, N., Pignata, L., Palumbo, P., Cubellis, M. V., Ramazanali, F., Ray, P., Varkiani, M., Reyhani-Sabet, F., Biglari, A., Sparago, A., Acurzio, B., Palumbo, O., Carella, M., Riccio, A., & Totonchi, M. (2021). Biallelic variant in cyclin B3 is associated with failure of maternal meiosis II and recurrent digynic triploidy. *J Med Genet, 58*(11), 783-788. doi:10.1136/jmedgenet-2020-106909

Faustova, I., Bulatovic, L., Matiyevskaya, F., Valk, E., Örd, M., & Loog, M. (2021). A new linear cyclin docking motif that mediates exclusively S-phase CDK-specific signaling. *Embo j, 40*(2), e105839. doi:10.15252/embj.2020105839

Ferby, I., Blazquez, M., Palmer, A., Eritja, R., & Nebreda, A. R. (1999). A novel p34(cdc2)-binding and activating protein that is necessary and sufficient to trigger G(2)/M progression in Xenopus oocytes. *Genes Dev, 13*(16), 2177-2189. doi:10.1101/gad.13.16.2177

Finidori-Lepicard, J., Schorderet-Slatkine, S., Hanoune, J., & Baulieu, E.-E. (1981). Progesterone inhibits membrane-bound adenylate cyclase in Xenopus laevis oocytes. *Nature, 292*(5820), 255-257. doi:10.1038/292255a0

Fisher, D. L., & Nurse, P. (1996). A single fission yeast mitotic cyclin B p34cdc2 kinase promotes both S-phase and mitosis in the absence of G1 cyclins. *Embo j, 15*(4), 850-860.

Fujimitsu, K., Grimaldi, M., & Yamano, H. (2016). Cyclin-dependent kinase 1–dependent activation of APC/C ubiquitin ligase. *Science, 352*(6289), 1121-1124. doi:10.1126/science.aad3925

Furuno, N., Nishizawa, M., Okazaki, K., Tanaka, H., Iwashita, J., Nakajo, N., Ogawa, Y., & Sagata, N. (1994). Suppression of DNA replication via Mos function during meiotic divisions in Xenopus oocytes. *Embo j, 13*(10), 2399-2410. doi:10.1002/j.1460-2075.1994.tb06524.x

Gaffré, M., Martoriati, A., Belhachemi, N., Chambon, J. P., Houliston, E., Jessus, C., & Karaiskou, A. (2011). A critical balance between Cyclin B synthesis and Myt1 activity controls meiosis entry in Xenopus oocytes. *Development, 138*(17), 3735-3744. doi:10.1242/dev.063974

Gallant, P., & Nigg, E. A. (1994). Identification of a novel vertebrate cyclin: cyclin B3 shares properties with both A- and B-type cyclins. *Embo j, 13*(3), 595-605. doi:10.1002/j.1460-2075.1994.tb06297.x

Garrido, D., Bourouh, M., Bonneil, É., Thibault, P., Swan, A., & Archambault, V. (2020). Cyclin B3 activates the Anaphase-Promoting Complex/Cyclosome in meiosis and mitosis. *PLOS Genetics, 16*(11), e1009184. doi:10.1371/journal.pgen.1009184

Gerhart, J., Wu, M., & Kirschner, M. (1984). Cell cycle dynamics of an M-phase-specific cytoplasmic factor in Xenopus laevis oocytes and eggs. *J Cell Biol, 98*(4), 1247-1255. doi:10.1083/jcb.98.4.1247

Gheghiani, L., Loew, D., Lombard, B., Mansfeld, J., & Gavet, O. (2017). PLK1 Activation in Late G2 Sets Up Commitment to Mitosis. *Cell Reports, 19*(10), 2060-2073. doi:10.1016/j.celrep.2017.05.031

Gibson, T. J., Thompson, J. D., Blocker, A., & Kouzarides, T. (1994). Evidence for a protein domain superfamily shared by the cyclins, TFIIB and RB/p107. *Nucleic Acids Res, 22*(6), 946-952. doi:10.1093/nar/22.6.946

Glotzer, M., Murray, A. W., & Kirschner, M. W. (1991). Cyclin is degraded by the ubiquitin pathway. *Nature, 349*(6305), 132-138. doi:10.1038/349132a0

Gross, S. D., Schwab, M. S., Taieb, F. E., Lewellyn, A. L., Qian, Y.-W., & Maller, J. L. (2000). The critical role of the MAP kinase pathway in meiosis II in Xenopus oocytes is mediated by p90Rsk. *Current Biology, 10*(8), 430-438. doi:10.1016/S0960-9822(00)00425-5

Gutiérrez-Escribano, P., & Nurse, P. (2015). A single cyclin–CDK complex is sufficient for both mitotic and meiotic progression in fission yeast. *Nature Communications, 6*(1), 6871. doi:10.1038/ncomms7871

Haccard, O., Lewellyn, A., Hartley, R. S., Erikson, E., & Maller, J. L. (1995). Induction of Xenopus oocyte meiotic maturation by MAP kinase. *Dev Biol, 168*(2), 677-682. doi:10.1006/dbio.1995.1112

Haider, S. R., Reid, H. J., & Sharp, B. L. (2012). Tricine-SDS-PAGE. *Methods Mol Biol, 869*, 81-91. doi:10.1007/978-1-61779-821-4_8

Hara, M., Abe, Y., Tanaka, T., Yamamoto, T., Okumura, E., & Kishimoto, T. (2012). Greatwall kinase and cyclin B-Cdk1 are both critical constituents of M-phase-promoting factor. *Nat Commun, 3*, 1059. doi:10.1038/ncomms2062

Hardt, S. E., & Sadoshima, J. (2002). Glycogen synthase kinase-3beta: a novel regulator of cardiac hypertrophy and development. *Circ Res, 90*(10), 1055-1063. doi:10.1161/01.res.0000018952.70505.f1

Heim, A., Tischer, T., & Mayer, T. U. (2018). Calcineurin promotes APC/C activation at meiotic exit by acting on both XErp1 and Cdc20. *EMBO Rep, 19*(12). doi:10.15252/embr.201846433

Hochegger, H., Klotzbücher, A., Kirk, J., Howell, M., le Guellec, K., Fletcher, K., Duncan, T., Sohail, M., & Hunt, T. (2001). New B-type cyclin synthesis is required between meiosis I and II during Xenopus oocyte maturation. *Development, 128*(19), 3795-3807. doi:10.1242/dev.128.19.3795

Hoffmann, I., Clarke, P. R., Marcote, M. J., Karsenti, E., & Draetta, G. (1993). Phosphorylation and activation of human cdc25-C by cdc2--cyclin B and its involvement in the self-amplification of MPF at mitosis. *Embo j, 12*(1), 53-63. doi:10.1002/j.1460-2075.1993.tb05631.x

Huchon, D., Ozon, R., Fischer, E. H., & Demaille, J. G. (1981). The pure inhibitor of cAMP-dependent protein kinase initiates Xenopus laevis meiotic maturation. A 4-step scheme for meiotic maturation. *Mol Cell Endocrinol, 22*(2), 211-222. doi:10.1016/0303-7207(81)90092-7

Hutti, J. E., Jarrell, E. T., Chang, J. D., Abbott, D. W., Storz, P., Toker, A., Cantley, L. C., & Turk, B. E. (2004). A rapid method for determining protein kinase phosphorylation specificity. *Nat Methods, 1*(1), 27-29. doi:10.1038/nmeth708

Inoue, D., Ohe, M., Kanemori, Y., Nobui, T., & Sagata, N. (2007). A direct link of the Mos-MAPK pathway to Erp1/Emi2 in meiotic arrest of Xenopus laevis eggs. *Nature, 446*(7139), 1100-1104. doi:10.1038/nature05688

Isoda, M., Sako, K., Suzuki, K., Nishino, K., Nakajo, N., Ohe, M., Ezaki, T., Kanemori, Y., Inoue, D., Ueno, H., & Sagata, N. (2011). Dynamic regulation of Emi2 by Emi2-bound Cdk1/Plk1/CK1 and PP2A-B56 in meiotic arrest of Xenopus eggs. *Dev Cell, 21*(3), 506-519. doi:10.1016/j.devcel.2011.06.029

Izumi, T., & Maller, J. L. (1993). Elimination of cdc2 phosphorylation sites in the cdc25 phosphatase blocks initiation of M-phase. *Mol Biol Cell, 4*(12), 1337-1350. doi:10.1091/mbc.4.12.1337

Jackson, P. K., Chevalier, S., Philippe, M., & Kirschner, M. W. (1995). Early events in DNA replication require cyclin E and are blocked by p21CIP1. *J Cell Biol, 130*(4), 755-769. doi:10.1083/jcb.130.4.755

Jacobs, D., Glossip, D., Xing, H., Muslin, A. J., & Kornfeld, K. (1999). Multiple docking sites on substrate proteins form a modular system that mediates recognition by ERK MAP kinase. *Genes Dev, 13*(2), 163-175. doi:10.1101/gad.13.2.163

Jacobs, H. W., Knoblich, J. A., & Lehner, C. F. (1998). Drosophila Cyclin B3 is required for female fertility and is dispensable for mitosis like Cyclin B. *Genes & Development, 12*(23), 3741-3751. doi:10.1101/gad.12.23.3741

Jessus, C., Munro, C., & Houliston, E. (2020). Managing the Oocyte Meiotic Arrest—Lessons from Frogs and Jellyfish. *Cells, 9*(5), 1150. doi:10.3390/cells9051150

Jorgensen, A., & Rajpert-De Meyts, E. (2014). Regulation of meiotic entry and gonadal sex differentiation in the human: normal and disrupted signaling. *Biomol Concepts, 5*(4), 331-341. doi:10.1515/bmc-2014-0014

Karaïskou, A., Jessus, C., Brassac, T., & Ozon, R. (1999). Phosphatase 2A and polo kinase, two antagonistic regulators of cdc25 activation and MPF auto-amplification. *J Cell Sci, 112 (Pt 21)*, 3747-3756. doi:10.1242/jcs.112.21.3747

Karaiskou, A., Perez, L. H., Ferby, I., Ozon, R., Jessus, C., & Nebreda, A. R. (2001). Differential regulation of Cdc2 and Cdk2 by RINGO and cyclins. *J Biol Chem, 276*(38), 36028-36034. doi:10.1074/jbc.M104722200

Karasu, M. E., Bouftas, N., Keeney, S., & Wassmann, K. (2019). Cyclin B3 promotes anaphase I onset in oocyte meiosis. *J Cell Biol, 218*(4), 1265-1281. doi:10.1083/jcb.201808091

Knuesel, M. T., Meyer, K. D., Bernecky, C., & Taatjes, D. J. (2009). The human CDK8 subcomplex is a molecular switch that controls Mediator coactivator function. *Genes Dev, 23*(4), 439-451. doi:10.1101/gad.1767009

Kõivomägi, M., Örd, M., Iofik, A., Valk, E., Venta, R., Faustova, I., Kivi, R., Balog, E. R. M., Rubin, S. M., & Loog, M. (2013). Multisite phosphorylation networks as signal processors for Cdk1. *Nature Structural & Molecular Biology, 20*(12), 1415-1424. doi:10.1038/nsmb.2706

Kõivomägi, M., Valk, E., Venta, R., Iofik, A., Lepiku, M., Balog, E. R., Rubin, S. M., Morgan, D. O., & Loog, M. (2011). Cascades of multisite phosphorylation control Sic1 destruction at the onset of S phase. *Nature, 480*(7375), 128-131. doi:10.1038/nature10560

Kõivomägi, M., Valk, E., Venta, R., Iofik, A., Lepiku, M., Morgan, D. O., & Loog, M. (2011). Dynamics of Cdk1 substrate specificity during the cell cycle. *Mol Cell, 42*(5), 610-623. doi:10.1016/j.molcel.2011.05.016

Lefebvre, C., Terret, M. E., Djiane, A., Rassinier, P., Maro, B., & Verlhac, M. H. (2002). Meiotic spindle stability depends on MAPK-interacting and spindle-stabilizing protein (MISS), a new MAPK substrate. *J Cell Biol, 157*(4), 603-613. doi:10.1083/jcb.200202052

Lemonnier, T., Daldello, E. M., Poulhe, R., Le, T., Miot, M., Lignières, L., Jessus, C., & Dupré, A. (2021). The M-phase regulatory phosphatase PP2A-B55δ opposes protein kinase A on Arpp19 to initiate meiotic division. *Nature Communications, 12*(1), 1837. doi:10.1038/s41467-021-22124-0

Li, J., Tang, J. X., Cheng, J. M., Hu, B., Wang, Y. Q., Aalia, B., Li, X. Y., Jin, C., Wang, X. X., Deng, S. L., Zhang, Y., Chen, S. R., Qian, W. P., Sun, Q. Y., Huang, X. X., & Liu, Y. X. (2018). Cyclin B2 can compensate for Cyclin B1 in oocyte meiosis I. *J Cell Biol, 217*(11), 3901-3911. doi:10.1083/jcb.201802077

Li, Y., Wang, L., Zhang, L., He, Z., Feng, G., Sun, H., Wang, J., Li, Z., Liu, C., Han, J., Mao, J., Li, P., Yuan, X., Jiang, L., Zhang, Y., Zhou, Q., & Li, W. (2019). Cyclin B3 is required for metaphase to anaphase transition in oocyte meiosis I. *J Cell Biol, 218*(5), 1553-1563. doi:10.1083/jcb.201808088

Liu, J., Grimison, B., & Maller, J. L. (2007). New insight into metaphase arrest by cytostatic factor: from establishment to release. *Oncogene, 26*(9), 1286-1289. doi:10.1038/sj.onc.1210203

Loog, M., & Morgan, D. O. (2005). Cyclin specificity in the phosphorylation of cyclin-dependent kinase substrates. *Nature, 434*(7029), 104-108. doi:10.1038/nature03329

Lorca, T., Cruzalegui, F. H., Fesquet, D., Cavadore, J.-c., Méry, J., Means, A., & Dorée, M. (1993). Calmodulin-dependent protein kinase II mediates inactivation of MPF and CSF upon fertilization of Xenopus eggs. *Nature, 366*(6452), 270-273. doi:10.1038/366270a0

Lowery, D. M., Lim, D., & Yaffe, M. B. (2005). Structure and function of Polo-like kinases. *Oncogene, 24*(2), 248-259. doi:10.1038/sj.onc.1208280

Lozano, J. C., Vergé, V., Schatt, P., Juengel, J. L., & Peaucellier, G. (2012). Evolution of cyclin B3 shows an abrupt three-fold size increase, due to the extension of a single exon in placental mammals, allowing for new protein-protein interactions. *Mol Biol Evol, 29*(12), 3855-3871. doi:10.1093/molbev/mss189

Maller, J. L., & Krebs, E. G. (1977). Progesterone-stimulated meiotic cell division in Xenopus oocytes. Induction by regulatory subunit and inhibition by catalytic subunit of adenosine 3':5'-monophosphate-dependent protein kinase. *J Biol Chem, 252*(5), 1712-1718. doi:10.1016/S0021-9258(17)40606-5

Maller, J. L., Schwab, M. S., Gross, S. D., Taieb, F. E., Roberts, B. T., & Tunquist, B. J. (2002). The mechanism of CSF arrest in vertebrate oocytes. *Mol Cell Endocrinol, 187*(1-2), 173-178. doi:10.1016/s0303-7207(01)00695-5

Malumbres, M., & Barbacid, M. (2001). To cycle or not to cycle: a critical decision in cancer. *Nat Rev Cancer, 1*(3), 222-231. doi:10.1038/35106065

Margolis, S. S., Perry, J. A., Weitzel, D. H., Freel, C. D., Yoshida, M., Haystead, T. A., & Kornbluth, S. (2006). A role for PP1 in the Cdc2/Cyclin B-mediated positive feedback activation of Cdc25. *Mol Biol Cell, 17*(4), 1779-1789. doi:10.1091/mbc.e05-08-0751

Martínez-Alonso, D., & Malumbres, M. (2020). Mammalian cell cycle cyclins. *Semin Cell Dev Biol, 107*, 28-35. doi:10.1016/j.semcdb.2020.03.009

Masui, Y., & Markert, C. L. (1971). Cytoplasmic control of nuclear behavior during meiotic maturation of frog oocytes. *Journal of Experimental Zoology, 177*(2), 129-145. doi:10.1002/jez.1401770202

McGrath, D. A., Balog, E. R. M., Kõivomägi, M., Lucena, R., Mai, M. V., Hirschi, A., Kellogg, D. R., Loog, M., & Rubin, S. M. (2013). Cks confers specificity to phosphorylation-dependent CDK signaling pathways. *Nature Structural & Molecular Biology, 20*(12), 1407-1414. doi:10.1038/nsmb.2707

Meng, T. G., Lei, W. L., Li, J., Wang, F., Zhao, Z. H., Li, A., Wang, Z. B., Sun, Q. Y., & Ou, X. H. (2020). Degradation of Ccnb3 is essential for maintenance of MII arrest in oocyte. *Biochem Biophys Res Commun, 521*(1), 265-269. doi:10.1016/j.bbrc.2019.10.124

Michowski, W., Chick, J. M., Chu, C., Kolodziejczyk, A., Wang, Y., Suski, J. M., Abraham, B., Anders, L., Day, D., Dunkl, L. M., Li Cheong Man, M., Zhang, T., Laphanuwat, P., Bacon, N. A., Liu, L., Fassl, A., Sharma, S., Otto, T., Jecrois, E., Han, R., Sweeney, K. E., Marro, S., Wernig, M., Geng, Y., Moses, A., Li, C., Gygi, S. P., Young, R. A., & Sicinski, P. (2020). Cdk1 Controls Global Epigenetic Landscape in Embryonic Stem Cells. *Mol Cell, 78*(3), 459-476.e413. doi:10.1016/j.molcel.2020.03.010

Mochida, S., & Hunt, T. (2007). Calcineurin is required to release Xenopus egg extracts from meiotic M phase. *Nature, 449*(7160), 336-340. doi:10.1038/nature06121

Mochida, S., Ikeo, S., Gannon, J., & Hunt, T. (2009). Regulated activity of PP2A–B55δ is crucial for controlling entry into and exit from mitosis in Xenopus egg extracts. *Embo j, 28*(18), 2777-2785. doi:10.1038/emboj.2009.238

Mochida, S., Rata, S., Hino, H., Nagai, T., & Novák, B. (2016). Two Bistable Switches Govern M Phase Entry. *Curr Biol, 26*(24), 3361-3367. doi:10.1016/j.cub.2016.10.022

Morgan, D. O. (2007). *The cell cycle: Principles of control*: New Science Press Ltd.

Mueller, P. R., Coleman, T. R., Kumagai, A., & Dunphy, W. G. (1995). Myt1: a membrane-associated inhibitory kinase that phosphorylates Cdc2 on both threonine-14 and tyrosine-15. *Science, 270*(5233), 86-90. doi:10.1126/science.270.5233.86

Mulner, O., Huchon, D., Thibier, C., & Ozon, R. (1979). Cyclic AMP synthesis in Xenopus laevis oocytes inhibition by progesterone. *Biochimica et Biophysica Acta (BBA) - General Subjects, 582*(1), 179-184. doi:10.1016/0304-4165(79)90301-5

Murphy, L. O., Smith, S., Chen, R. H., Fingar, D. C., & Blenis, J. (2002). Molecular interpretation of ERK signal duration by immediate early gene products. *Nat Cell Biol, 4*(8), 556-564. doi:10.1038/ncb822

Nguyen, T. B., Manova, K., Capodieci, P., Lindon, C., Bottega, S., Wang, X. Y., Refik-Rogers, J., Pines, J., Wolgemuth, D. J., & Koff, A. (2002). Characterization and expression of mammalian cyclin b3, a prepachytene meiotic cyclin. *J Biol Chem, 277*(44), 41960-41969. doi:10.1074/jbc.M203951200

Nishiyama, T., Ohsumi, K., & Kishimoto, T. (2007). Phosphorylation of Erp1 by p90rsk is required for cytostatic factor arrest in Xenopus laevis eggs. *Nature, 446*(7139), 1096-1099. doi:10.1038/nature05696

Noble, M. E., Endicott, J. A., Brown, N. R., & Johnson, L. N. (1997). The cyclin box fold: protein recognition in cell-cycle and transcription control. *Trends Biochem Sci, 22*(12), 482-487. doi:10.1016/s0968-0004(97)01144-4

Ohe, M., Inoue, D., Kanemori, Y., & Sagata, N. (2007). Erp1/Emi2 is essential for the meiosis I to meiosis II transition in Xenopus oocytes. *Developmental Biology, 303*(1), 157-164. doi:10.1016/j.ydbio.2006.10.044

Ohe, M., Kawamura, Y., Ueno, H., Inoue, D., Kanemori, Y., Senoo, C., Isoda, M., Nakajo, N., & Sagata, N. (2010). Emi2 inhibition of the anaphase-promoting complex/cyclosome absolutely requires Emi2 binding via the C-terminal RL tail. *Molecular Biology of the Cell, 21*(6), 905-913. doi:10.1091/mbc.e09-11-0974

Okano-Uchida, T., Okumura, E., Iwashita, M., Yoshida, H., Tachibana, K., & Kishimoto, T. (2003). Distinct regulators for Plk1 activation in starfish meiotic and early embryonic cycles. *Embo j, 22*(20), 5633-5642. doi:10.1093/emboj/cdg535

Örd, M., Venta, R., Möll, K., Valk, E., & Loog, M. (2019). Cyclin-Specific Docking Mechanisms Reveal the Complexity of M-CDK Function in the Cell Cycle. *Molecular Cell, 75*(1), 76-89.e73. doi:10.1016/j.molcel.2019.04.026

Palmer, A., Gavin, A.-C., & Nebreda, A. R. (1998). A link between MAP kinase and p34cdc2/cyclin B during oocyte maturation: p90rsk phosphorylates and inactivates the p34cdc2 inhibitory kinase Myt1. *Embo j, 17*(17), 5037-5047. doi:10.1093/emboj/17.17.5037

Patra, D., & Dunphy, W. G. (1996). Xe-p9, a Xenopus Suc1/Cks homolog, has multiple essential roles in cell cycle control. *Genes Dev, 10*(12), 1503-1515. doi:10.1101/gad.10.12.1503

Patra, D., & Dunphy, W. G. (1998). Xe-p9, a Xenopus Suc1/Cks protein, is essential for the Cdc2-dependent phosphorylation of the anaphase- promoting complex at mitosis. *Genes Dev, 12*(16), 2549-2559. doi:10.1101/gad.12.16.2549

Patra, D., Wang, S. X., Kumagai, A., & Dunphy, W. G. (1999). The xenopus Suc1/Cks protein promotes the phosphorylation of G(2)/M regulators. *J Biol Chem, 274*(52), 36839-36842. doi:10.1074/jbc.274.52.36839

Peter, M., Labbé, J.-C., Dorée, M., & Mandart, E. (2002). A new role for Mos in Xenopus oocyte maturation: targeting Myt1 independently of MAPK. *Development, 129*(9), 2129-2139. doi:10.1242/dev.129.9.2129

Petracchi, F., Colaci, D. S., Igarzabal, L., & Gadow, E. (2009). Cytogenetic analysis of first trimester pregnancy loss. *Int J Gynaecol Obstet, 104*(3), 243-244. doi:10.1016/j.ijgo.2008.10.014

Pines, J. (1996). Cell cycle: Reaching for a role for the Cks proteins. *Current Biology, 6*(11), 1399-1402. doi:10.1016/S0960-9822(96)00741-5

Piqué, M., López, J. M., Foissac, S., Guigó, R., & Méndez, R. (2008). A Combinatorial Code for CPE-Mediated Translational Control. *Cell, 132*(3), 434-448. doi:10.1016/j.cell.2007.12.038

Pomerening, J. R., Sontag, E. D., & Ferrell, J. E., Jr. (2003). Building a cell cycle oscillator: hysteresis and bistability in the activation of Cdc2. *Nat Cell Biol, 5*(4), 346-351. doi:10.1038/ncb954

Posada, J., Yew, N., Ahn, N. G., Vande Woude, G. F., & Cooper, J. A. (1993). Mos stimulates MAP kinase in Xenopus oocytes and activates a MAP kinase kinase in vitro. *Mol Cell Biol, 13*(4), 2546-2553. doi:10.1128/mcb.13.4.2546-2553.1993

Qian, Y. W., Erikson, E., & Maller, J. L. (1999). Mitotic effects of a constitutively active mutant of the Xenopus polo-like kinase Plx1. *Mol Cell Biol, 19*(12), 8625-8632. doi:10.1128/mcb.19.12.8625

Quandt, E., Ribeiro, M. P. C., & Clotet, J. (2020). Atypical cyclins: the extended family portrait. *Cell Mol Life Sci, 77*(2), 231-242. doi:10.1007/s00018-019-03262-7

Rauh, N. R., Schmidt, A., Bormann, J., Nigg, E. A., & Mayer, T. U. (2005). Calcium triggers exit from meiosis II by targeting the APC/C inhibitor XErp1 for degradation. *Nature, 437*(7061), 1048-1052. doi:10.1038/nature04093

Ren, S., & Rollins, B. J. (2004). Cyclin C/cdk3 promotes Rb-dependent G0 exit. *Cell, 117*(2), 239-251. doi:10.1016/s0092-8674(04)00300-9

Rezaei, M., Buckett, W., Bareke, E., Surti, U., Majewski, J., & Slim, R. (2021). A protein-truncating mutation in CCNB3 in a patient with recurrent miscarriages and failure of meiosis I. *J Med Genet*. doi:10.1136/jmedgenet-2021-107875

Rudner, A. D., & Murray, A. W. (2000). Phosphorylation by Cdc28 activates the Cdc20-dependent activity of the anaphase-promoting complex. *J Cell Biol, 149*(7), 1377-1390. doi:10.1083/jcb.149.7.1377

Ruiz, E. J., Hunt, T., & Nebreda, A. R. (2008). Meiotic inactivation of Xenopus Myt1 by CDK/XRINGO, but not CDK/cyclin, via site-specific phosphorylation. *Mol Cell, 32*(2), 210-220. doi:10.1016/j.molcel.2008.08.029

Sadler, S. E., & Maller, J. L. (1981). Progesterone inhibits adenylate cyclase in Xenopus oocytes. Action on the guanine nucleotide regulatory protein. *Journal of Biological Chemistry, 256*(12), 6368-6373. doi:10.1016/S0021-9258(19)69173-8

Sagata, N., Oskarsson, M., Copeland, T., Brumbaugh, J., & Vande Woude, G. F. (1988). Function of c-mos proto-oncogene product in meiotic maturation in Xenopus oocytes. *Nature, 335*(6190), 519-525. doi:10.1038/335519a0

Sagata, N., Oskarsson, M., Copeland, T., Brumbaugh, J., & Woude, G. F. V. (1988). Function of c-mos proto-oncogene product in meiotic maturation in Xenopus oocytes. *Nature, 335*(6190), 519-525. doi:10.1038/335519a0

Sako, K., Suzuki, K., Isoda, M., Yoshikai, S., Senoo, C., Nakajo, N., Ohe, M., & Sagata, N. (2014). Emi2 mediates meiotic MII arrest by competitively inhibiting the binding of Ube2S to the APC/C. *Nat Commun, 5*, 3667. doi:10.1038/ncomms4667

Santamaría, D., Barrière, C., Cerqueira, A., Hunt, S., Tardy, C., Newton, K., Cáceres, J. F., Dubus, P., Malumbres, M., & Barbacid, M. (2007). Cdk1 is sufficient to drive the mammalian cell cycle. *Nature, 448*(7155), 811-815. doi:10.1038/nature06046

Satyanarayana, A., & Kaldis, P. (2009). Mammalian cell-cycle regulation: several Cdks, numerous cyclins and diverse compensatory mechanisms. *Oncogene, 28*(33), 2925-2939. doi:10.1038/onc.2009.170

Schmidt, A., Duncan, P. I., Rauh, N. R., Sauer, G., Fry, A. M., Nigg, E. A., & Mayer, T. U. (2005). Xenopus polo-like kinase Plx1 regulates XErp1, a novel inhibitor of APC/C activity. *Genes & Development, 19*(4), 502-513. doi:10.1101/gad.320705

Schmidt, A., Rauh, N. R., Nigg, E. A., & Mayer, T. U. (2006). Cytostatic factor: an activity that puts the cell cycle on hold. *J Cell Sci, 119*(Pt 7), 1213-1218. doi:10.1242/jcs.02919

Session, A. M., Uno, Y., Kwon, T., Chapman, J. A., Toyoda, A., Takahashi, S., Fukui, A., Hikosaka, A., Suzuki, A., Kondo, M., van Heeringen, S. J., Quigley, I., Heinz, S., Ogino, H., Ochi, H., Hellsten, U., Lyons, J. B., Simakov, O., Putnam, N., Stites, J., Kuroki, Y., Tanaka, T., Michiue, T., Watanabe, M., Bogdanovic, O., Lister, R., Georgiou, G., Paranjpe, S. S., van Kruijsbergen, I., Shu, S., Carlson, J., Kinoshita, T., Ohta, Y., Mawaribuchi, S., Jenkins, J., Grimwood, J., Schmutz, J., Mitros, T., Mozaffari, S. V., Suzuki, Y., Haramoto, Y., Yamamoto, T. S., Takagi, C., Heald, R., Miller, K., Haudenschild, C., Kitzman, J., Nakayama, T., Izutsu, Y., Robert, J., Fortriede, J., Burns, K., Lotay, V., Karimi, K., Yasuoka, Y., Dichmann, D. S., Flajnik, M. F., Houston, D. W., Shendure, J., DuPasquier, L., Vize, P. D., Zorn, A. M., Ito, M., Marcotte, E. M., Wallingford, J. B., Ito, Y., Asashima, M., Ueno, N., Matsuda, Y., Veenstra, G. J. C., Fujiyama, A., Harland, R. M., Taira, M., & Rokhsar, D. S. (2016). Genome evolution in the allotetraploid frog Xenopus laevis. *Nature, 538*(7625), 336-343. doi:10.1038/nature19840

Setoyama, D., Yamashita, M., & Sagata, N. (2007). Mechanism of degradation of CPEB during Xenopus oocyte maturation. *Proc Natl Acad Sci U S A, 104*(46), 18001-18006. doi:10.1073/pnas.0706952104

Sha, W., Moore, J., Chen, K., Lassaletta, A. D., Yi, C. S., Tyson, J. J., & Sible, J. C. (2003). Hysteresis drives cell-cycle transitions in Xenopus laevis egg extracts. *Proc Natl Acad Sci U S A, 100*(3), 975-980. doi:10.1073/pnas.0235349100

Sheridan, D. L., Kong, Y., Parker, S. A., Dalby, K. N., & Turk, B. E. (2008). Substrate discrimination among mitogen-activated protein kinases through distinct docking sequence motifs. *J Biol Chem, 283*(28), 19511-19520. doi:10.1074/jbc.M801074200

Shoji, S., Muto, Y., Ikeda, M., He, F., Tsuda, K., Ohsawa, N., Akasaka, R., Terada, T., Wakiyama, M., Shirouzu, M., & Yokoyama, S. (2014). The zinc-binding region (ZBR) fragment of Emi2 can inhibit APC/C by targeting its association with the coactivator Cdc20 and UBE2C-mediated ubiquitylation. *FEBS Open Bio, 4*, 689-703. doi:10.1016/j.fob.2014.06.010

Shoji, S., Yoshida, N., Amanai, M., Ohgishi, M., Fukui, T., Fujimoto, S., Nakano, Y., Kajikawa, E., & Perry, A. C. (2006). Mammalian Emi2 mediates cytostatic arrest and transduces the signal for meiotic exit via Cdc20. *Embo j, 25*(4), 834-845. doi:10.1038/sj.emboj.7600953

Slizynski, B. M. (1957). Meiotic prophase in female mice. *Nature, 179*(4560), 638. doi:10.1038/179638a0

Solomon, M. J., Lee, T., & Kirschner, M. W. (1992). Role of phosphorylation in p34cdc2 activation: identification of an activating kinase. *Molecular Biology of the Cell, 3*(1), 13-27. doi:10.1091/mbc.3.1.13

Songyang, Z., Lu, K. P., Kwon, Y. T., Tsai, L. H., Filhol, O., Cochet, C., Brickey, D. A., Soderling, T. R., Bartleson, C., Graves, D. J., DeMaggio, A. J., Hoekstra, M. F., Blenis, J., Hunter, T., & Cantley, L. C. (1996). A structural basis for substrate specificities of protein Ser/Thr kinases: primary sequence preference of casein kinases I and II, NIMA, phosphorylase kinase, calmodulin-dependent kinase II, CDK5, and Erk1. *Mol Cell Biol, 16*(11), 6486-6493. doi:10.1128/mcb.16.11.6486

Spruck, C. H., de Miguel, M. P., Smith, A. P. L., Ryan, A., Stein, P., Schultz, R. M., Lincoln, A. J., Donovan, P. J., & Reed, S. I. (2003). Requirement of Cks2 for the First Metaphase/Anaphase Transition of Mammalian Meiosis. *Science, 300*(5619), 647-650. doi:doi:10.1126/science.1084149

Spruck, C. H., Strohmaier, H., Watson, M., Smith, A. P., Ryan, A., Krek, T. W., & Reed, S. I. (2001). A CDK-independent function of mammalian Cks1: targeting of SCF(Skp2) to the CDK inhibitor p27Kip1. *Mol Cell, 7*(3), 639-650. doi:10.1016/s1097-2765(01)00210-6

Stern, B., & Nurse, P. (1996). A quantitative model for the cdc2 control of S phase and mitosis in fission yeast. *Trends Genet, 12*(9), 345-350. doi:10.1016/S0168-9525(96)80016-3

Tang, W., Wu, J. Q., Chen, C., Yang, C. S., Guo, J. Y., Freel, C. D., & Kornbluth, S. (2010). Emi2-mediated inhibition of E2-substrate ubiquitin transfer by the anaphase-promoting complex/cyclosome through a D-box-independent mechanism. *Mol Biol Cell, 21*(15), 2589-2597. doi:10.1091/mbc.E09-08-0708

Tanoue, T., Adachi, M., Moriguchi, T., & Nishida, E. (2000). A conserved docking motif in MAP kinases common to substrates, activators and regulators. *Nat Cell Biol, 2*(2), 110-116. doi:10.1038/35000065

Tassan, J. P., Jaquenoud, M., Léopold, P., Schultz, S. J., & Nigg, E. A. (1995). Identification of human cyclin-dependent kinase 8, a putative protein kinase partner for cyclin C. *Proc Natl Acad Sci U S A, 92*(19), 8871-8875. doi:10.1073/pnas.92.19.8871

Terret, M. E., Lefebvre, C., Djiane, A., Rassinier, P., Moreau, J., Maro, B., & Verlhac, M. H. (2003). DOC1R: a MAP kinase substrate that control microtubule organization of metaphase II mouse oocytes. *Development, 130*(21), 5169-5177. doi:10.1242/dev.00731

Tischer, T., Hörmanseder, E., & Mayer, T. U. (2012). The APC/C inhibitor XErp1/Emi2 is essential for Xenopus early embryonic divisions. *Science, 338*(6106), 520-524. doi:10.1126/science.1228394

Tung, J. J., Hansen, D. V., Ban, K. H., Loktev, A. V., Summers, M. K., Adler, J. R., 3rd, & Jackson, P. K. (2005). A role for the anaphase-promoting complex inhibitor Emi2/XErp1, a homolog of early mitotic inhibitor 1, in cytostatic factor arrest of Xenopus eggs. *Proc Natl Acad Sci U S A, 102*(12), 4318-4323. doi:10.1073/pnas.0501108102

Tung, J. J., Padmanabhan, K., Hansen, D. V., Richter, J. D., & Jackson, P. K. (2007). Translational Unmasking of Emi2 Directs Cytostatic Factor Arrest in Meiosis II. *Cell Cycle, 6*(6), 725-731. doi:10.4161/cc.6.6.3936

Uhlmann, F., Bouchoux, C., & López-Avilés, S. (2011). A quantitative model for cyclin-dependent kinase control of the cell cycle: revisited. *Philosophical Transactions of the Royal Society B: Biological Sciences, 366*(1584), 3572-3583. doi:doi:10.1098/rstb.2011.0082

Valk, E., Örd, M., Faustova, I., & Loog, M. (2023). CDK signaling via nonconventional CDK phosphorylation sites. *Mol Biol Cell, 34*(12), pe5. doi:10.1091/mbc.E22-06-0196 van der Voet, M., Lorson, M. A., Srinivasan, D. G., Bennett, K. L., & van den Heuvel, S. (2009). C. elegans mitotic cyclins have distinct as well as overlapping functions in chromosome segregation. *Cell Cycle, 8*(24), 4091-4102. doi:10.4161/cc.8.24.10171

van Hooff, J. J., Tromer, E., van Wijk, L. M., Snel, B., & Kops, G. J. (2017). Evolutionary dynamics of the kinetochore network in eukaryotes as revealed by comparative genomics. *EMBO Rep, 18*(9), 1559-1571. doi:10.15252/embr.201744102

Vigneron, S., Brioudes, E., Burgess, A., Labbé, J. C., Lorca, T., & Castro, A. (2009). Greatwall maintains mitosis through regulation of PP2A. *Embo j, 28*(18), 2786-2793. doi:10.1038/emboj.2009.228

Vigneron, S., Sundermann, L., Labbé, J. C., Pintard, L., Radulescu, O., Castro, A., & Lorca, T. (2018). Cyclin A-cdk1-Dependent Phosphorylation of Bora Is the Triggering Factor Promoting Mitotic Entry. *Dev Cell, 45*(5), 637-650.e637. doi:10.1016/j.devcel.2018.05.005

Von Stetina, J. R., & Orr-Weaver, T. L. (2011). Developmental control of oocyte maturation and egg activation in metazoan models. *Cold Spring Harb Perspect Biol, 3*(10), a005553. doi:10.1101/cshperspect.a005553

Wang, J., Cao, W. L., & Liu, X. J. (2006). Protein kinase A(PKA)-restrictive and PKA-permissive phases of oocyte maturation. *Cell Cycle, 5*(2), 213-217. doi:10.4161/cc.5.2.2365

Wang, R., He, G., Nelman-Gonzalez, M., Ashorn, C. L., Gallick, G. E., Stukenberg, P. T., Kirschner, M. W., & Kuang, J. (2007). Regulation of Cdc25C by ERK-MAP kinases during the G2/M transition. *Cell, 128*(6), 1119-1132. doi:10.1016/j.cell.2006.11.053

Warburton, D., & Fraser, F. C. (1964). Spontaneous Abortion Risks in Man: Data from Reproductive Histories Collected in a Medical Genetics Unit. *Am J Hum Genet, 16*(1), 1-25. Retrieved from https://www.ncbi.nlm.nih.gov/pmc/articles/PMC1932458/pdf/ajhg00547-0015.pdf

Weinberg, R. A. (1995). The retinoblastoma protein and cell cycle control. *Cell, 81*(3), 323-330. doi:10.1016/0092-8674(95)90385-2

Wood, D. J., & Endicott, J. A. (2018). Structural insights into the functional diversity of the CDK-cyclin family. *Open Biol, 8*(9). doi:10.1098/rsob.180112

Wu, J. Q., Hansen, D. V., Guo, Y., Wang, M. Z., Tang, W., Freel, C. D., Tung, J. J., Jackson, P. K., & Kornbluth, S. (2007). Control of Emi2 activity and stability through Mos-mediated recruitment of PP2A. *Proceedings of the National Academy of Sciences, 104*(42), 16564-16569. doi:doi:10.1073/pnas.0707537104

Wu, Q., Guo, Y., Yamada, A., Perry, J. A., Wang, M. Z., Araki, M., Freel, C. D., Tung, J. J., Tang, W., Margolis, S. S., Jackson, P. K., Yamano, H., Asano, M., & Kornbluth, S. (2007). A role for Cdc2- and PP2A-mediated regulation of Emi2 in the maintenance of CSF arrest. *Curr Biol, 17*(3), 213-224. doi:10.1016/j.cub.2006.12.045

Yang, K., Hitomi, M., & Stacey, D. W. (2006). Variations in cyclin D1 levels through the cell cycle determine the proliferative fate of a cell. *Cell division, 1*, 32. doi:10.1186/1747-1028-1-32

Yu, J., Raia, P., Ghent, C. M., Raisch, T., Sadian, Y., Cavadini, S., Sabale, P. M., Barford, D., Raunser, S., Morgan, D. O., & Boland, A. (2021). Structural basis of human separase regulation by securin and CDK1-cyclin B1. *Nature, 596*(7870), 138-142. doi:10.1038/s41586-021-03764-0

Yuan, K., & O'Farrell, P. H. (2015). Cyclin B3 is a mitotic cyclin that promotes the metaphase-anaphase transition. *Curr Biol, 25*(6), 811-816. doi:10.1016/j.cub.2015.01.053

Zhang, T., Qi, S. T., Huang, L., Ma, X. S., Ouyang, Y. C., Hou, Y., Shen, W., Schatten, H., & Sun, Q. Y. (2015). Cyclin B3 controls anaphase onset independent of spindle assembly checkpoint in meiotic oocytes. *Cell Cycle, 14*(16), 2648-2654. doi:10.1080/15384101.2015.1064567

9. Acknowledgements

First of all, I want to thank Thomas Mayer for giving me the opportunity to do my PhD thesis in his lab. The PhD position gave me the chance to see a different part of Germany and to work at a beautiful location. I also want to thank Thomas for his patience and encouraging behaviour and for giving us the chance to get in touch with other researchers within the project and the invited speaker during the VTKs.

I further want to thank Christine Peter and Martin Scheffner for being members of my graduate school committee and my examination committee. Thank you for the valuable scientific input and the enriching discussions.
I like to acknowledge the Konstanz Research School Chemical Biology (KoRS-CB) and the SFB969 of the University of Konstanz for supporting me and my work and for providing always interesting and relevant courses and programs to support the exchange among the different PhD students.

I want to thank my two Master's students Mona Urban and Michael Schäfer for their help in my project. I also want to acknowledge all my VTK students David, Konstantin, Carolin, Elena, Marvin, Alisa, Kara, Lena, Vanessa, and Elif who taught me patience and gave me the opportunity to spread my excitement about my projects.

I also want to thank the whole Mayer Lab with all former and recent members. Especially I want to thank Andreas Heim for all the time he came up with another idea of how to make things work and who is a better search engine than Google when it comes to cell cycle-related questions. Also thank you for proofreading my thesis—without your comments this thesis would not be as it is now! Another big thank you goes to Martina Baack and her great job in purification whatever needs to be purified, like XErp1 antibody or cycB3/Cdk complexes. You (almost) always made it work and therefore saved me a lot of time. I also want to thank Melanie Walter for always supporting me by preparing buffers or doing some cloning. Without you, lunches would have been less enjoyable. Also, I would never have been able to finish the cycB3-project in such a short time without the previous work done by so many people in the lab, thank you for that: Janina Müller, Camilla Kleinhempel, Hiba Al-Abdallah, Lena Schneider, Patrick Wehrle, and Elijah Johannes. Also thanks to the other former and recent members Franziska Teusel, Lars Henschke, Christian Heinzle, Marc Halder, Deniz Strohmaier, and all the Master's and Bachelor's students working in the lab during my PhD work.

Thanks also to Sophia and Yannick for exciting game nights and excellent food. Without your sofa, the last month of my PhD would have been more stressful.

I also want to say thank you to my family, especially to my parents. Without your support and your faith in me, I would have never reached that point in my life.

Last but not least, I want to thank you, Fabian, for being the best thing that happened to me in Konstanz and at any other place—without you something would be missing in my life.